TR-81-111-01

DISPERSION MODEL STUDIES FOR SPACE SHUTTLE ENVIRONMENTAL EFFECTS ACTIVITIES

Final Report Under Contract No. NAS8-31841

Prepared For:

NATIONAL AERONAUTICS AND SPACE ADMINISTRATION
George C. Marshall Space Flight Center
Marshall Space Flight Center, Alabama 35812

April 1981

H. E. CRAMER COMPANY, INC.
University of Utah Research Park
Post Office Box 8049
Salt Lake City, Utah 84108

TABLE OF CONTENTS

SECTION 1
INTRODUCTION

The H. E. Cramer Company, Inc. began work under NASA Contract No. NAS8-31841 in March 1976 and completed work, including all modifications to the contract, in December 1980. The work under the contract has principally involved the development of the NASA/MSFC REED computer code for predicting concentrations, dosage and deposition downwind from rocket vehicle launches and the development and application of dispersion modeling techniques for use in NASA environmental studies concerned with launch support and associated fuel storage and handling problems. In this final report, we describe the calculation procedures and results of nine studies performed during the course of the work which were not included in the two formal technical reports previously submitted under the contract (Stephens and Dumbauld, 1979; Dumbauld, Rafferty and Saterlie, 1977).

SECTION 2

SIMPLIFIED DISPERSION MODEL FOR THE MOMENTUM PHASE OF PLUME EXPANSION

A Momentum Phase Dispersion Model computer program was developed for use on the REEDA system for calculating concentrations in the jet plumes from various ducts at MSFC facilities. The mathematical equations used in the computer program as well as the solutions for example problems are given below for the following source configurations:

- A horizontal exhaust duct near ground level located at the Marshall Hot Gas Facility (MHGF)
- A horizontal exhaust duct at a height of 30.5 meters above the ground located at the T/Acoustic Facility
- A vertical exhaust duct at a height of 9.15 meters above the ground located at LRLF

Effluent composition and other source parameters for the three exhaust ducts are given in Tables 2-1 through 2-4. The concentrations χ_o at the duct exit of potentially hazardous gases contained in the exhaust effluent at each facility are given in Tables 2-1 through 2-3. Table 2-4 gives the remaining source parameters required for input to the models. Threshold hazard concentrations (THC) for the various constituents of the exhaust gases are given in Table 2-5.

The plume expansion formula used in the calculations is based on expressions for the expansion of plumes from jets described by Briggs (1971) where the source emissions are assumed to be continuous for a period of sixty seconds or longer. Observations of plumes from jets indicate that the plume radius r increases with distance from the exit plane according to the expression

TABLE 2-1

CONCENTRATIONS IN THE EXHAUST DUCT (χ_o) AT THE MHGF

Fuel	Concentration (ppm)				
	CO	HCN	$COCl_2$	HCl	Cl
CPR-488	666.9	99.3	129.7	47.5	92.5
TEXTHANE	642.9	86.8	165.4	61.0	118.7
BX-250	654.1	94.3	150.3	52.8	102.7
PD-200	664.9	0	0	0	0
DC-3-6548	683.3	0	0	0	0
SLA-561	752.1	0	0	0	0
MXSA	662.1	113.0	71.35	26.5	51.4

TABLE 2-2

CONCENTRATIONS IN THE EXHAUST DUCT
(χ_o) AT THE T/ACOUSTIC FACILITY

Fuel	Concentration (ppm)				
	CO	HCN	$COCl_2$	HCl	Cl
CPR-488	218.6	32.4	42.3	15.6	30.3
TEXTHANE	209.6	28.3	53.9	19.9	38.6
BX-250	213.6	30.2	44.5	11.3	22.0
PD-200	260.3	0	0	0	0
DC-3-6548	267.5	0	0	0	0
SLA-561	294.5	0	0	0	0
MXSA	260.2	77.1	27.9	10.3	20.0

TABLE 2-3

CONCENTRATIONS IN THE EXHAUST DUCT
(χ_o) AT THE LRLF

Fuel	Concentration (ppm)				
	CO	HCN	$COCl_2$	HCl	Cl
CPR-488	25.1	3.7	4.9	1.8	3.5
TEXTHANE	24.2	3.27	4.73	1.74	3.39
BX-250	24.7	3.5	5.1	1.3	2.5
PD-200	81.4	0	0	0	0
DC-3-6548	83.6	0	0	0	0
SLA-561	92.1	0	0	0	0
MXSA	81.5	5.0	8.7	3.2	6.3

TABLE 2-4

OTHER SOURCE PARAMETERS

Parameter	Facility		
	MHGF	LRLF	T/Acoustic
Duct Dimensions (m)	Height = .363 Width = .629	Diameter = 0.762	Height = .915 Width = .915
Height Above Ground Level (m)	1.32	9.15	30.5
Exit Speed (m/sec)	145.8	48.8	220
Orientation of Exit Plane	Horizontal	Vertical	Horizontal

TABLE 2-5

THRESHOLD HAZARD CONCENTRATIONS FOR THE VARIOUS EXHAUST-GAS CONSTITUENTS

Exhaust Gas Constituents	Threshold Hazard Concentration (ppm)
CO	50
HCN	10
$COCl_2$	0.1
HCl	5
Cl	0.5

$$r = \left(\frac{1}{3} + \frac{\bar{u}}{v_o}\right) x \qquad (2\text{-}1)$$

where

$\bar{u}$ = ambient wind speed

v_o = exit velocity at the source

x = distance from the exit plane

The radius r_x of the plume at a distance x from the exit plane is

$$r_x = r_o + \left(\frac{1}{3} + \frac{\bar{u}}{v_o}\right) x \qquad (2\text{-}2)$$

where

r_o = effective radius of the exit

For rectangular shaped exits, the program assumes

$$r_o = \left(A_o/\pi\right)^{1/2} \qquad (2\text{-}3)$$

where

A_o = area of the duct exit

When the jet is directed horizontally, Equation (2-2) is strictly valid out to the distance at which the jet velocity becomes equal to the ambient wind speed. Assuming the wind direction is along the axis of the jet, the distance x' where v_o equals $\bar{u}$ is given by

$$x' = \frac{3 v_o r_o}{v_o + 3\bar{u}} \left(\sqrt{\frac{v_o}{\bar{u}}} - 1 \right) \qquad (2\text{-}4)$$

If the jet is directed vertically, the plume rises due to the momentum generated by the jet and the stabilization height H is given by the expression

$$H = h + \frac{6 v_o r_o}{\bar{u}} \qquad (2\text{-}5)$$

where

h = height of the jet exit plane

The distance downwind x' at which distance the stabilization height H is achieved is given by

$$x' = \frac{8 r_o \bar{u}}{v_o} \left(\frac{v_o}{\bar{u}} + 3 \right)^2 \qquad (2\text{-}6)$$

Assuming that the material in the plume has a Gaussian distribution, the concentration at the plume centerline at height z above the ground and distance $x<x'$ from the exhuast is given by

$$\chi\{x<x'\} = \frac{\chi_o r_o^2}{2 \sigma_r^2} \left\{ \exp \left[-.5 \left(\frac{H - z}{\sigma_r} \right)^2 \right] + \exp \left[-.5 \left(\frac{H + z}{\sigma_r} \right)^2 \right] \right\} \qquad (2\text{-}7)$$

Similarly, at distances $x>x'$, the concentration is given by

$$\chi\{x>x'\} = \frac{\chi_o r_o^2}{2\sigma_y\sigma_z}\left\{\exp\left[-.5\left(\frac{H-z}{\sigma_z}\right)^2\right] + \exp\left[-.5\left(\frac{H+z}{\sigma_z}\right)^2\right]\right\} \quad (2\text{-}8)$$

In Equation (2-7) and (2-8),

χ_o = gas concentration at the exit plane

$$\sigma_r = \frac{r_o + \left(\frac{1}{3} + \frac{\bar{u}}{v_o}\right) x}{2.15} \quad (2\text{-}9)$$

$$\sigma_y = 50\,\sigma'_A\left[\frac{x + x_y}{45}\right]^{0.9} \quad (2\text{-}10)$$

$$x_y = 45\left[\frac{\sigma_r\{x = x'\}}{50\,\sigma'_A}\right]^{1/.9} - x' \quad (2\text{-}11)$$

σ'_A = standard deviation of the wind azimuth angle in radians

$$\sigma_z = \sigma'_E\left(x + x_z\right) \quad (2\text{-}12)$$

$$\sigma_z = \left[\frac{\sigma_r\{x = x'\}}{\sigma'_E}\right] - x' \quad (2\text{-}13)$$

σ'_E = standard deviation of the wind elevation angle in radians

Concentrations at distances greater than x' downwind from vertically oriented jets are calculated from Equation (2-8). The program does not contain provision for calculating concentrations from vertically oriented jets for distances less than x'. The critical distance x_{crit} at which $\chi \leq THC$ is obtained by solving Equation (2-7) or Equation (2-8) using iterative procedures to determine the value of x that is equal to x_{crit}.

Requisite model inputs include the height z and the meteorological parameters $\bar{u}$, σ'_A and σ'_E. To obtain maximum estimates of x_{crit} for the MHGF, the height z was set equal to H (1.32 meters). In the remaining calculations, z was set equal to 2 meters. Concentrations downwind from horizontal jets tend to very inversely with the wind speed $\bar{u}$ because σ_r in Equation (2-9) increases with increasing wind speed. Concentrations donwwind from vertically oriented jets tend to vary directly with wind speed because plume rise decreases with increasing wind speed. For these reasons, $\bar{u}$ was set equal to 1 meter per second for calculations of x_{crit} downwind from the T/Acoustic Facility and MHGF and equal to 10 meters per second for the calculations of x_{crit} downwind from the LRLF. The turbulence parameters σ'_A and σ'_E were set equal to 0.08727 radians (5 degrees) in the calculations to take account of the turbulence induced by the buildings associated with the three facilities.

The values of the hazard distance calculated for the chemical constituents of emissions from the exhaust duct at the MHGF are given in Table 2-6. The largest calculated value for x_{crit} of 118 meters occurs for the phosgene ($COCl_2$) component of the fuel texthane. It should be noted that no credit has been taken in the calculation for any increase in the height of the exhuast plume due to thermal buoyancy. The calculated distances may therefore be overestimates.

Similar calculations made for the T/Acoustic Facility and LRLF showed that near ground-level concentrations of the exhaust gas constituents are always below the threshold hazard concentrations.

TABLE 2-6

CALCULATED CRITICAL DISTANCES FROM THE EXHAUST DUCT OF THE MHGF FOR THE CHEMICAL CONSTITUENTS OF THE VARIOUS FUELS

Fuel	Critical Distances (m)					
	CO	HCN	$COCl_2$	HCl	Cl	All
CPR-488	3.7	3.1	103	3.0	30	103
TEXTHANE	3.6	2.8	118	3.5	36	118
BX-250	3.6	3.0	112	3.2	33	112
PD-200	3.7	-	-	-	-	3.7
DC-3-6548	3.7	-	-	-	-	3.7
SLA-561	3.9	-	-	-	-	3.9
MXSA	3.6	3.3	72	2.0	19	73
All Fuels	3.9	3.3	118	3.5	36	118

SECTION 3

VAPORIZATION OF OXYGEN VENTED DURING LAUNCH OPERATIONS

Estimates of the time required for liquid oxygen to evaporate after venting from LOX tanks during launch operations were made for MSFC. The evaporation rate for liquid drops depends principally on the rate at which heat from the surrounding environment is absorbed by the drops. The rate of decrease in the drop diameter D_p caused by evaporation, according to Fuchs (1959), is given by the expression

$$\frac{d\,D_p}{dt} = \frac{-4M_v D_v}{M_m D_p} \cdot \frac{\rho_a}{\rho_p} \cdot \frac{\Delta p}{p_f} \left[2 + 0.6\ Sc^{1/3} \cdot Re^{1/2}\right] \qquad (3\text{-}1)$$

where

M_v = molecular weight of the evaporating vapor

M_m = mean molecular weight of resulting vapor-air mixture

D_v = molecular diffusivity of evaporating vapor in air

ρ_a = density of air

ρ_p = density of liquid

Δp = vapor pressure of evaporating liquid at the droplet surface minus the vapor pressure in ambient air

p_f = air partial pressure

Sc = Schmidt number

$$= \frac{D_v \rho_a}{\mu_a} \tag{3-2}$$

μ_a = absolute viscosity of air

Re = Reynolds number

$$= \frac{V_t D_p \rho_a}{\mu_a} \tag{3-3}$$

V_t = terminal velocity of the falling drop

To determine the time required for the drop to evaporate, Equation (3-1) must be integrated over all drop diameters D'_p of the liquid oxygen ranging from the initial diameter at venting to zero when the drop is fully evaporated. Since the Reynolds number and terminal velocity of the drop are functions of the drop diameter, the integral is not easily evaluated. To avoid a time consuming numerical integration, the Reynolds number, Re, was approximated and taken to be constant during the evaporation period. When Re is held constant, the integral of Equation (3-1) yields the following expression for time required for the drop to evaporate

$$t_E = \frac{\bar{D}_\rho^2}{2\left(\frac{4M_v D_v}{M_m} \cdot \frac{\rho_a}{\rho_p} \cdot \frac{\Delta p}{\rho_f}\right)\left(2 + 0.6\ Sc^{1/3} \cdot Re^{1/2}\right)} \tag{3-4}$$

where

$\bar{D}_p$ = average drop diameter used to determine the constant value of Re

We assumed the value of $\bar{D}_p$ can be determined from the expression

$$\bar{D}_p = \left[\frac{(D'_p)^{\frac{1}{2}} + 0^{\frac{1}{2}}}{2} \right]^2 \qquad (3\text{-}5)$$

Table 3-1 presents values of the parameters in Equation (3-4) we have used to solve for the evaporation time of drops with diameters of 1, 1.5 and 3 mm. Since water drops with diameters greater than about 3 mm quickly break up into smaller drops and liquid oxygen has a viscosity about one-fifth that of water, we have assumed that the drops of liquid oxygen will also not be larger than about 3 mm. The results of the calculations are shown in Table 3-2, along with the average drop diameters from Equation (3-5) and the values of V_t corresponding to these average diameters calculated using the McDonald (1960) technique.

TABLE 3-1

INPUT PARAMETERS

Parameter	Value
M_v	32 g · mole^{-1}
M_m	28.94 g · mole^{-1}
D_v	0.187 cm^2 · s^{-1}
ρ_a	1.2566 x 10^{-3} g · cm^{-3}
ρ_p	1.144 g · cm^{-3}
Δp	~ 0.8 atmosphere
p_f	~ 1.0 atmosphere
μ_a	1.7448 x 10^{-4} g · cm^{-1} · s^{-1}
T	280.94 ^{o}K

TABLE 3-2

EVAPORATION TIMES FOR SELECTED DROP SIZES OF LIQUID OXYGEN

Initial Drop Diameter, D'_p (mm)	Average Drop Diameter, $\overline{D}_p$ (mm)	Terminal Velocity, V_t ($cm \cdot s^{-1}$)	Evaporation Time, t_E (s)
1.0	0.250	97.9	1.4
1.5	0.375	160.2	2.4
3.0	0.750	320.0	5.8

SECTION 4

ESTIMATES OF DOWNWIND CONCENTRATIONS FOR SPACE SHUTTLE ORBITER EMERGENCY LANDINGS AT WHITE SANDS MISSILE RANGE

Hazard calculations were made for a hypothetical crash of the Space Shuttle Orbiter during an emergency landing at White Sands Missile Range. The model calculations were performed using a slightly modified version of a computer program developed for Dugway Proving Ground (Bjorklund and Dumbauld, 1977) and meteorological data based on a previous study we completed for White Sands Missile Range (Dumbauld and Bjorklund, 1977). Details of the calculations and their results are described below.

Dispersion Model

The peak centerline concentration downwind from an instantaneous source can be expressed as the product of two terms:

$$\text{Peak Centerline Concentration} = \{\text{Peak Concentration Term}\}\{\text{Vertical Term}\} \tag{4-1}$$

The Peak Concentration Term is defined by the expression

$$\frac{KQ}{(2\pi)^{3/2}\sigma_x\sigma_y\sigma_z} \tag{4-2}$$

where

K = parameter used to convert inputs into dimensionally consistent units

Q = total source strength

σ_x = standard deviation of the alongwind distribution of materials

σ_y = standard deviation of the crosswind distribution of material

σ_z = standard deviation of the vertical distribution of material

The Vertical Term is given by the expression

$$f_i \left\{ \sum_{a=0}^{\infty} \left[\gamma_i^a \exp\left[-\frac{1}{2}\left(\frac{2aH_m - H + z + V_{si}x/\bar{u}}{\sigma_z} \right)^2 \right] + \gamma_i^{a+1} \exp\left[-\frac{1}{2}\left(\frac{2aH_m + H + z - V_{si}x/\bar{u}}{\sigma_z} \right)^2 \right] \right] \right. \quad (4\text{-}3)$$

$$\left. + \sum_{a=1}^{\infty} \left[\gamma_i^a \exp\left[-\frac{1}{2}\left(\frac{2aH_m + H - z - V_{si}x/\bar{u}}{\sigma_z} \right)^2 \right] + \gamma_i^{a-1} \exp\left[-\frac{1}{2}\left(\frac{2aH_m - H - z + V_{si}x/\bar{u}}{\sigma_z} \right)^2 \right] \right] \right\}$$

where

f_i = fraction of the total source strength comprised of material in the i^{th} size category

γ_i = fraction of material in the i^{th} size category reflected at the ground surface (1 for complete reflection and 0 for no reflection)

H_m = depth of the surface mixing layer

H = effective source height

z = height above ground

V_{si} = gravitational settling velocity of the i^{th} size category

x = distance from the source

$\bar{u}$ = mean wind speed in the layer containing the cloud

For convenience in writing Equation (4-3), 0^0 (zero to the zero power) is defined to be equal to unity. Inspection of Equation (4-3) shows that the Vertical Term accounts for cloud depletion due to gravitational settling ($V_{si} > 0$) and due to retention of meterial at the surface ($\gamma_i < 1$).

The standard deviation of the vertical distribution of meterial is given by the expression

$$\sigma_z = \sigma'_E x_{rz} \left[\frac{x+x_z - x_{rz}(1-\beta)}{\beta x_{rz}} \right]^{\beta} \qquad (4\text{-}4)$$

where

σ'_E = standard deviation of the elevation wind angle in radians

x_{rz} = distance over which rectilinear vertical cloud expansion occurs downwind from an ideal point source

β = vertical diffusion coefficient

x_z = vertical virtual distance

$$= \begin{cases} \dfrac{\sigma_{zR}}{\sigma'_E} - x_{Rz} & ; \ \sigma_{zR} \leq \sigma'_E x_{rz} \\ \beta x_{rz} \left(\dfrac{\sigma_{zR}}{\sigma'_E x_{rz}} \right)^{1/\beta} - x_{Rz} + x_{rz}(1-\beta) & ; \ \sigma_{zR} > \sigma'_E x_{rz} \end{cases} \qquad (4\text{-}5)$$

σ_{zR} = standard deviation of the vertical concentration distribution at a distance x_{Rz} downwind from the source

The standard deviation of alongwind concentration distribution is given by the expression

$$\sigma_x = \left[\left(\frac{L\{x\}}{4.3} \right)^2 + \sigma_{xo}^2 \right]^{1/2} \tag{4-6}$$

where

$L\{x\}$ = alongwind cloud length at distance x from the source

$$= \left\{ \begin{array}{ll} \dfrac{0.6 \ \Delta\bar{u} \ x}{\bar{u}} & ; \ \Delta\bar{u} > 0 \\ \\ 0 & ; \ \Delta\bar{u} \leq 0 \end{array} \right\} \tag{4-7}$$

$\Delta\bar{u}$ = vertical wind-speed shear in the layer containing the cloud

$$= \frac{\bar{u}_R}{(z_R)^p} \left[(z_2)^p - (z_1)^p \right] \tag{4-8}$$

σ_{xo} = standard deviation of the alongwind concentration distribution at the source

$\bar{u}_R$ = mean wind speed at the reference height z_R

p = wind profile power-law exponent

z_2 = effective upper bound of the cloud

$$= \left\{ \begin{array}{ll} H + 2.15 \ \sigma_z & ; \ z_2 < H_m \\ \\ H_m & ; \ z_2 \geq H_m \end{array} \right\} \tag{4-9}$$

z_1 = effective lower bound of the cloud

$$= \left\{ \begin{array}{ll} H - 2.15\,\sigma_z & ; \quad z_1 > 2 \\ 2 & ; \quad z_1 \leq 2 \end{array} \right\} \tag{4-10}$$

$$\bar{u} = \left\{ \begin{array}{ll} \dfrac{\bar{u}_R \left[(z_2)^{1+p} - (z_1)^{1+p} \right]}{(z_2 - z_1)(z_R)^p \, (1+p)} & ; \quad \bar{u} > \bar{u}_R \\ \bar{u}_R & ; \quad \bar{u} < \bar{u}_R \end{array} \right\} \tag{4-11}$$

It should be noted that the factor 0.6 appearing in Equation (4-7) is based on theoretical work by Tyldesly and Wallington (1965) and measurements from recent experiments at Dugway and other locations.

The standard deviation of the crosswind distribution of material is given by the expression

$$\sigma_y = \left[\left(\sigma'_A\{\tau\} \quad x_{ry} \left(\frac{x + x_y - x_{ry}(1-\alpha)}{\alpha \, x_{ry}} \right)^{\alpha} \right)^2 + \left(\frac{\Delta\theta' \, x}{4.3} \right)^2 \right]^{1/2} \tag{4-12}$$

where

$\sigma'_A\{\tau\}$ = standard deviation of the azimuth wind angle in radians measured over the source emission time τ

where

$$\sigma'_A\{\tau\} = \sigma'_A\{\tau_o\} \left(\frac{\tau}{\tau_o}\right)^{1/5} \quad ; \quad 1 < \tau_o \leq 600 \text{ seconds} \tag{4-13}$$

$\sigma'_A\{\tau_o\}$ = standard deviation of the azimuth wind angle in radians in the surface mixing layer measured over the reference time τ_o

x_{ry} = distance over which rectilinear crosswind cloud expansion occurs downwind from the virtual point source

α = crosswind diffusion coefficient

x_y = crosswind virtual distance

$$x_y = \begin{cases} \dfrac{\sigma_{yR}}{\sigma'_A\{\tau\}} - x_{Ry} & ; \sigma_{yR} \leq \sigma'_A\{\tau\}\, x_{ry} \\ \alpha\, x_{ry} \left(\dfrac{\sigma_{yR}}{\sigma'_A\{\tau\}\, x_{ry}}\right) - x_{Ry} + x_{ry}(1-\alpha) & ; \sigma_{yR} > \sigma'_A\{\tau\}\, x_{ry} \end{cases} \tag{4-14}$$

σ_{yR} = standard deviation of the crosswind concentration distribution at a distance x_{Ry} downwind from the source

$\Delta\theta'$ = azimuth wind direction shear in radians within the layer containing the cloud

$$= \frac{\Delta\theta}{\Delta z} \cdot \left(\frac{\pi}{180}\right)\left(z_2 - z_1\right) \tag{4-15}$$

$\frac{\Delta\theta}{\Delta z}$ = rate change of wind direction in degrees with height in the surface mixing layer where $\Delta\theta$ is positive in the clockwise sense

Peak centerline time-average concentrations are obtained by multiplying Equation (4-1) by the expression

$$\frac{\sqrt{2\pi}\ \sigma_x}{\bar{u}\ T_a} \left\{ \text{erf} \left(\frac{\bar{u}\ T_a}{2\sqrt{2}\ \sigma_x} \right) \right\} \tag{4-16}$$

where

T_a = averaging time in seconds

Source Model Inputs

Source inputs used in the model calculations are shown in Table (4-1). The source strengths Q shown in the table were supplied by MSFC. The values of K are used to convert the source strength to cubic centimeters of gas at STP under the assumption that the pollutants will behave as ideal gases. These source strengths, when used in the models described above, will thus yield concentrations in units of parts per million parts of air (ppm) at STP. At the suggestion of MSFC, the source dimensions σ_{zR}, σ_{yR} and σ_{xo} were calculated from the expression

$$\sigma_{zR} = \sigma_{yR} = \sigma_{xo} = \left(\frac{3V}{4\pi} \right)^{1/3} \tag{4-17}$$

where V = total volume of gases comprising the source in cubic meters

and under the assumption that one standard deviation of the source distribution is equal to the radius of a sphere containing the released gases. Also at the suggestion of MSFC, the height of the release was set equal to twice the vertical source dimension. The net effect of these assumptions is to maximize the ground-level concentrations downwind from the source, because it is likely that any accident in which these fuels were released would result in a fire and buoyant rise of the combustion products and thus reduced surface concentrations. The source emission time τ was set to 2.5 seconds. Also, because the pollutants are gaseous, the settling velocities V_{si} were set to zero and the reflection coefficient γ_i set to unity (complete reflection).

TABLE 4-1

SOURCE INPUTS

Parameter		Value
Q (lbs)	Monomethylhydrazine	1886
	Hydrazine	283
	Nitrogen Tetraoxide	3016
	Ammonia	51
K ($cm^3 . lb^{-1}$)	Monomethylhydrazine	2.2055×10^5
	Hydrazine	3.1706×10^5
	Nitrogen Tetraoxide	1.1043×10^5
	Ammonia	5.9769×10^5
σ_{zR} (m)		5.92
σ_{yR} (m)		5.92
σ_{xo} (m)		5.92
$x_{ry} = x_{rz}$ (m)		0
H (m)		12.73
τ (s)		2.5
f_i		1
Y_i		1
V_{si} ($m\ s^{-1}$)		0

Meteorological Inputs

The meteorological inputs for nighttime and daytime accidents shown in Table 4-2 were selected from dispersion model inputs suggested for use at White Sands Missile Range (WSMR) by Dumbauld and Bjorklund (1977) and are based on measurements made at WSMR. The mixing depths H_m represent minimum values measured at WSMR during daytime and nighttime hours (see Table 3-1, Dumbauld and Bjorklund, 1977). The values of σ'_A, σ'_E and p shown in Table 4-2 are also based on measurements at WSMR and have been selected from Tables 3-4 and 3-5 of the report by Dumbauld and Bjorklund (1977). The nighttime values are for net radiation indices of -1 and -2 and the daytime values are for a net radiation index of +1. Thus, the selected inputs represent poor dispersion conditions which are intended to maximize ground-level concentrations. The lateral α and vertical β dispersion coefficients for instantaneous sources were set to unity in the calculations. Finally, the wind direction shear term $\Delta\theta/\Delta Z$ has been set to zero to maximize concentrations downwind from the source.

Results of the Calculations

The results of the calculations are shown in Figures 4-1 through 4-8. Figure 4-1 shows daytime and nighttime peak centerline monomethylhydrazine concentrations downwind from the hypothetical Orbiter accident at WSMR and Figure 4-2 shows the peak centerline ten-minute average concentrations. As might be expected, the peak centerline concentrations are much greater than the peak centerline ten-minute average concentrations near the source where the cloud passage time is shorter than the ten-minute averaging time. As the cloud grows alongwind with increasing travel distance from the source, the peak-centerline ten-minute average concentrations become more nearly equal to the peak centerline concentrations. Figure 4-3 through 4-8 show similar profiles for the remaining pollutants.

TABLE 4-2

METEOROLOGICAL INPUTS

Parameter	Value	
	Night	Day
H_m (m)	30	200
$\bar{u}_R$ (m s^{-1}; z_R = 2 m)	2	4
p	.25	.17
$\sigma_E^{\cdot}$ (radians)	.0506	.0524
$\sigma_A^{\cdot}$ {τ_o = 600 s} (radians)	.1501	.1571
α	1	1
β	1	1
$\Delta\theta/\Delta Z$	0	0

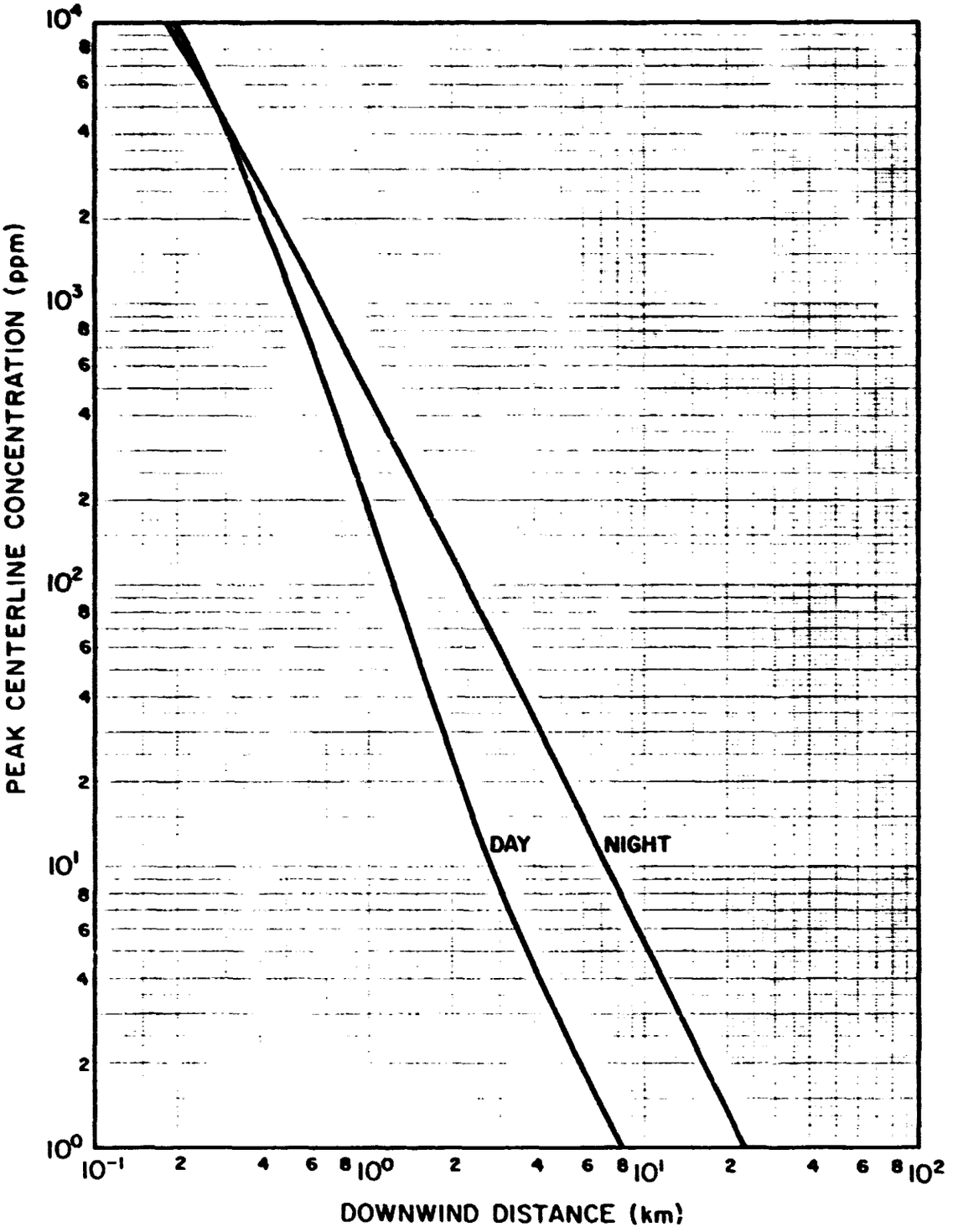

FIGURE 4-1. Daytime and nighttime peak centerline monomethylhydrazine concentrations (ppm) downwind from a hypothetical Orbiter accident at White Sands Missile Range.

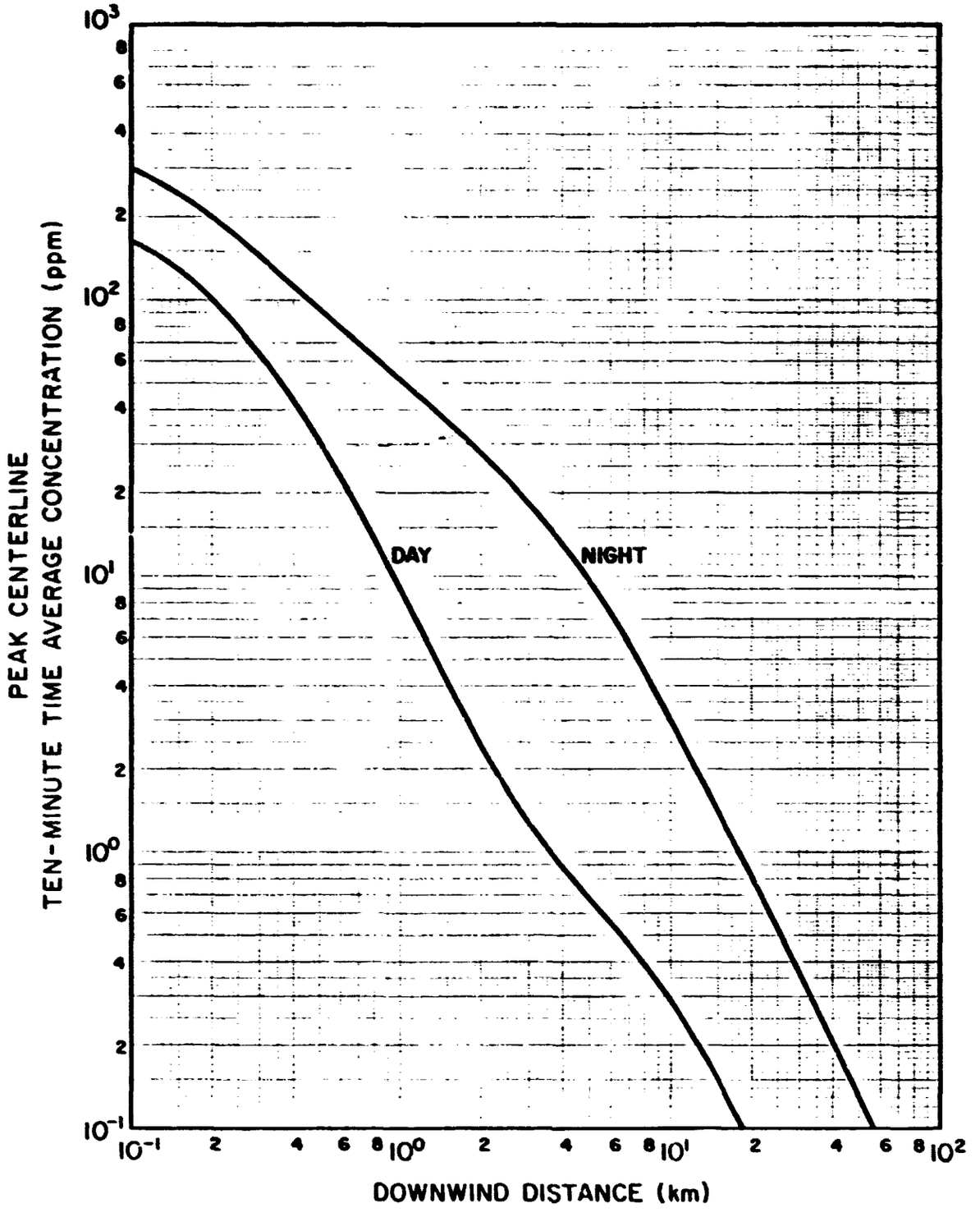

FIGURE 4-2. Daytime and nighttime peak centerline ten-minute average monomethylhydrazine concentrations (ppm) downwind from a hypothetical Orbiter accident at White Sands Missile Range.

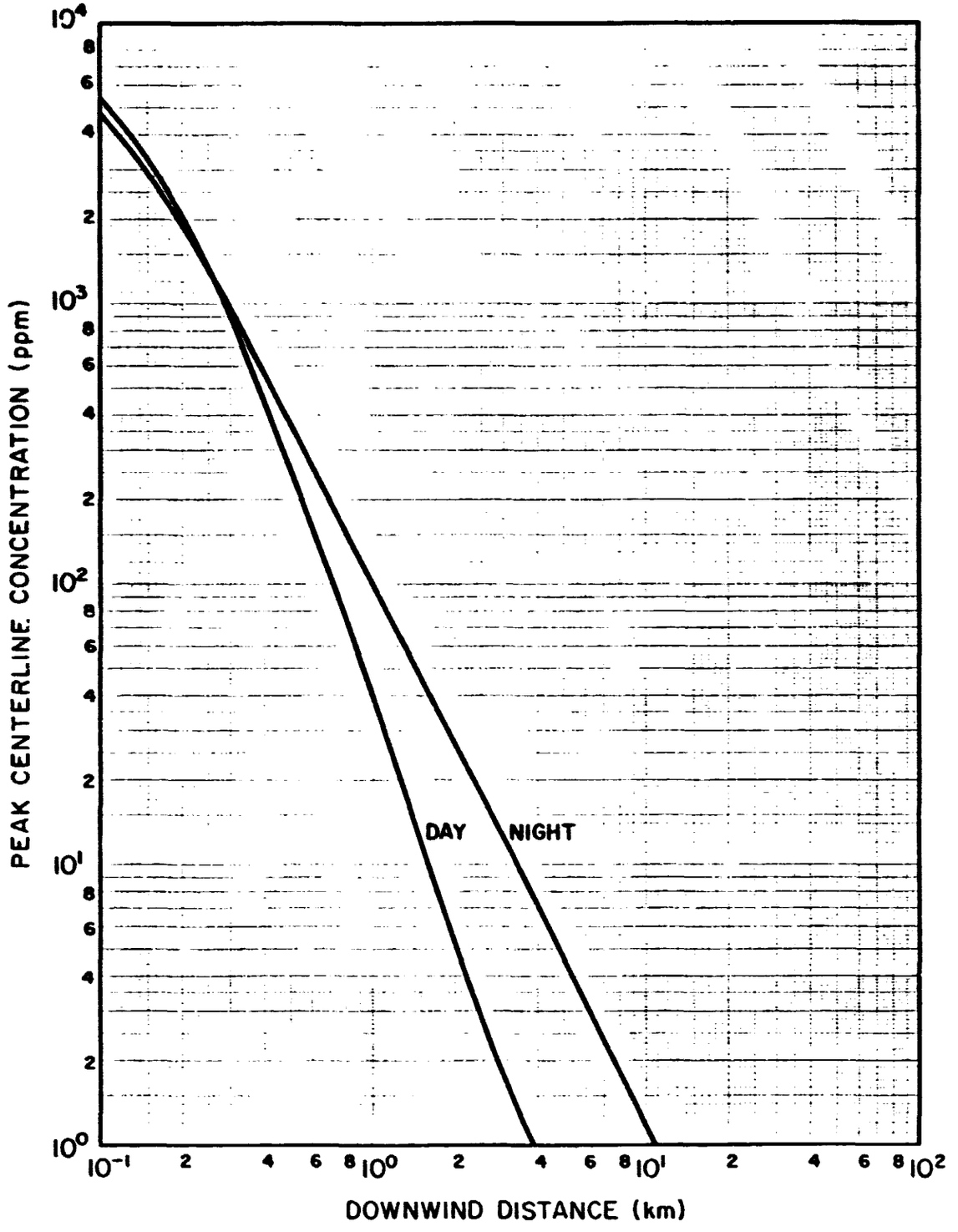

FIGURE 4-3. Daytime and nighttime peak centerline hydrazine concentrations (ppm) downwind from a hypothetical Orbiter accident at White Sands Missile Range.

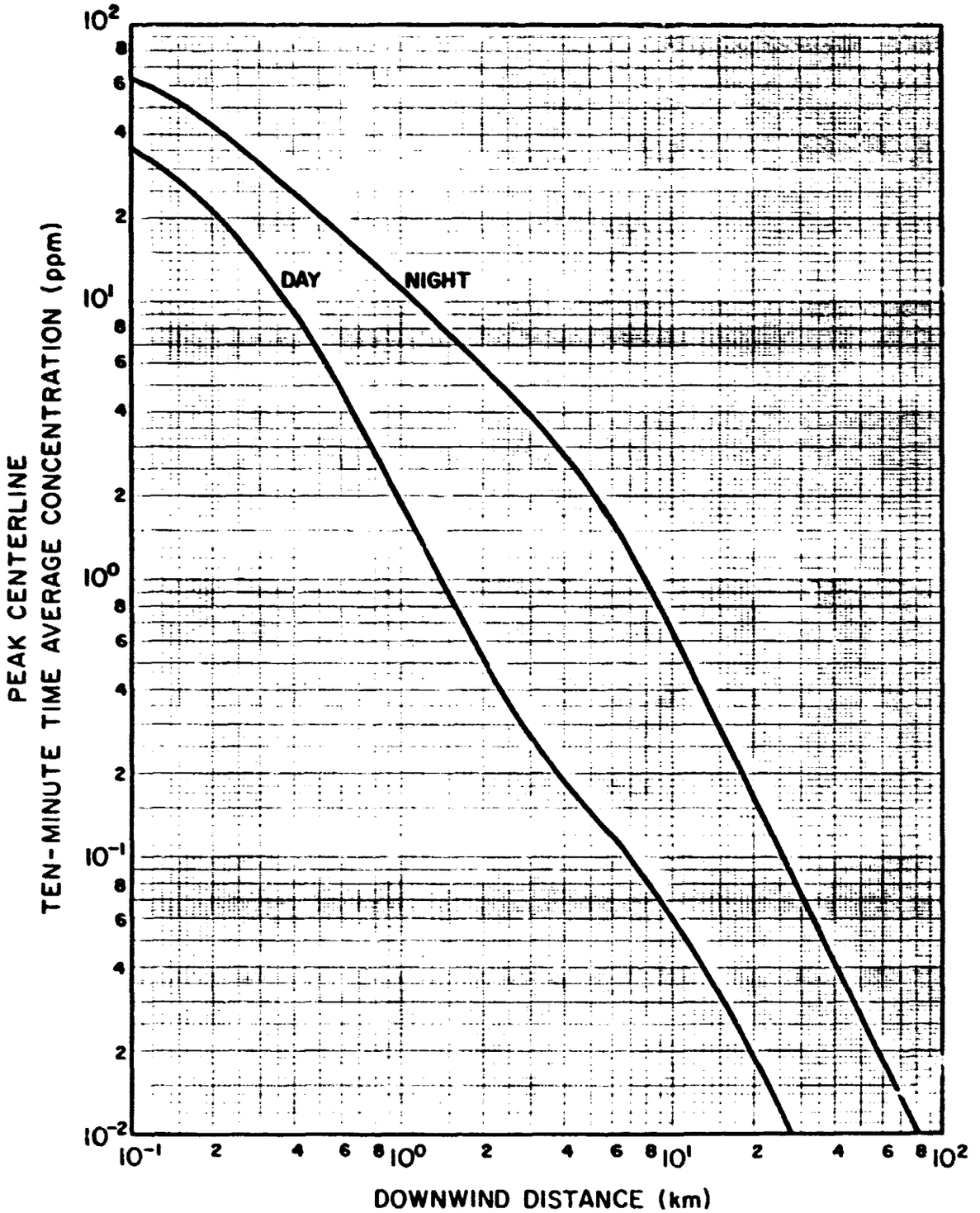

FIGURE 4-4. Daytime and nighttime peak centerline ten-minute average hydrazine concentrations (ppm) downwind from a hypothetical Orbiter accident at White Sands Missile Range.

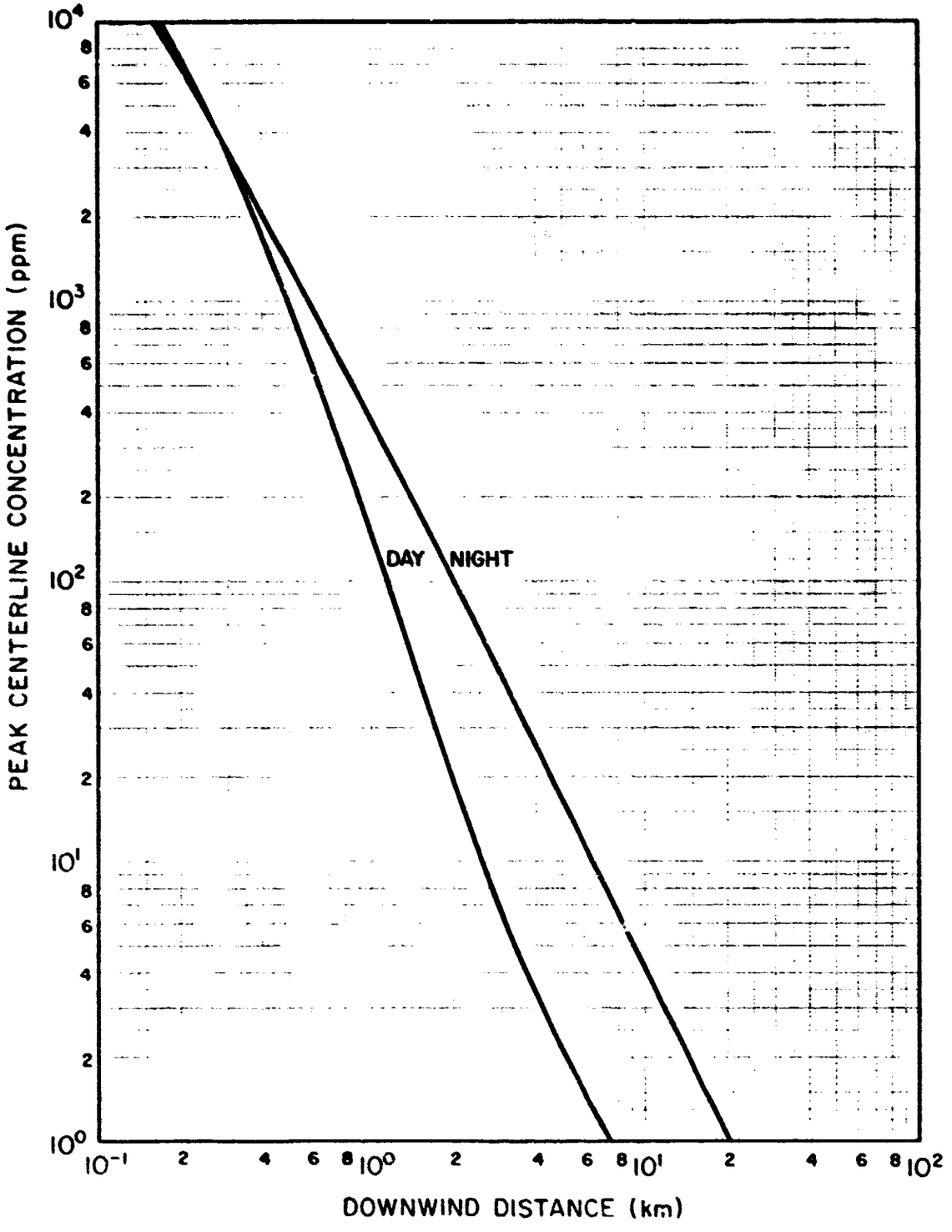

FIGURE 4-5. Daytime and nighttime peak centerline nitrogen tetraoxide concentrations (ppm) downwind from a hypothetical Orbiter accident at White Sands Missile Range.

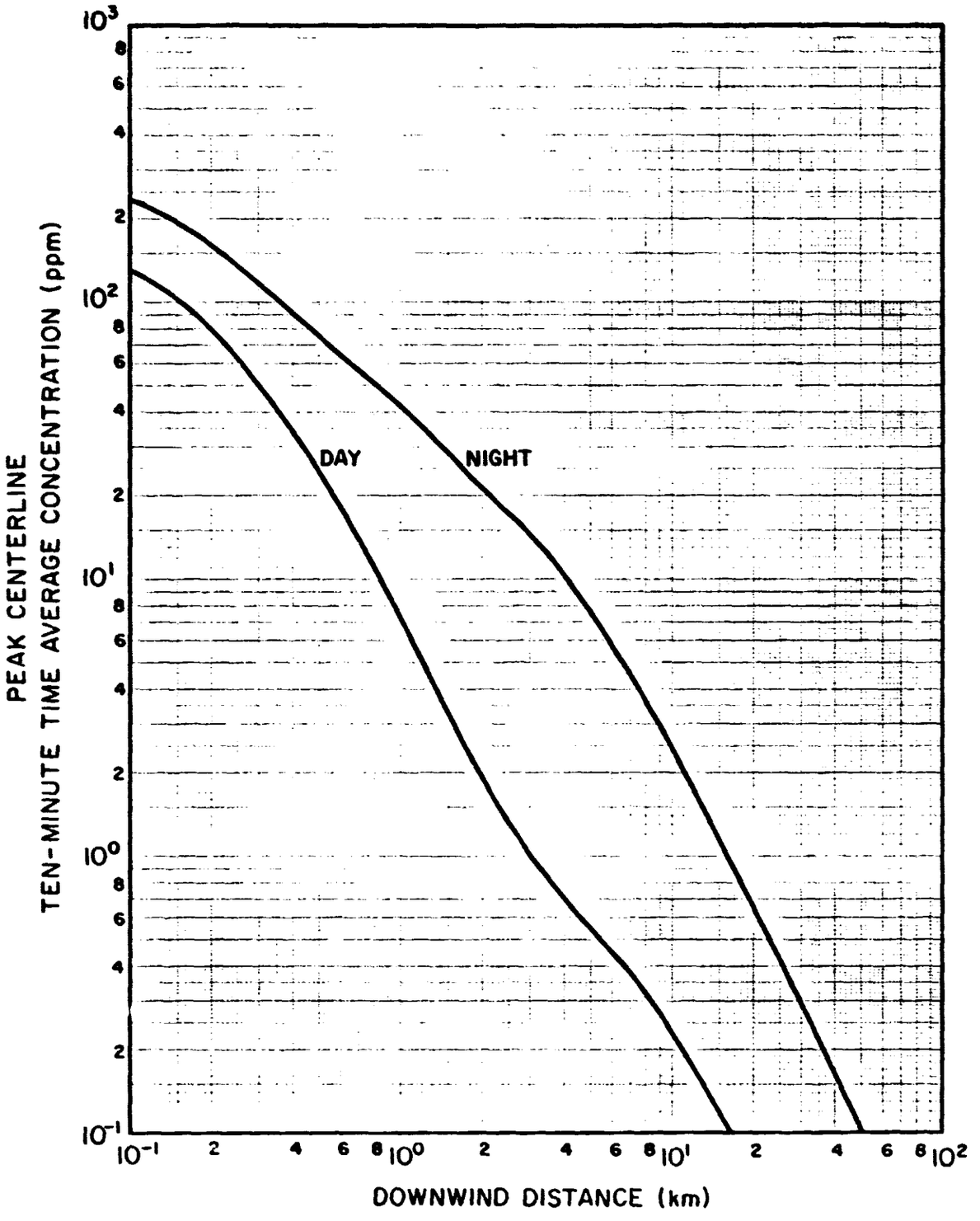

FIGURE 4-6. Daytime and nighttime peak centerline ten-minute average nitrogen tetraoxide concentrations (ppm) downwind from a hypothetical Orbiter accident at White Sands Missile Range.

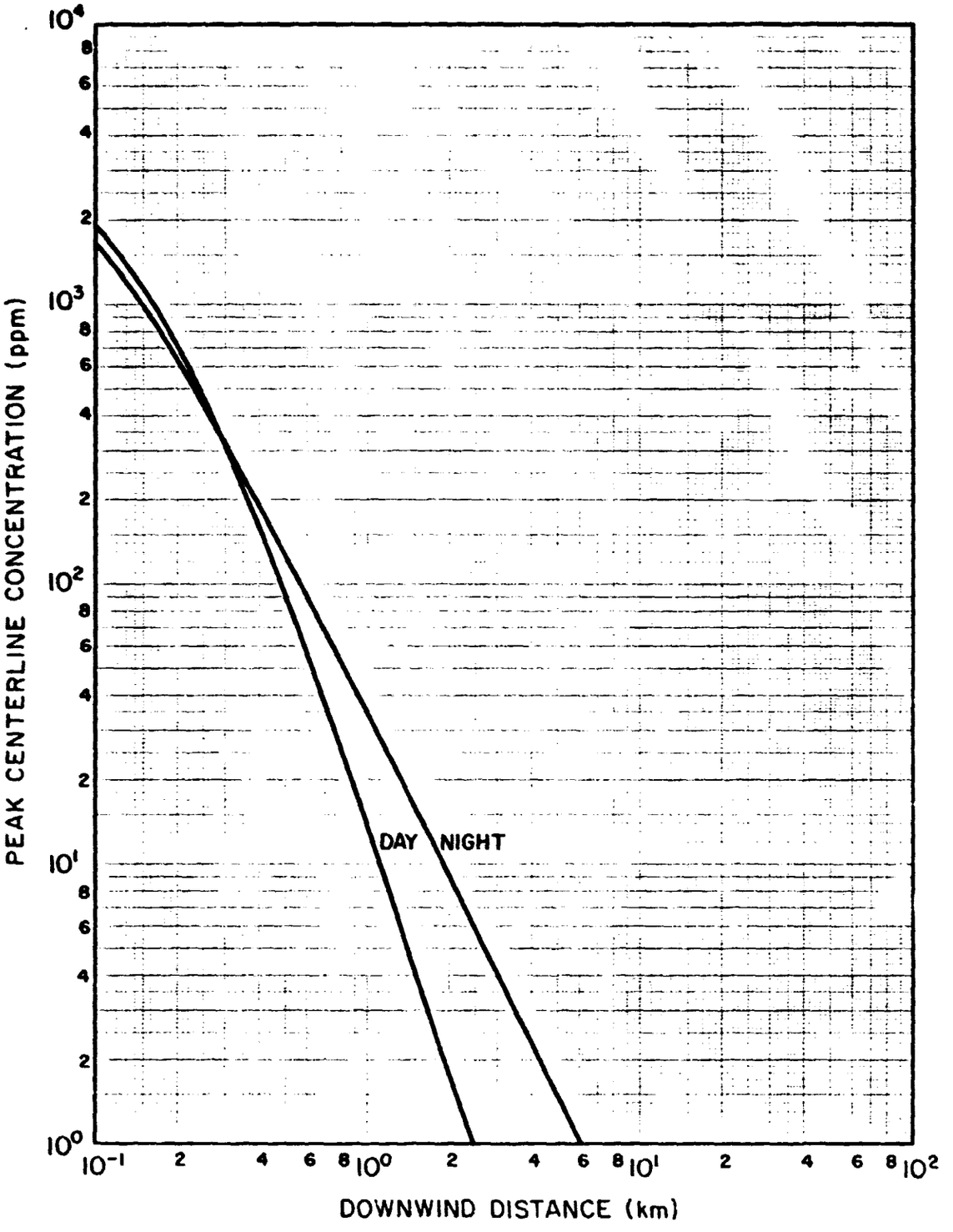

FIGURE 4-7. Daytime and nighttime peak centerline ammonia concentrations (ppm) downwind from a hypothetical Orbiter accident at White Sands Missile Range.

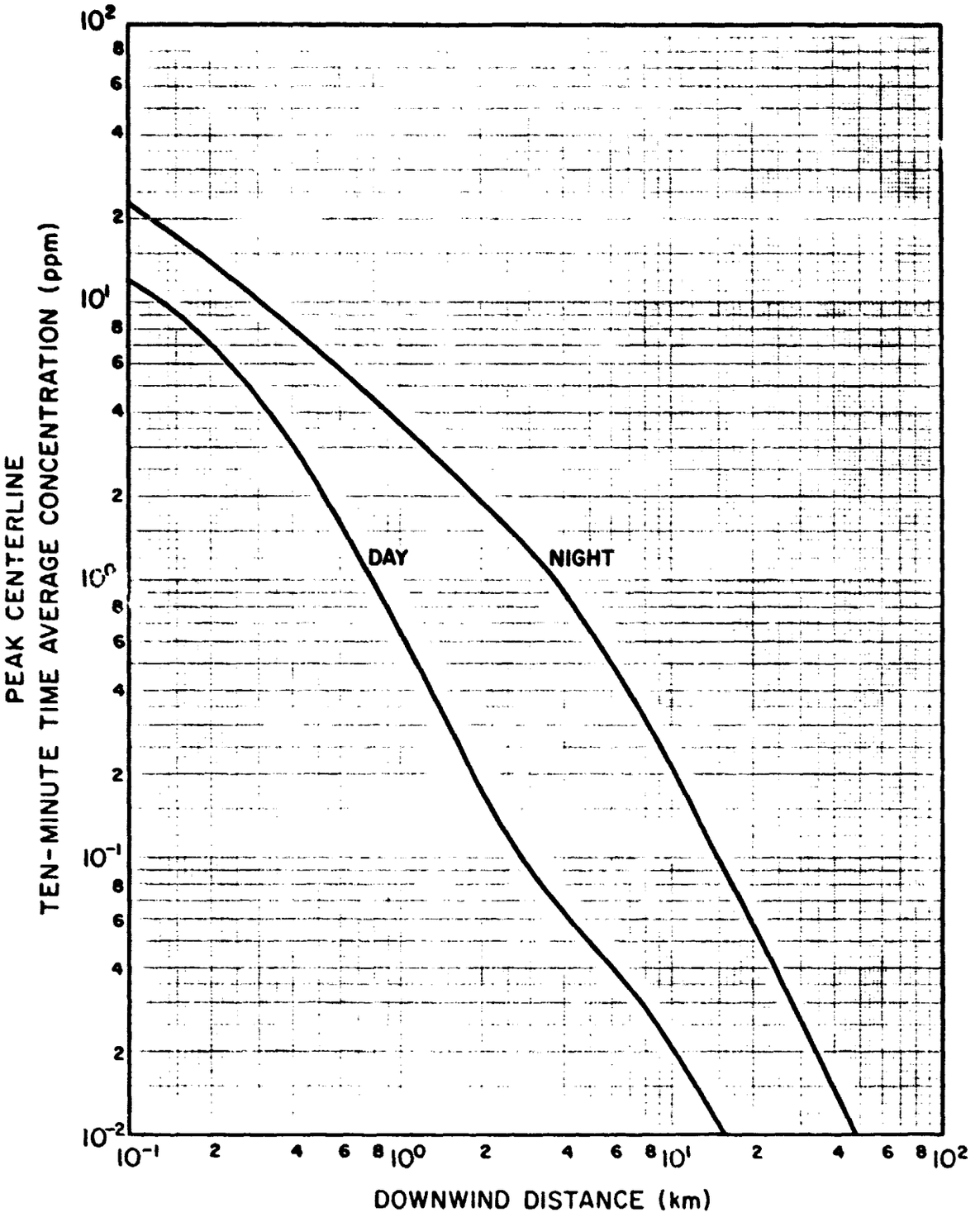

FIGURE 4-8. Daytime and nighttime peak centerline ten-minute average ammonia concentrations (ppm) downwind from a hypothetical Orbiter accident at White Sands Missile Range.

SECTION 5

ESTIMATES OF DOWNWIND CONCENTRATIONS FOR SPACE SHUTTLE ORBITER EMERGENCY LANDINGS AT KENNEDY SPACE CENTER

Hazard calculations, similar to those discribed in Section 4 above, were also made for Orbiter emergency landings at KSC using the dispersion model described in Section 4.

Source Model Inputs

Source inputs used in the model calculations for an Orbiter emergency landing at KSC are shown in Table 5-1. The source strengths Q shown in the table were supplied by MSFC. The remaining source parameters were derived using the procedures outlined above in Section 4.

Meteorological Inputs

The meteorological inputs for three atmospheric stability categories at KSC selected for use in this study are shown in Table 5-2. The values of the mixing depths H_m shown in the table were selected by reviewing rawinsonde data presented in a series of reports by Stephens, Hickey and Greene (for example, see Stephens, Hickey and Greene, 1978). The values of H_m in the table are some of the lowest values found in reviewing the rawinsonde data for the selected atmospheric conditions and are intended to maximize ground-level concentrations at the longer distances from the accident. The values of the wind speed $\bar{u}_R$, power-law coefficient p, and standard deviations σ'_A and σ'_E shown in Table 5-2 also represent poor dispersion conditions for the selected atmospheric stability categories (see Table 5-1, Dumbauld, Bjorklund, Cramer and Record, 1970). The lateral α and vertical β dispersion coefficients for instantaneous sources were set equal to unity in the calculations. Finally, the wind direction shear term $\Delta\theta/\Delta z$ was set to zero to maximize concentrations downwind from the accident.

TABLE 5-1

SOURCE INPUTS

Parameter		Value
Q (lbs)	Monomethylhydrazine	2298
	Hydrazine	278
	Nitrogen Tetraoxide	3791
K ($cm^3 . lb^{-1}$)	Monomethylhydrazine	2.2055×10^5
	Hydrazine	3.1706×10^5
	Nitrogen Tetraoxide	1.1043×10^5
σ_{zR} (m)		6.23
σ_{yR} (m)		6.23
σ_{xo} (m)		6.23
$x_{ry} = x_{rz}$ (m)		0
H (m)		13.4
τ (s)		2.5
f_i		1
γ_i		1
V_{si} ($m\ s^{-1}$)		0

TABLE 5-2

METEOROLOGICAL INPUTS

Parameter	Atmospheric Stability Category		
	Stable	Near Neutral	Slightly Unstable
H_m(m)	100	145	300
$\bar{u}_R$(ms^{-1}) at z_R{2m}	1.50	4.00	2.00
p	0.40	0.20	0.25
σ'_E(radians)	0.0321	0.0496	0.0496
$\sigma'_A\{\tau_o$=600s}radians	0.0960	0.1484	0.1484
α	1	1	1
β	1	1	1
$\Delta\theta/\Delta z$	0	0	0

Results of the Calculations

The results of the calculations are presented in Figure 5-1 through 5-6. Figure 5-1 shows peak centerline concentrations of monomethylhydrazine (solid line), nitrogen tetraoxide (dashed line) and hydrazine (dotted line) donwwind from the hypothetical Orbiter accident at KSC for stable atmospheric conditions. Figure 5-2 shows the peak centerline ten-minute average concentrations for the same pollutants and stable atmospheric conditions. As might be expected, the peak centerline concentrations are much greater than the peak centerline ten-minute average concentrations near the source where the cloud passage time is shorter than the ten-minute averaging time. As the cloud grows alongwind with increasing travel distance from the source, the peak centerline ten-minute average concentrations become more nearly equal to the peak centerline concentrations. Figures 5-3 and 5-4 show similar profiles for neutral atmospheric conditions and Figures 5-5 and 5-6 are for unstable atmospheric conditions.

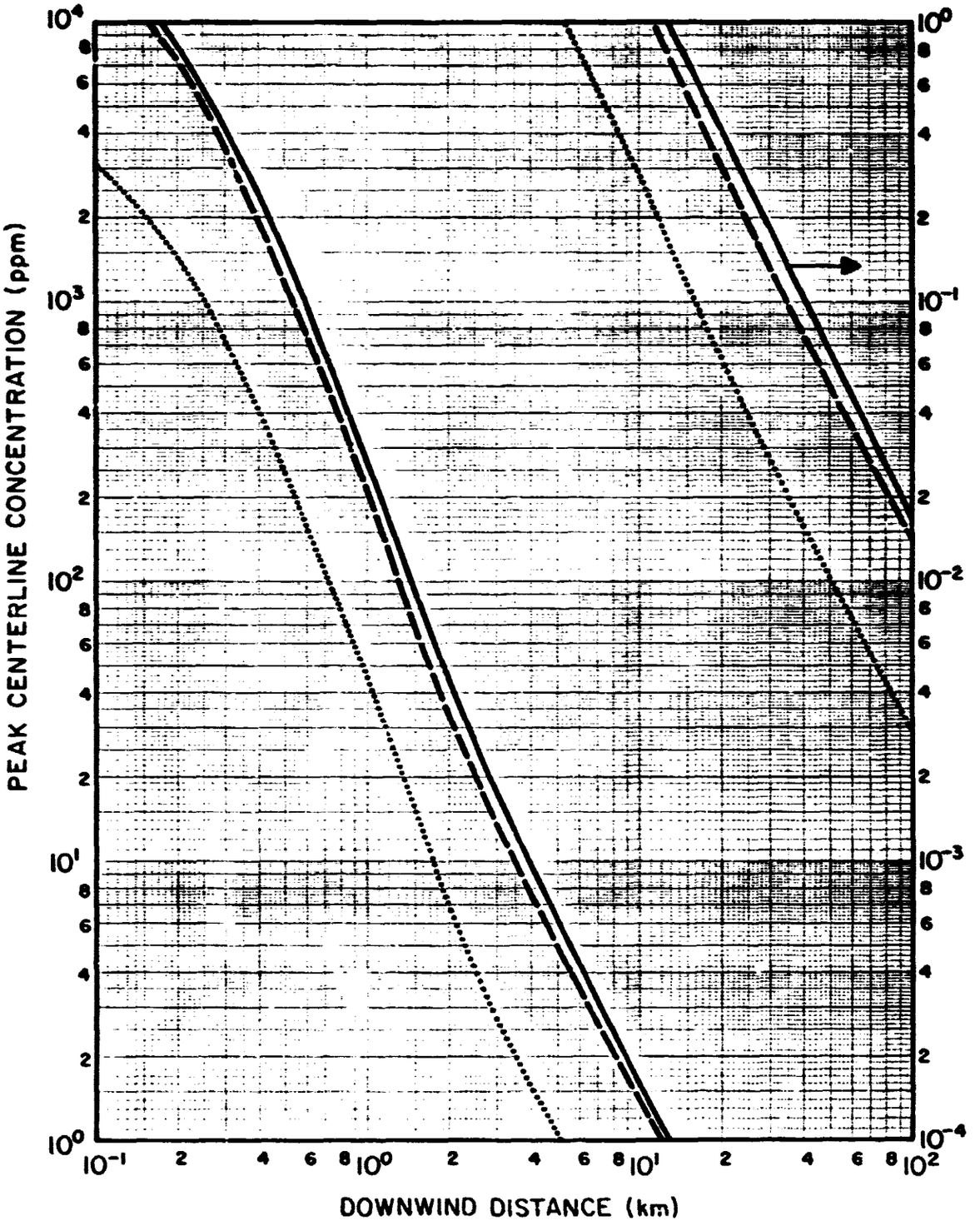

FIGURE 5-1. Peak centerline concentrations (ppm) of monomethylhydrazine (solid line), nitrogen tetraoxide (dashed line) and hydrazine (dotted line) downwind from a hypothetical Orbiter accident at Kennedy Space Center in stable atmospheric conditions.

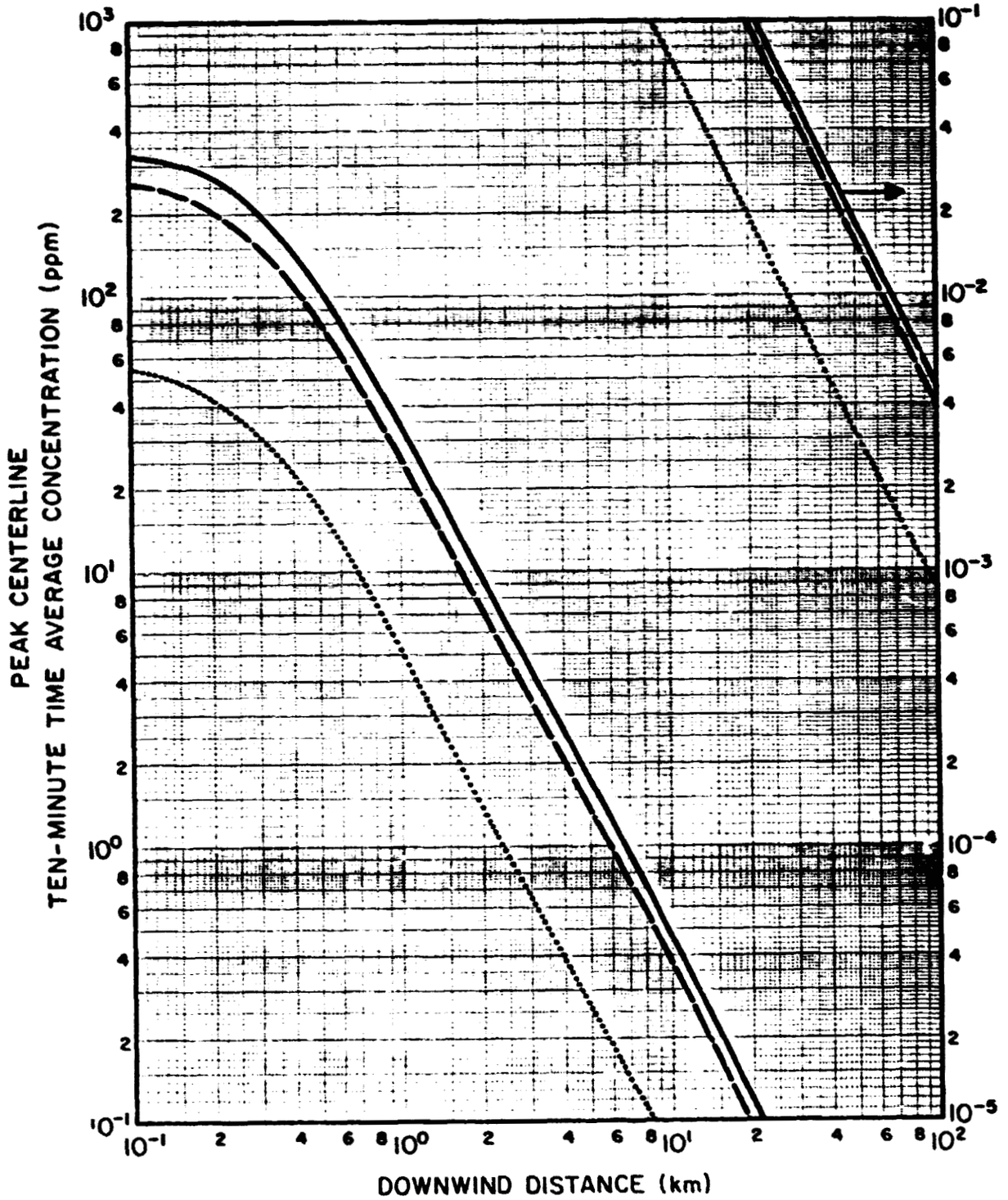

FIGURE 5-2. Peak centerline ten-minute average concentrations (ppm) of monomethylhydrazine (solid line), nitrogen tetraoxide (dashed line) and hydrazine (dotted line) downwind from a hypothetical Orbiter accident at Kennedy Space Center in stable atmospheric conditions.

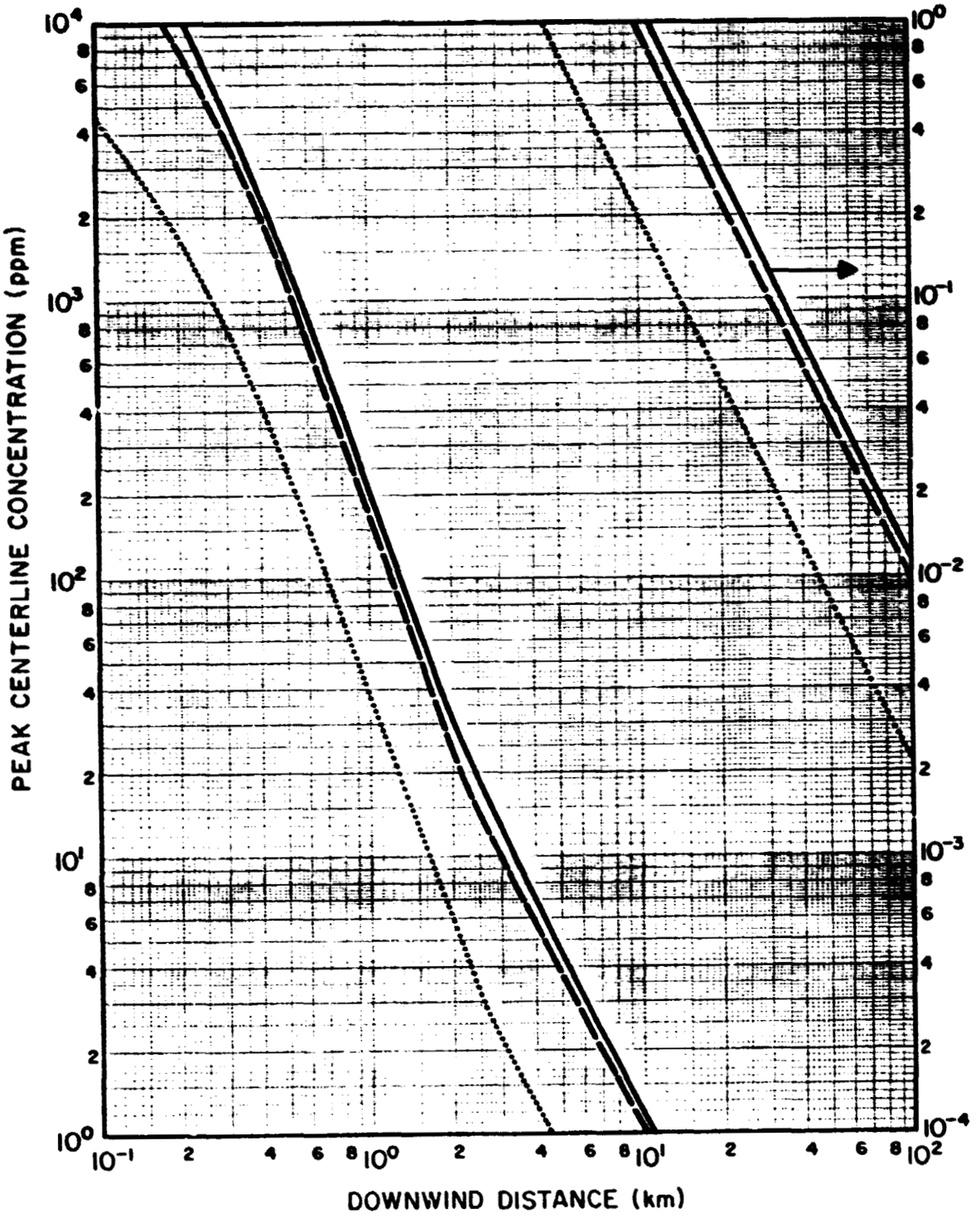

FIGURE 5-3. Peak centerline concentrations (ppm) of monomethylhydrazine (solid line), nitrogen tetraoxide (dashed line) and hydrazine (dotted line) downwind from a hypothetical Orbiter accident at Kennedy Space Center in neutral atmospheric conditions.

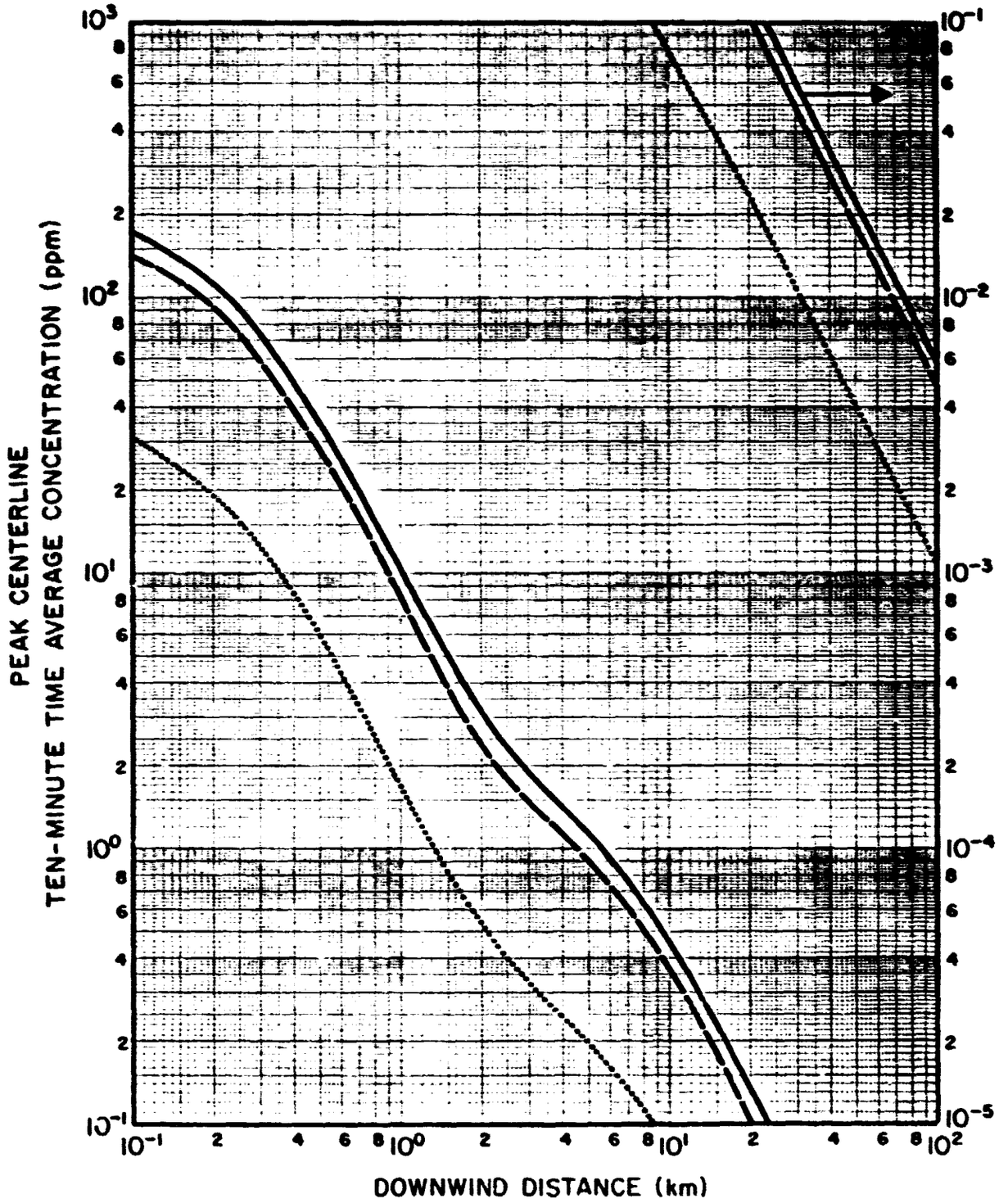

FIGURE 5-4. Peak centerline ten-minute average concentrations (ppm) of monomethylhydrazine (solid line), nitrogen tetraoxide (dashed line) and hydrazine (dotted line) downwind from a hypothetical Orbiter accident at Kennedy Space Center in neutral atmospheric conditions.

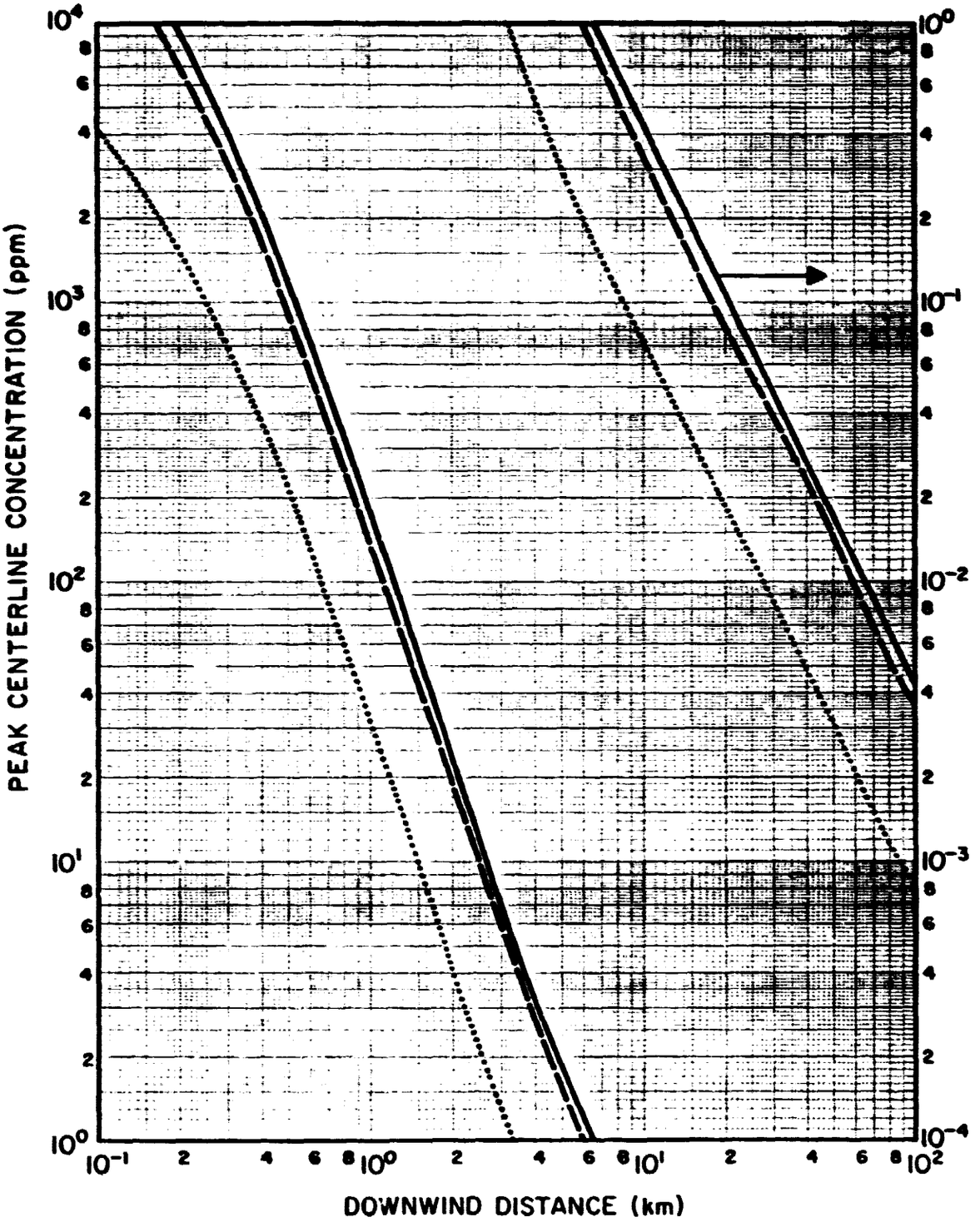

FIGURE 5-5. Peak centerline concentrations (ppm) of monomethylhydrazine (solid line), nitrogen tetraoxide (dashed line) and hydrazine (dotted line) downwind from a hypothetical Orbiter accident at Kennedy Space Center in unstable atmospheric conditions.

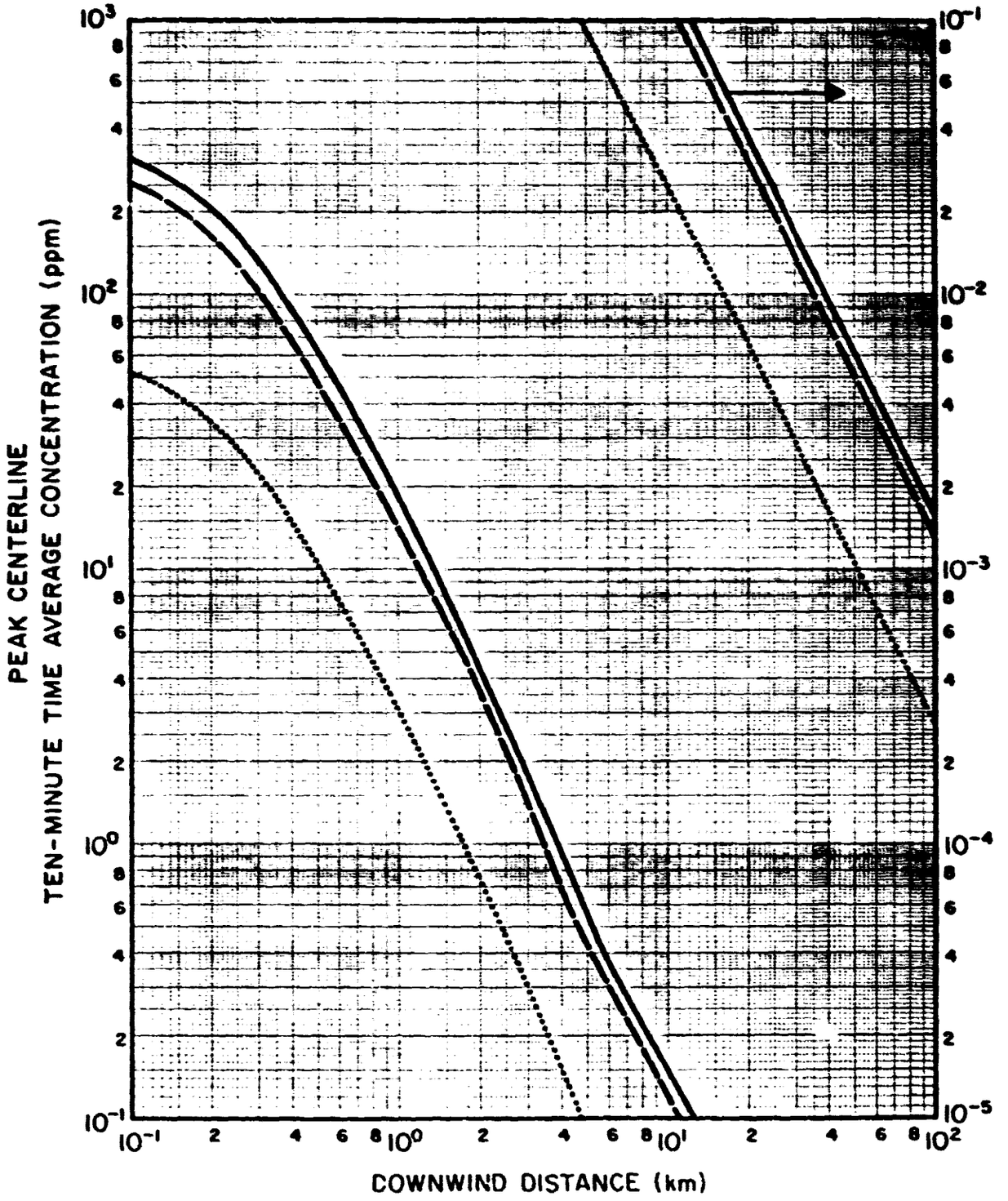

FIGURE 5-6. Peak centerline ten-minute average concentrations (ppm) of monomethylhydrazine (solid line), nitrogen tetraoxide (dashed line) and hydrazine (dotted line downwind from a hypothetical Orbiter accident at Kennedy Space Center in unstable atmospheric conditions.

SECTION 6

HCl CONCENTRATIONS DOWNWIND FROM ACCIDENTAL SRM IGNITION IN THE VAB AT KENNEDY SPACE CENTER

A preliminary analysis of HCl concentrations downwind from the VAB has been made for the following four types of postulated accidents:

- Type I -- Ignition of a single, plugged, center segment in High Bay 4 with the High Bay doors closed
- Type II -- Ignition of a single, plugged, center segment in High Bay 4 with the High Bay doors 50 percent open
- Type III -- Ignition of a three stack (2 center, 1 aft) group (unplugged) on the MLP in High Bay 3 with the High Bay doors closed
- Type IV -- Ignition of a three stack (2 center, 1 aft) group (unplugged) on the MLP in High Bay 3 with the High Bay doors 50 percent open

The source information for these four types of accidents was calculated for Dr. Koller by Dr. Bemiss, PRC System Services Company. Table 6-1 shows the parameters derived by Dr. Bemiss that are required for calculating HCl concentrations downwind from the VAB.

Cloud Rise Calculations

According to the guidelines published by the ASME (Smith, 1968) a cloud rise exceeding 1.5 times the building height would result in a cloud stabilization height above the region of disturbed flow and thus greatly

TABLE 6-1

SOURCE PARAMETERS FOR THE POSTULATED TYPES OF ACCIDENTS

Source Parameter	Accident Type			
	I	II	III	IV
Gas Exit Temperature (^{o}C)	167	167	458	458
Gas Exit Volume (m^3)	2.1520	3.1994	7.3346	9.3497
Gas Exit Area (m^2)	612	1955.4	612	1955.4
Release Time (s)	932	932	847	847
Exit Velocity ($m\ s^{-1}$)	3.77	1.76	14.15	5.65
HCl Release Rate ($kg\ s^{-1}$)	10.172	15.12	61.596	78.144

reduce ground-level concentration levels close to the source. For this reason, we have used the source information in Table 6-1 to calculate cloud rise for the four types of accidents outline above.

For the purposes of this study, cloud rise is calculated from the following expression (Briggs, 1971) for atmospheres with potential temperature gradients greater than zero:

$$\Delta h = \begin{cases} f\left[\dfrac{6F}{\bar{u}\{h\}\gamma^2 s}\right]^{1/3} & ; \quad \pi\bar{u}\{h\}s^{-1/2} < 10h \\ f\left[\dfrac{3F}{\bar{u}\{h\}\gamma^2 s}\left(1 - \cos\left(\dfrac{10s^{1/2}h}{\bar{u}\{h\}}\right)\right)\right]^{1/3} & ; \quad \pi\bar{u}\{h\}s^{-1/2} \geq 10h \end{cases} \qquad (6\text{-}1)$$

where

Δh = cloud rise

$$F = g A w\left(1 - \frac{T_a}{T_s}\right) \qquad (6\text{-}2)$$

g = acceleration due to gravity

A = exit area of the gas cloud

w = gas exit velocity

T_a = ambient air temperature

T_s = gas exit temperature

$$s = \frac{g}{T}\frac{\partial\theta}{\partial z} \qquad (6\text{-}3)$$

$\frac{\partial\theta}{\partial z}$ = vertical potential temperature gradient

γ = entrainment coefficient

f = correction factor limiting cloud rise as the mean wind speed at stack height approaches or exceeds the exit velocity w

$$= \begin{cases} 1 & ; \ \bar{u}\{h\} \\ \left(\frac{3w - 3\bar{u}\{h\}}{w}\right) & ; \ \frac{w}{1.5} < \bar{u}\{h\} < w \\ 0 & ; \ \bar{u}\{h\} \geq w \end{cases} \qquad (6\text{-}4)$$

$\bar{u}\{h\}$ = mean wind speed at the building height h

$$= \bar{u}\{2m\}\left(\frac{h}{2}\right)^{p} \qquad (6\text{-}5)$$

$\bar{u}\{2m\}$ = mean wind speed at a height of 2 meters in an area not influenced by the building

p = wind power-law coefficient

The source and meteirological parameters required to calculate cloud rise using Equation 6-1 are respectively shown in Tables 6-2 and 6-3. The area A shown in Table 6-2 is for 4 roof ventilators commonly found in a group on the roof of the VAB. Inspection of Equation 6-1 shows that the cloud rise increases as the value of A increases, if all other parameters are held constant. Since we wished to make conservative estimates of cloud rise, we selected the area of 4 ventilators as a minimum

TABLE 6-2

SOURCE PARAMETERS FOR CALCULATING
CLOUD RISE

Source Parameter	Accident Type			
	Type I	Type II	Type III	Type IV
A (m^2)	23.5	23.5	23.5	23.5
w (ms^{-1})	3.77	1.76	14.15	5.65
h (m)	160	160	160	160
T_s	440.2	440.2	731	731
γ	0.66	0.66	0.66	0.66

TABLE 6-3

METEOROLOGICAL PARAMETERS FOR CALCULATING
COULD RISE

Meteorological Parameter	Wind Speeds $\bar{u}\{2m\}$ (ms^{-1})		
	1 (Very Light)	2 (Light)	4 (Moderate)
T_a (^oK)	298.2	298.2	298.2
$\frac{\partial\theta}{\partial z}$ (deg m^{-1})	0.02	0.01	0.005
p	0.25	0.20	0.15

area through which the exit velocity w was equivalent to the value shown in the table. The value of 0.66 for γ is the value suggested by Briggs (1972) for stacks. We made cloud-rise calculations for three nominal 2-meter wind speeds, as shown in Table 6-3. Values of $\partial\theta/\partial z$ and p were assigned to these mean wind speeds on the basis of previous experience and knowledge of meteorological tower measurements made at KSC.

The results of the cloud-rise calculations are given in Table 6-4 and show zero cloud rise is calculated for Type II accidents, for Type I accidents with mean wind speeds of 2 and 4 meters per second and for Type IV accidents with a mean wind speed of 4 meters per second. However, none of the cloud rise values calculated for the other cases results in a cloud stabilization height greater than 2.5 times the building height (400 m) which is the upper boundary of the region of disturbed flow as specified in the ASME guidelines. It should be noted that if we assumed the exit velocity to apply to a larger cross-sectional area or considered the enhancement of plume rise due to the combining of plumes from other groups of vents (see Briggs, 1974), we could have calculated stabilization heights greater than 400 meters for some cases. However, because of the uncertainties associated with these plume-rise calculations and to preclude overestimates of the hazard distances, we have included building wake effects in all the model calculations.

Building Wake Effects

To our knowledge, the best quantitative description of building wake effects on concentration patterns downwind from buildings is provided by wind-tunnel tests conducted by EPA (Thompson and Lombardi, 1977). The results of the EPA study are very similar to results reported by Robins and Castro (1977a, 1977b). The VAB building dimensions provided by Dr. Koller (h = 160m, w = 156m, d = 127m) show that the VAB building is approximately cubical. Therefore, we have use of the results presented by Thompson and Lombardi for a cubical building to evaluate the wake effects

TABLE 6-4

CALCULATED CLOUD RISE (Δh) AND CLOUD STABILIZATION HEIGHT (h + Δh) IN METERS FOR FOUR TYPES OF POSTULATED ACCIDENTS

Mean 2-meter Wind Speed $\bar{u}\{2m\}$ (ms^{-1})	Accident Type							
	I		II		III		IV	
	Δh	h+Δh	Δh	h+Δh	Δh	h+Δh	Δh	h+Δh
1	53.3	213.3	0	160	162.7	322.7	119.8	279.8
2	0	160	0	160	175.0	335.0	57.9	217.9
4	0	160	0	160	188.2	348.2	0	160

of the VAB building with the wind direction at a 45-degree angle to a building wall (their Case 2). This wind direction produces the highest ground-level concentrations downwind from a cubical building.

As explained below, we used the data for Case 2 in the Thompson and Lombardi report to develop the model source inputs and the lateral and vertical dispersion coefficients to be used in our model calculations. The wind-tunnel measurements of vertical concentration profiles for Case 2 (see Figure 12 on page 22 of the Thompson and Lombardi report) show that the plume centerline is brought to the ground by the building wake circulation at a distance of three to five building heights. To simplify our model calculations, we assumed a ground-level source located at the base of the VAB building with an initial vertical dimension ($2.15\ \sigma_{zR}$) given by the height of the VAB building and an initial lateral dimension ($4.30\ \sigma_{yR}$) given by the diagonal of the horizontal cross section of the VAB building. Values for the lateral and vertical turbulent intensities to be used in the model calculations were selected by a cut-and-try procedure where the objective was to obtain a normalized ground-level concentration profile from the model calculations, using the above source parameters in our quasi-continuous dispersion model described below, that matched the normalized ground-level concentration profile for Case 2 at distances from 5 to 20 building heights. Using the source parameters described above, with the lateral and vertical dispersion coefficients thus determined in the quasi-continuous dispersion model, we were also able to calculate vertical concentration profiles at distances of 5 and 8 building heights and a lateral concentration profile at a distance of 5 building heights which were in good agreement with the corresponding measurements presented by Thompson and Lombardi (see Figures 12 and 13 in their report) for Case 2.

Quasi-Continuous Source Model

The Guassian model for a quasi-continuous source emitting at a constant rate over the time t_B is given by the expression

$$\chi(x,y,z,t) = \frac{Q}{2\pi\,\sigma_y\,\sigma_z\,\bar{u}} \left\{\exp\left[-\frac{1}{2}\left(\frac{y}{\sigma_y}\right)^2\right]\right\}$$

$$\frac{1}{2}\left\{\operatorname{erf}\left[\frac{x-\bar{u}(t-t_B)}{\sqrt{2}\,\sigma_x}\right] - \operatorname{erf}\left[\frac{x-\bar{u}t}{\sqrt{2}\,\sigma_x}\right]\right\} \qquad (6\text{-}6)$$

$$\left\{\sum_{a=0}^{\infty}\left[\exp\left[-\frac{1}{2}\left(\frac{2aH_m-H+z}{\sigma_z}\right)^2\right] + \exp\left[-\frac{1}{2}\left(\frac{2aH_m+H+z}{\sigma_z}\right)^2\right]\right]\right.$$

$$\left. + \sum_{a=1}^{\infty}\left[\exp\left[-\frac{1}{2}\left(\frac{2aH_m+H-z}{\sigma_z}\right)^2\right] + \exp\left[-\frac{1}{2}\left(\frac{2aH_m-H-z}{\sigma_z}\right)^2\right]\right]\right\}$$

where

Q = source emission rate

σ_y = standard deviation of the crosswind concentration distribution

$$= \sigma'_A\, x_{ry}\left(\frac{x + x_y - x_{ry}\,(1-\alpha)}{x_{ry}}\right)^{\alpha} \qquad (6\text{-}7)$$

σ'_A = standard deviation of the wind azimuth angle in radians

x = downwind distance from the source

x_y = crosswind virtual distance

$$x_y = \alpha x_{ry} \left(\frac{\sigma_{yR}}{\sigma'_A \, x_{ry}} \right)^{1/\alpha} - x_R + x_{ry} \, (1 - \alpha) \qquad (6\text{-}8)$$

α = crosswind dispersion coefficient

x_{ry} = distance over which rectilinear crosswind cloud expansion occurs downwind from a virtual point source

σ_{yR} = standard deviation of the crosswind concentration distribution at a distance x_R form the source

σ_z = standard deviation of the vertical concentration distribution

$$= \sigma'_E \left(x + x_z \right) \qquad (6\text{-}9)$$

σ'_E = standard deviation of the wind elevation angle in radians

x_z = vertical virtual distance

$$= \frac{\sigma_{zR}}{\sigma'_E} - x_R \qquad (6\text{-}10)$$

σ_{zR} = standard deviation of the vertical concentration distribution at x_R

$\bar{u}$ = mean wind speed

$$\bar{u} = \left\{ \begin{array}{ll} \dfrac{\bar{u}_R \left[(z_2)^{1+p} - (z_1)^{1+p} \right]}{(z_2 - z_1)(z_R)^p (1+p)} & ; \quad \bar{u} > \bar{u}_R \\ \\ \bar{u}_R & ; \quad \bar{u} \leq \bar{u}_R \end{array} \right\} \qquad (6\text{-}11)$$

$\bar{u}_R$ = mean wind speed at the reference height z_R

p = wind profile power-law exponent

z_1 = effective lower bound of the cloud

$$= \left\{ \begin{array}{ll} H + 2.15\,\sigma_z & ; \quad z_1 > 2 \\ \\ 2 & ; \quad z_1 \leq 2 \end{array} \right\} \qquad (6\text{-}12)$$

z_2 = effective upper bound of the cloud

$$= \left\{ \begin{array}{ll} H + 2.15\,\sigma_z & ; \quad z_2 < H_m \\ \\ H_m & ; \quad z_2 \geq H_m \end{array} \right\} \qquad (6\text{-}13)$$

y = crosswind distance from the cloud centerline

H_m = depth of the surface mixing layer

H = effective height of the source above ground level

$$= h + \Delta h \qquad (6\text{-}14)$$

h = actual source height above ground level

Δh = cloud rise

z = height above ground level

t = time after release begins at the top of the roof

t_B = source emission time

σ_x = standard deviation of the alongwind concentration distribution

$$\sigma_x = \left[\left(\frac{L\{x\}}{4.3}\right)^2 + \sigma_{xc}^2\right]^{1/2} \qquad (6\text{-}14)$$

$$L\{x\} = \begin{cases} \dfrac{0.6\,\Delta\bar{u}}{\bar{u}}\,x \; ; & \Delta\bar{u} \geq 0 \\ 0 \; ; & \Delta\bar{u} < 0 \end{cases} \qquad (6\text{-}15)$$

$\Delta\bar{u}$ = vertical wind-speed shear in the layer containing the cloud

$$= \frac{\bar{u}_R}{z_R^p}\left[z_2^p - z_1^p\right] \qquad (6\text{-}16)$$

σ_{xo} = standard deviation of the alongwind cloud distribution at the source

Source and Meteorological Inputs for the Concentration Calculations

The source and meteorological inputs used in the concentration model given by Equation (6-6) are presented in Tables 6-5 and 6-6. The

TABLE 6-5

SOURCE INPUTS FOR THE CONCENTRATION CALCULATIONS

Source Parameter	Accident Type			
	I	II	III	IV
$Q(ppm\ m^3\ s^{-1}$	6.821×10^6	1.014×10^7	4.131×10^7	5.240×10^7
t_B	932	932	847	847
H (m)	0	0	0	0
$\sigma_{yR}=\sigma_{xo}$ (m)	46.9	46.9	46.9	46.9
σ_{zR} (m)	74.4	74.4	74.4	74.4
x_R (m)	0	0	0	0

TABLE 6-6

METEOROLOGICAL INPUTS FOR THE CONCENTRATION CALCULATIONS

Meteorological Parameter	Wind Speed		
	Very Light	Light	Moderate
σ'_A (radians)	0.1309	0.1309	0.1309
σ'_E (radians)	0.0400	0.0400	0.0400
α	0.9	0.9	0.9
$\bar{u}_R\{z_R=2m\}$ $(m\ s^{-1})$	1	2	4
p	0.25	0.20	0.15
H_m (m)	200	400	800

source emission rates in Table 6-5 were obtained by assuming that 1 kilogram per cubic meter of HCl at a pressure of 1013.2 millibars and temperature of 25° Celsius is equivalent to 6.7058×10^5 parts of HCl per million parts of air and then multiplying by the HCl emission rates specified by KSC (see Table 6-1). The source emission times t_B were also specified by KSC.

As noted earlier, we determined from an analysis of the measurements presented by Thompson and Lombardi (1977) for a cubical building oriented at a 45-degree angle to the mean wind direction that the normalized concentration profile at distances beyond 5 building heights was best represented by assuming a virtual volume source located at ground-level (H=0). This assumption was also found by Robins and Castro (1977b) to apply to their wind-tunnel concentration measurements. The lateral and alongwind source dimensions σ_{yR} and σ_{xo} were both set equal to the diagonal length of the building (201 meters) divided by 4.3 under the assumption that the crosswind and alongwind concentration distributions at the source were Gaussian. Because the source is located at ground-level, the vertical source dimension σ_{zR} was set equal to the building height h divided by 2.15 which follows from the assumption that the vertical concentration distribution is also Gaussian. Finally because the source dimension were defined at the downwind base of the building, the reference distance x_R was set to zero.

Table 6-6 shows the values for the lateral dispersion coefficient σ'_A and the vertical dispersion coefficient σ'_E obtained from the cut-and-try procedure using the dispersion model given by Equation 6-6 with the above source parameters, to calculate normalized concentrations equal to the normalized concentrations given by Thompson and Lombardi for Case 2 at downwind distances of 5 to 20 building heights. Also, the 2-meter wind speeds and the power-law coefficients in Table 6-6 are the same as those used in the cloud-rise calculations described earlier. Values for the depth of the surface mixing layer H_m shown in Table 6-6 are estimates we believe to be representative of conditions at KSC for the three mean wind speeds.

Results of the Calculations

Figures 6-1 through 6-4 show the calculated ground-level concentrations downwind from the VAB for the four types of postulated accidents during very light, light and moderate wind speeds.

The results of the concentration calculations are summarized in Table 6-7. The maximum HCl concentration occurs in every case at 275 to 300 meters downwind from the VAB. Inspection of Table 6-7 shows that ground-level concentrations are greatest, as expected, for Type IV accidents. Under very light wind speeds, HCl concentrations above 100 ppm extend to a distance of about 4 kilometers downwind from the VAB and concentrations above 5 ppm extend to a distance of about 18 kilometers downwind from the VAB.

We also calculated time concentration profiles for those cases in which the HCl concentration exceeded 100 ppm at distances greater than 800 meters from the VAB. In each of these cases, the time profile was calculated at the approximate distance where the HCl concentration was equal to 100 ppm. The results are shown in Figure 6-5 through 6-10. Figure 6-5 shows, for example, the time concentration profile at a distance of 3000 meters from the VAB for a Type III accident under very light wind speeds. At this distance, the HCl concentration exeeeds 5 ppm at 16.2 minutes after the cloud starts to exit the root vents and remains above 5 ppm until 38.2 minutes after the cloud starts to exit the roof vents.

Figure 6-11 illustrates the effect on the calculated ground-level HCl concentrations of including plume rise and neglecting building wake effects for a Type IV accident under light wind speeds. As shown in the figure, the maximum HCl concentration is reduced in magnitude from 1046 ppm to 40 ppm and the distance to the maximum is increased from about 275 meters to 3.3 kilometers if building wake effects are neglected. The threshold distance to an HCl concentration of 5 ppm is approximately 20 kilometers in both cases.

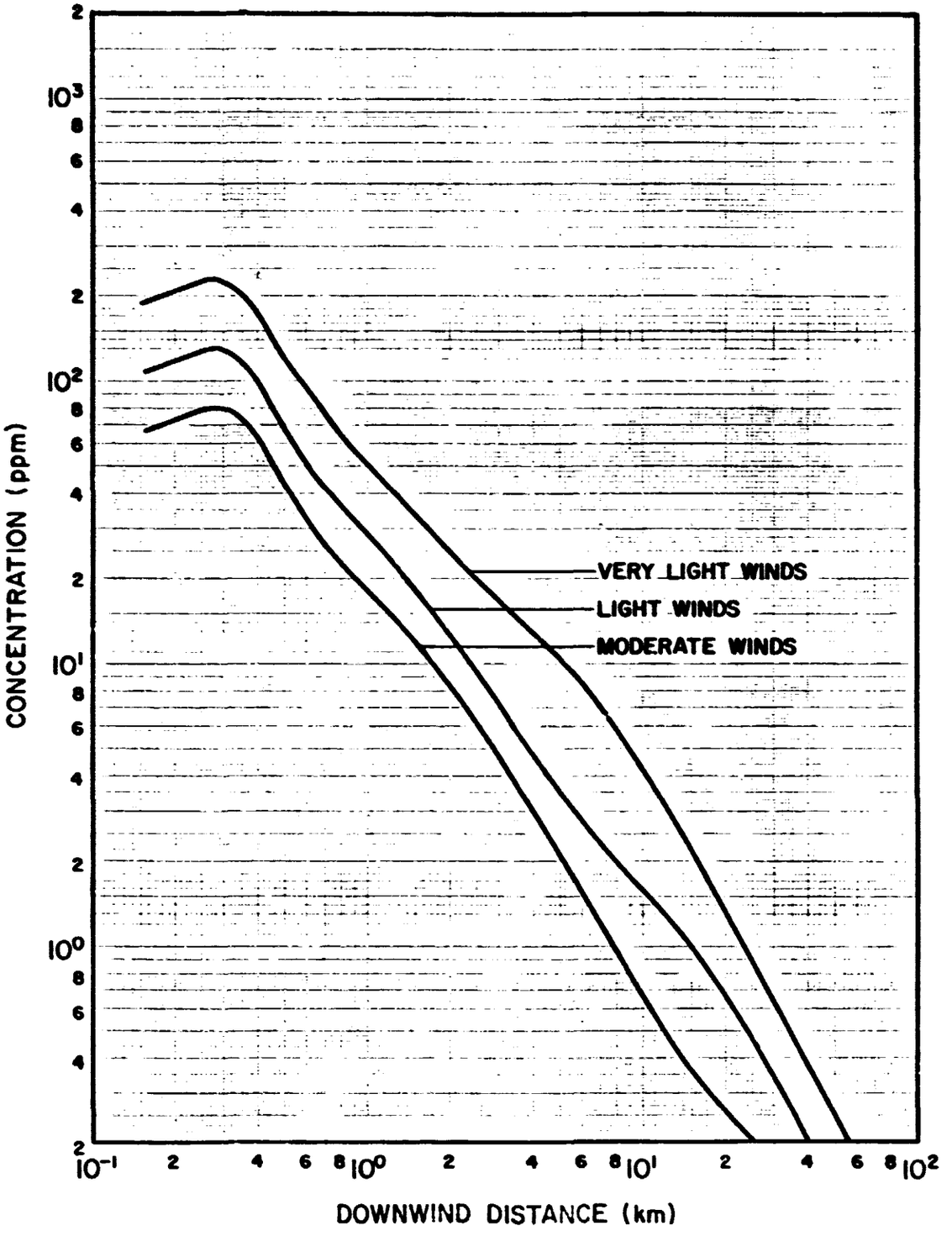

FIGURE 6-1. Ground-level HCl concentrations downwind from the VAB for a Type I postulated accident.

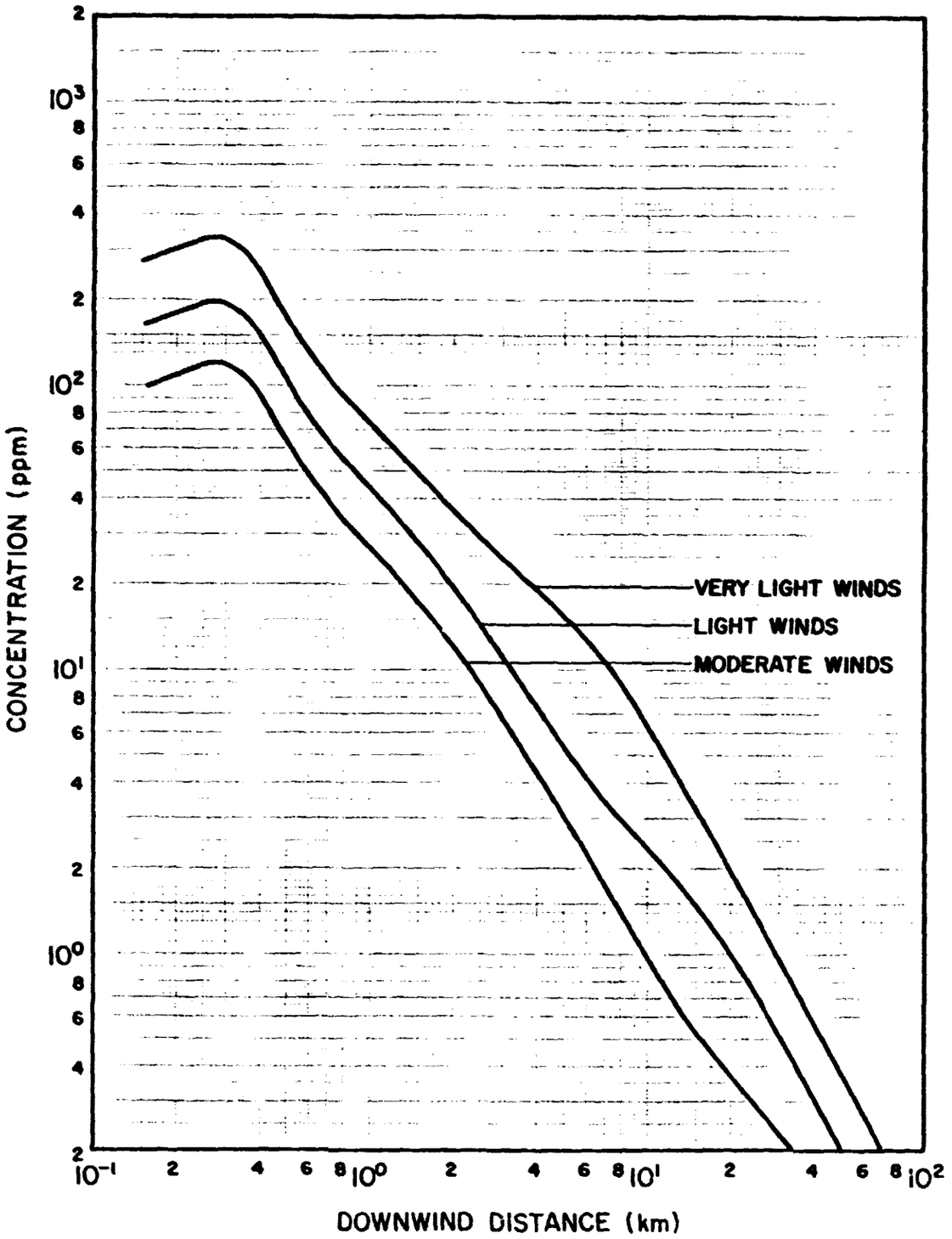

FIGURE 6-2. Ground-level HCl concentrations downwind from the VAB for a Type II postulated accident.

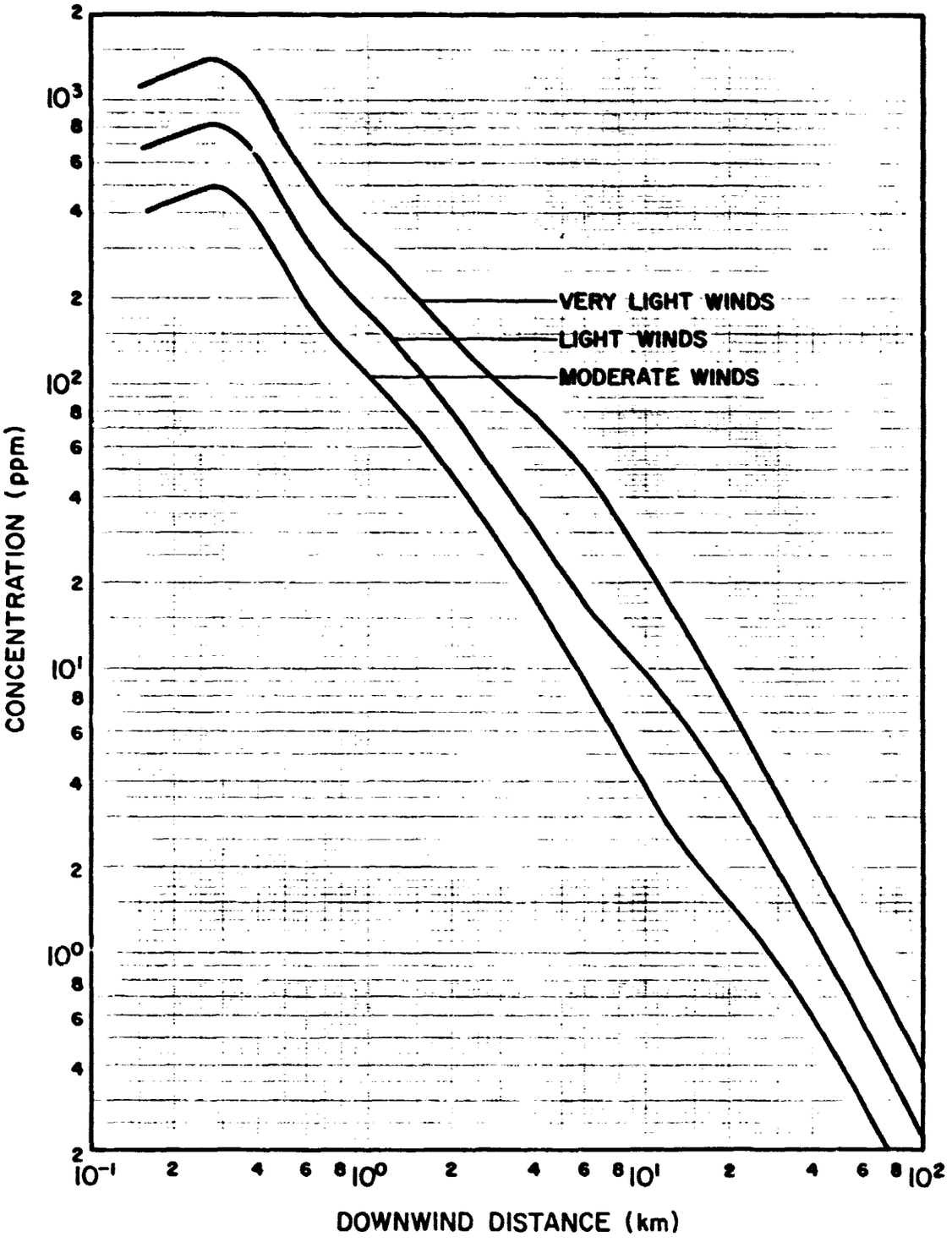

FIGURE 6-3. Ground-level HCl concentrations downwind from the VAB for a Type III postulated accident.

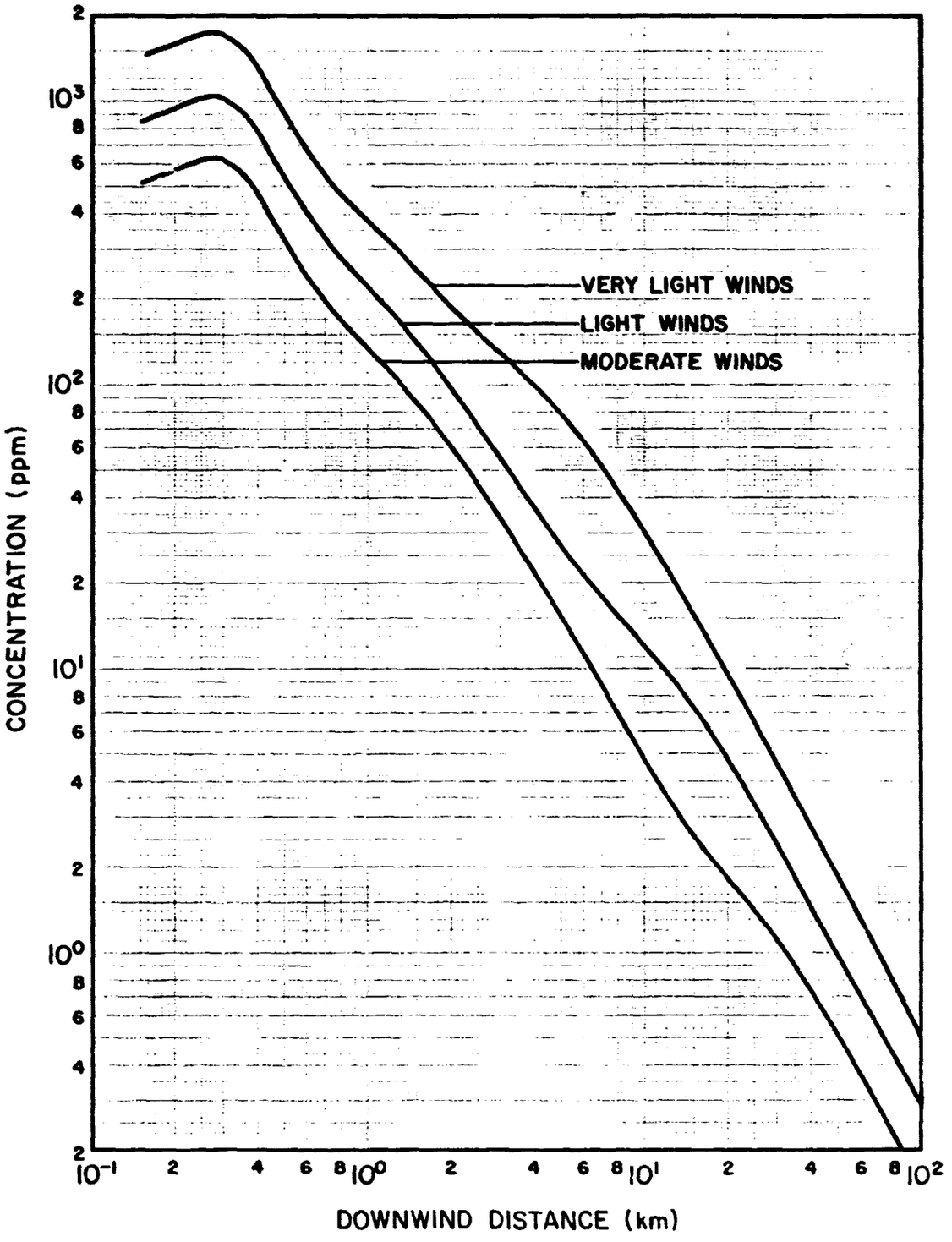

FIGURE 6-4. Ground-level HCl concentrations downwind from the VAB for a Type IV postulated accident.

TABLE 6-7

MAXIMUM HCl CONCENTRATIONS AND THRESHOLD DISTANCES TO HCl CONCENTRATIONS OF 100 and 5 PARTS PER MILLION (ppm)

Accident Type	Wind Speeds	Maximum Concentration (ppm)	Threshold Distance (meters)	
			100 ppm	5 ppm
I	Very Light	231	575	9200
	Light	136	400	3900
	Moderate	83	*	2900
II	Very Light	344	750	11500
	Light	202	510	5200
	Moderate	123	360	3600
III	Very Light	1401	3000	25000
	Light	824	1650	16500
	Moderate	501	1070	8500
IV	Very Light	1777	3950	28000
	Light	1046	1950	19000
	Moderate	635	1320	9600

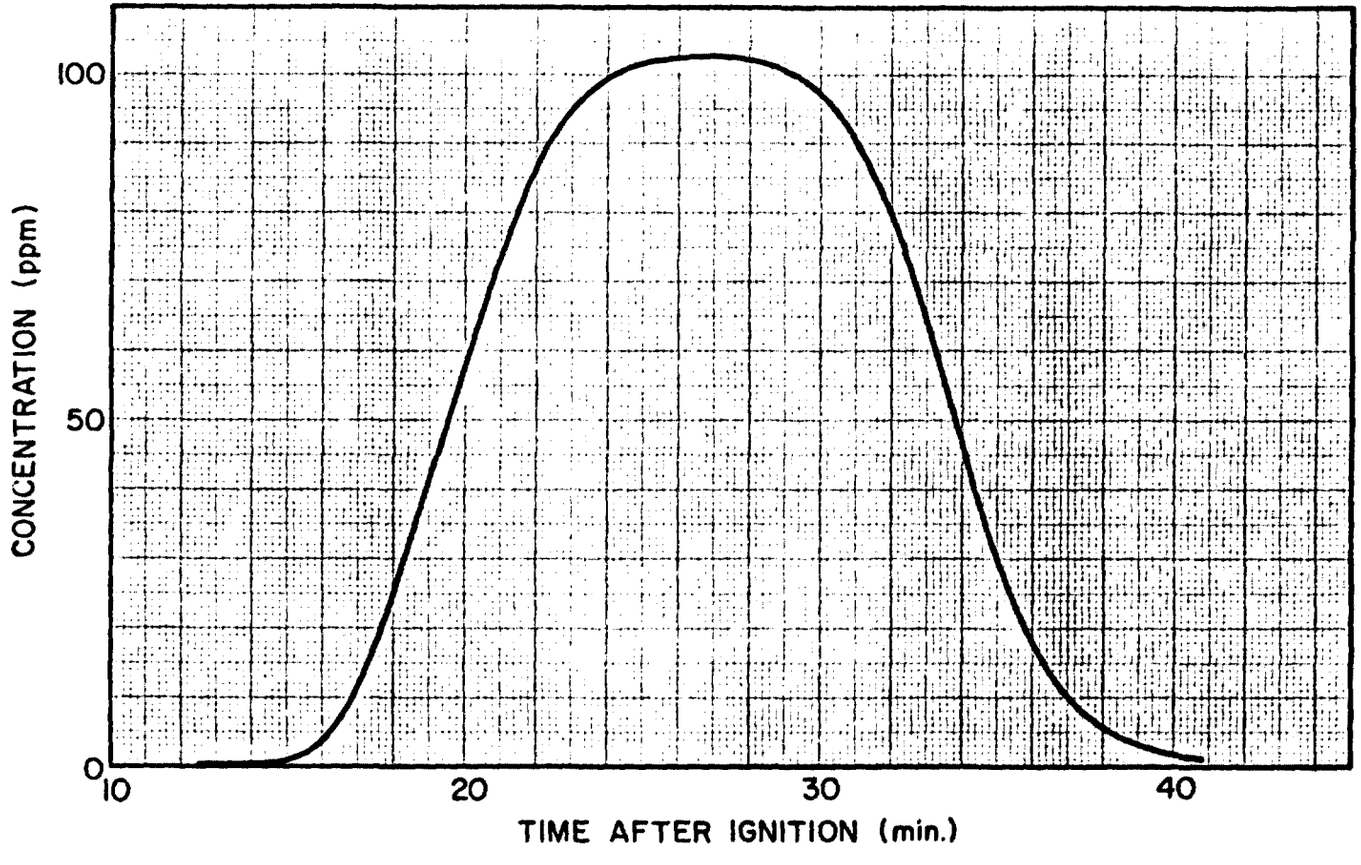

FIGURE 6-5. Time profile of HCl ground-level concentration at 3000 meters downwind from the VAB for a Type III postulated accident during very light winds.

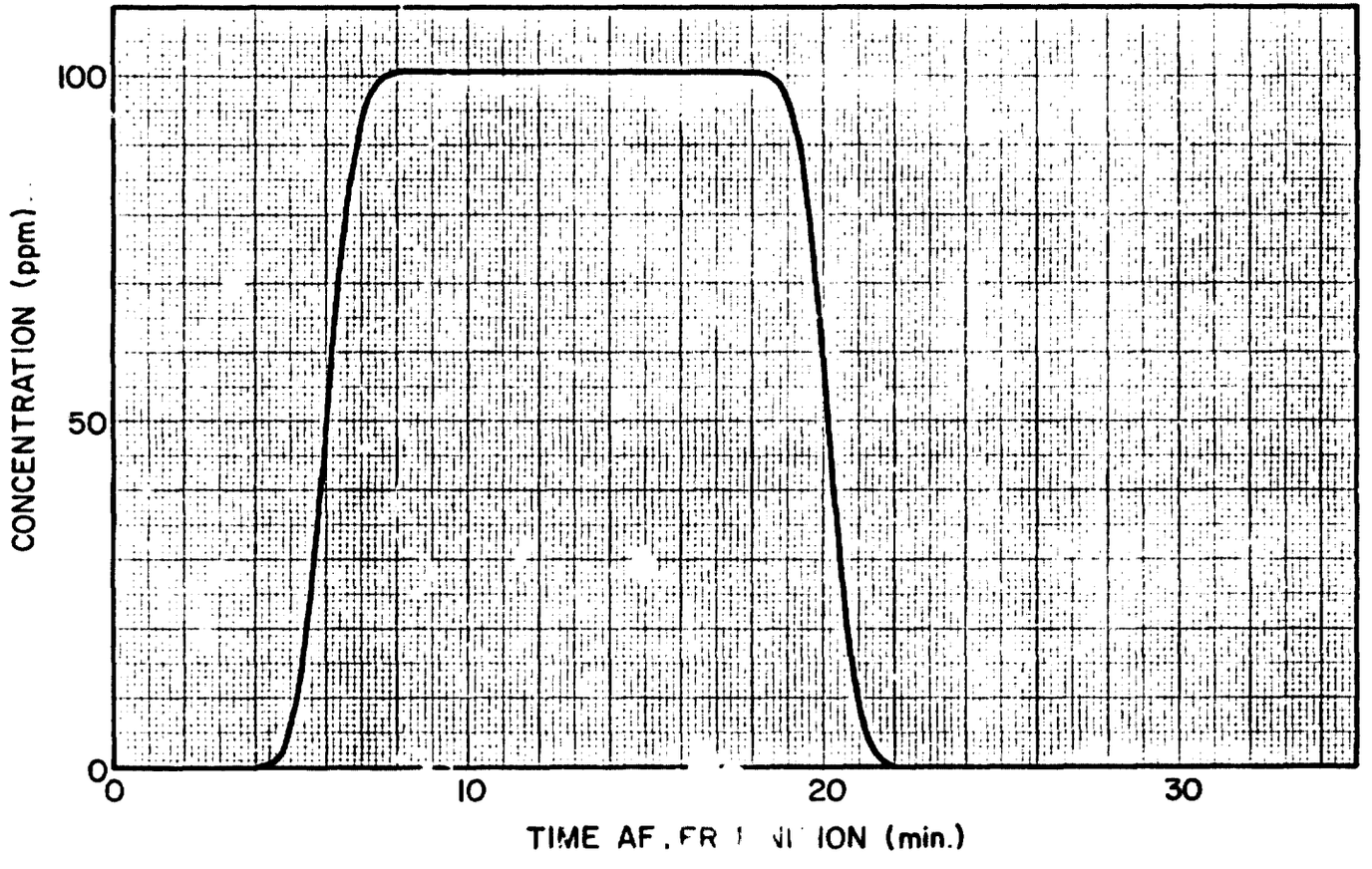

FIGURE 6-6. Time profile of HCl ground-level concentration at 1650 meters downwind from the VAB for a Type III postulated accident during light winds.

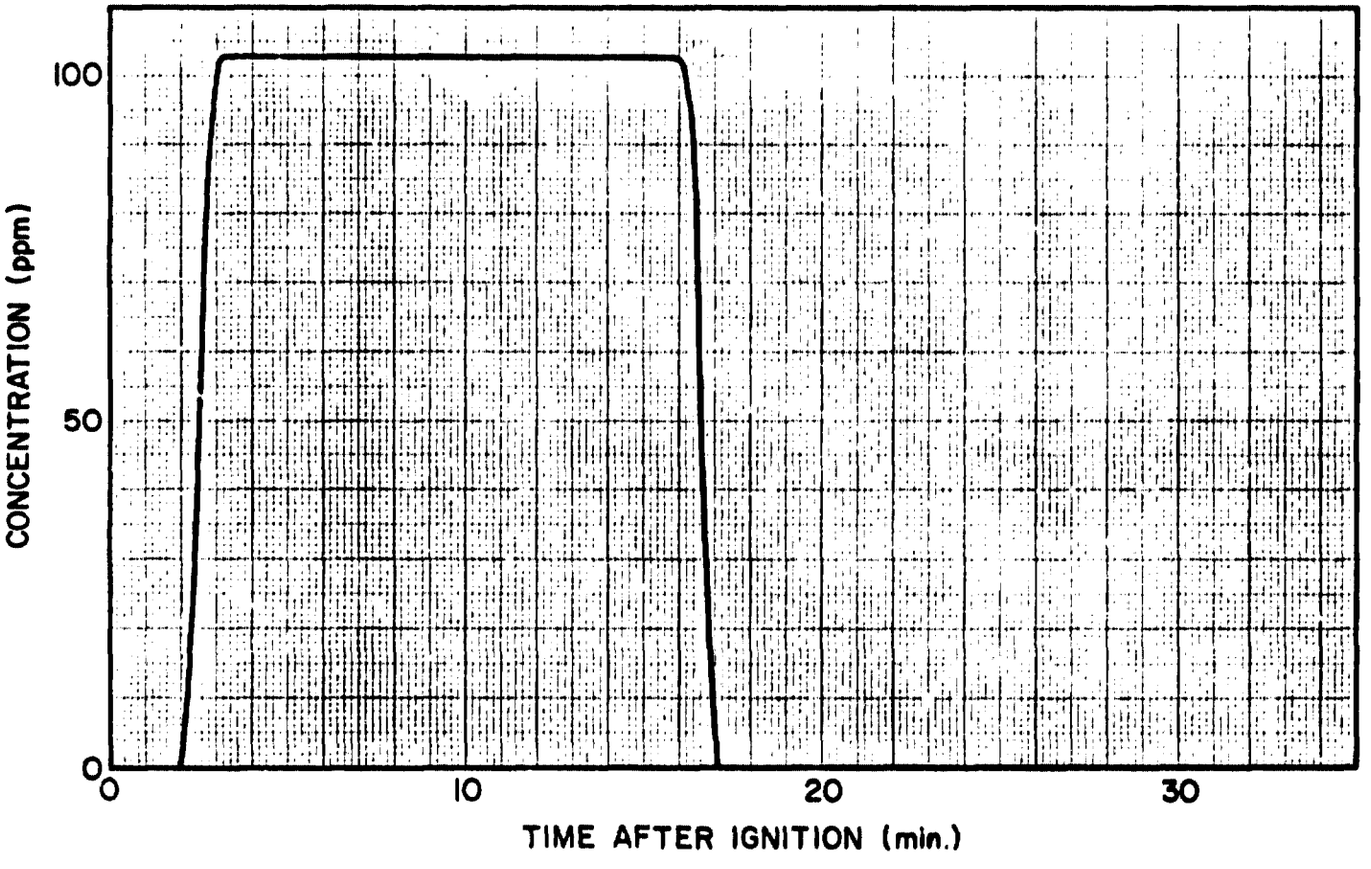

FIGURE 6-7. Time profile of HCl ground-level concentration at 1070 meters downwind from the VAB for a Type III postulated accident during moderate winds.

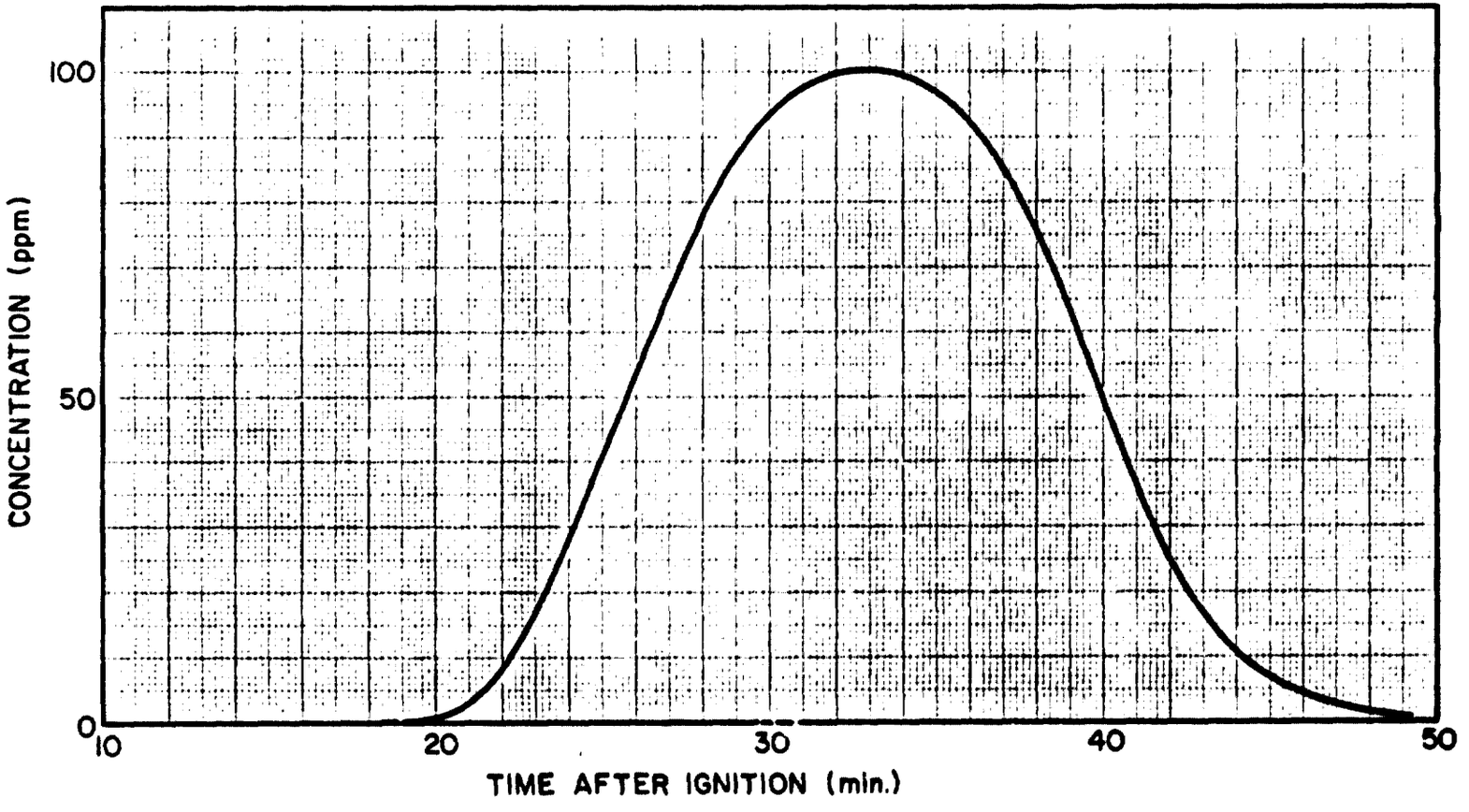

FIGURE 6-8. Time profile of HCl ground-level concentration at 3950 meters downwind from the VAB for a Type IV postulated accident during very light winds.

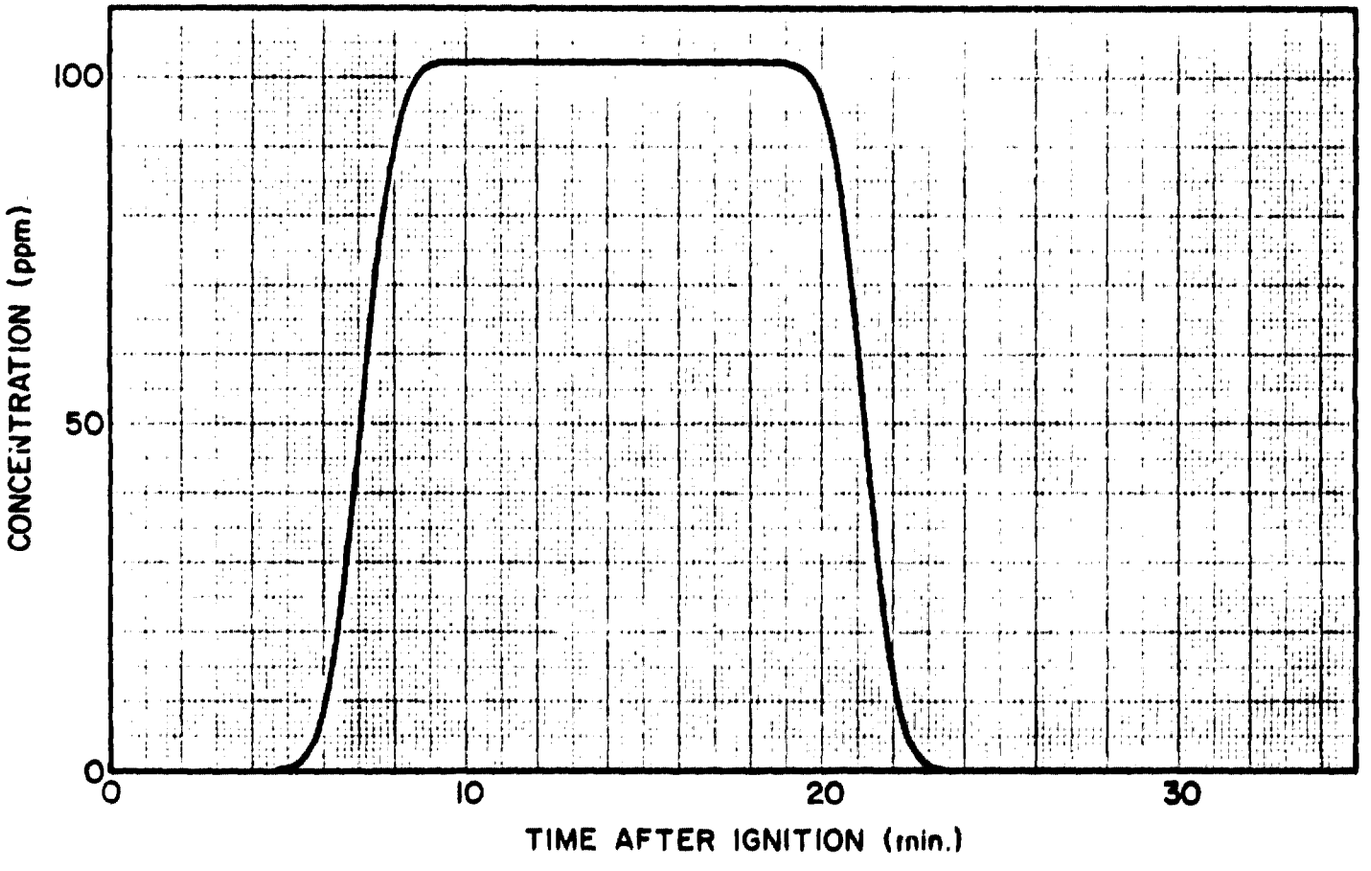

FIGURE 6-9. Time profile of HCl ground-level concentration at 1950 meters downwind from the VAB for a Type IV postulated accident during light winds.

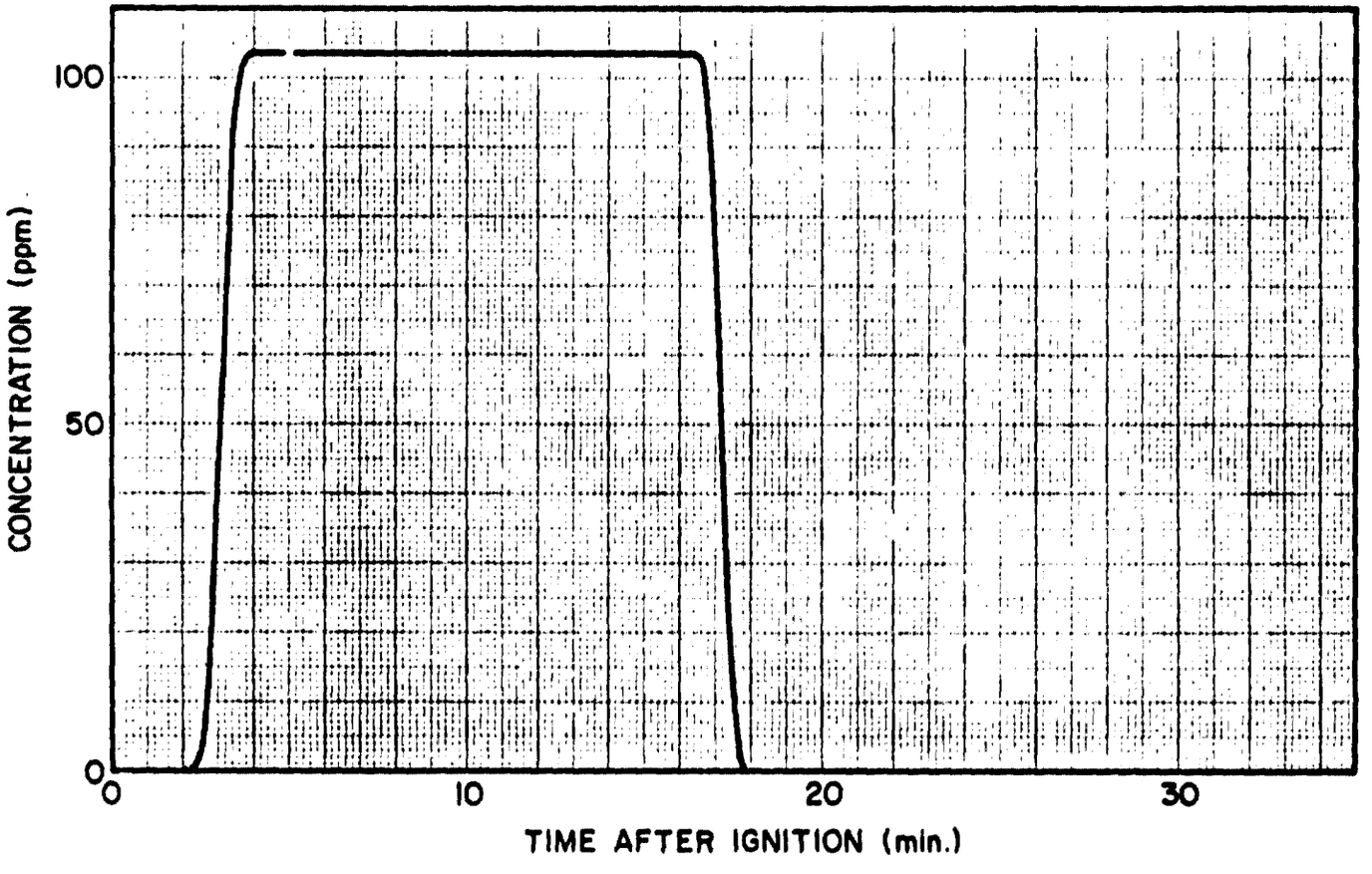

FIGURE 6-10. Time profile of HCl ground-level concentration at 1320 meters downwind from the VAB for a Type IV postulated accident during moderate winds.

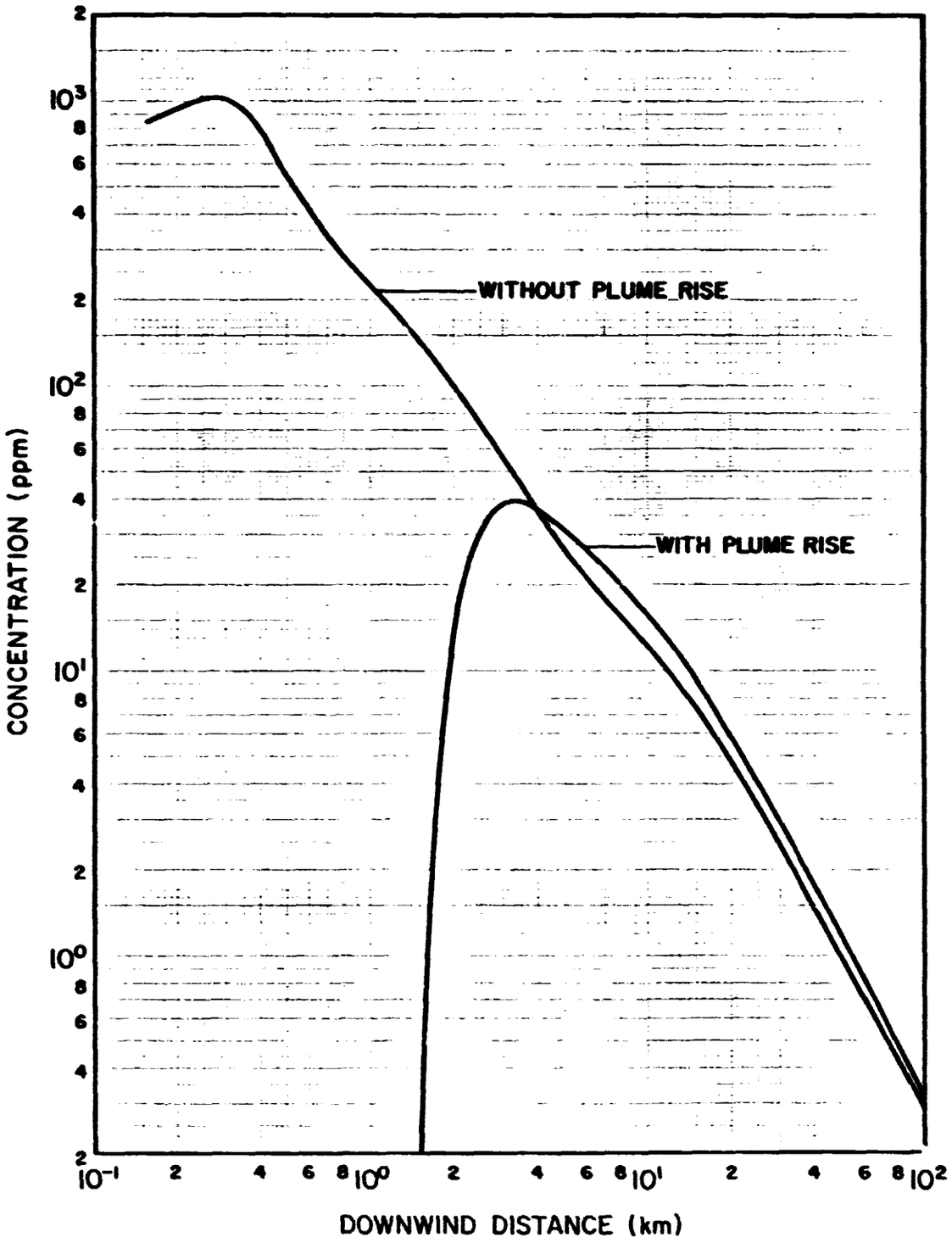

FIGURE 6-11. Ground-level HCl concentrations downwind from the VAB for a Type IV postulated accident during light winds.

SECTION 7

CALCULATIONS OF HYDRAZINE CONCENTRATIONS DOWNWIND FROM THE ORBITER PROCESSING FACILITY HYPER EXHAUST STACK

Calculations of hazard distances for the release of hydrazine from the Orbiter Processing Facility (OPF) Hyper Exhaust Stack were made using the quasi-continuous source model described above in Section 6. The exhaust stack has a height of 18.3 meters and a diameter of 1.83 meters. The flow rate through the stack, supplied to us by MSFC, is 434.2 $m^3 s^{-1}$ at a temperature of 23.89°C. According to MSFC, 1 liter of hydrazine is assumed to be spilled. Since no evaporation rate was supplied, we have made the assumption that the 1 liter of hydrazine is evaporated in 1 second.

Since the stack gases are near ambient temperature, only momentum forces contribute significantly to plume rise. Under this assumption, the final rise of the plume (see Dumbauld, Bjorklund and Bowers, 1973, p. A-11, Equation A-44) is

$$z = h + \left[\frac{3 w_o^2 r_o^2}{\gamma_c^2 \bar{u} s^{1/2}} + \left(\frac{r_o}{\gamma_c}\right)^3\right]^{1/3} - \frac{r_o}{\gamma_c} \qquad (7\text{-}1)$$

where

w_o = stack exit velocity = 16.53 m s^{-1}

r_o = stack exit radius = 0.9144 m

γ_c = entrainment coefficient = 0.6

s = stability parameter

$$= \frac{g}{T} \frac{\Delta\Phi}{\Delta z} \qquad (7\text{-}2)$$

g = 9.8 m s^{-1}

T = absolute temperature = 297.05°K

$\frac{\Delta\phi}{\Delta z}$ = lapse rate of potential temperature

$\bar{u}$ = mean wind speed

h = stack height = 18.3 m

For worst case conditions, we have set $\Delta\phi/\Delta z$ equal to 0.015°K m^{-1} and $\bar{u}$ equal to 2 m s^{-1}. Thus, the plume from the OPF stack stabilizes at a height of 51.74 meters and has a radius r equal to

$$r = \gamma(z - h) + r_o = 20.99 \text{ m} \qquad (7\text{-}3)$$

As noted above, the quasi-continuous source model described in Section 6 was used to calculate concentrations downwind from the stack. The source inputs based on the above assumptions and required for the calculations are given in Table 7-1. The source dimensions σ_{zR}, σ_{yR} and σ_{xo} were calculated from the expression

$$\sigma_{zR} = \sigma_{yR} = \sigma_{xo} = \frac{r}{4.3} = \frac{20.99}{4.3} = 9.76 \text{ m} \qquad (7\text{-}4)$$

The meteorological inputs used in the model calculations are shown in Table 7-2. A nominal value for H_m of 300 meters was used in the calculations. The value of the wind power-law coefficient p was set to zero, which means that the wind speed of 2 m s^{-1} is invariant with height under the worst-case conditions. Because of the proximity of the OPF stack to the VAB,

TABLE 7-1

SOURCE INPUTS

Parameter	Value
Q ($cm^3\ s^{-1}$)	1000
K	1
σ_{zR} (m)	9.76
σ_{yR} (m)	9.76
σ_{xo} (m)	9.76
$x_{Ry} = x_{Rz}$ (m)	0
$x_{ry} = x_{rz}$ (m)	50
H (m)	51.74
τ (s)	1

TABLE 7-2

METEOROLOGICAL INPUTS

Parameter	Value
H_m (m)	300
$\bar{u}_R$ (m s^{-1})	2
p	0
σ'_E (radians)	0.0971
σ'_A $\{\tau_o$=600s$\}$ (radians)	0.3491
α	1
β	1
$\frac{\Delta\Phi}{\Delta z}$	0

the value of σ_A was set equal to 20 degrees (.3491 radians) and the value of σ_E was set equal to $\sigma_A\{\tau=1\ s\}$, or 5.56 degrees (.0971 radians) to account for the enhanced turbulence caused by the VAB.

The results of the calculations are presented in Figure 7-1. The highest concentration of 1.7×10^{-3} ppm N_2H_4 occurs at a distance of 300 meters downwind from the stack. This concentration is well below the critical level of 3 ppm N_2H_4 for public and occupational emergency exposure limits. It should be noted that the concentration of N_2H_4 in the stack,

$$\frac{1000\ cm^3\ N_2H_4\ per\ second}{434.2\ m^3\ per\ second} = 2.3\ ppm,$$

is also below the critical exposure limits even when the 1 liter of N_2H_4 is released over a 1-second time period. Thus, these calculations show that the release of 1 liter of N_2H_4 through the OPF stack does not represent an exposure hazard.

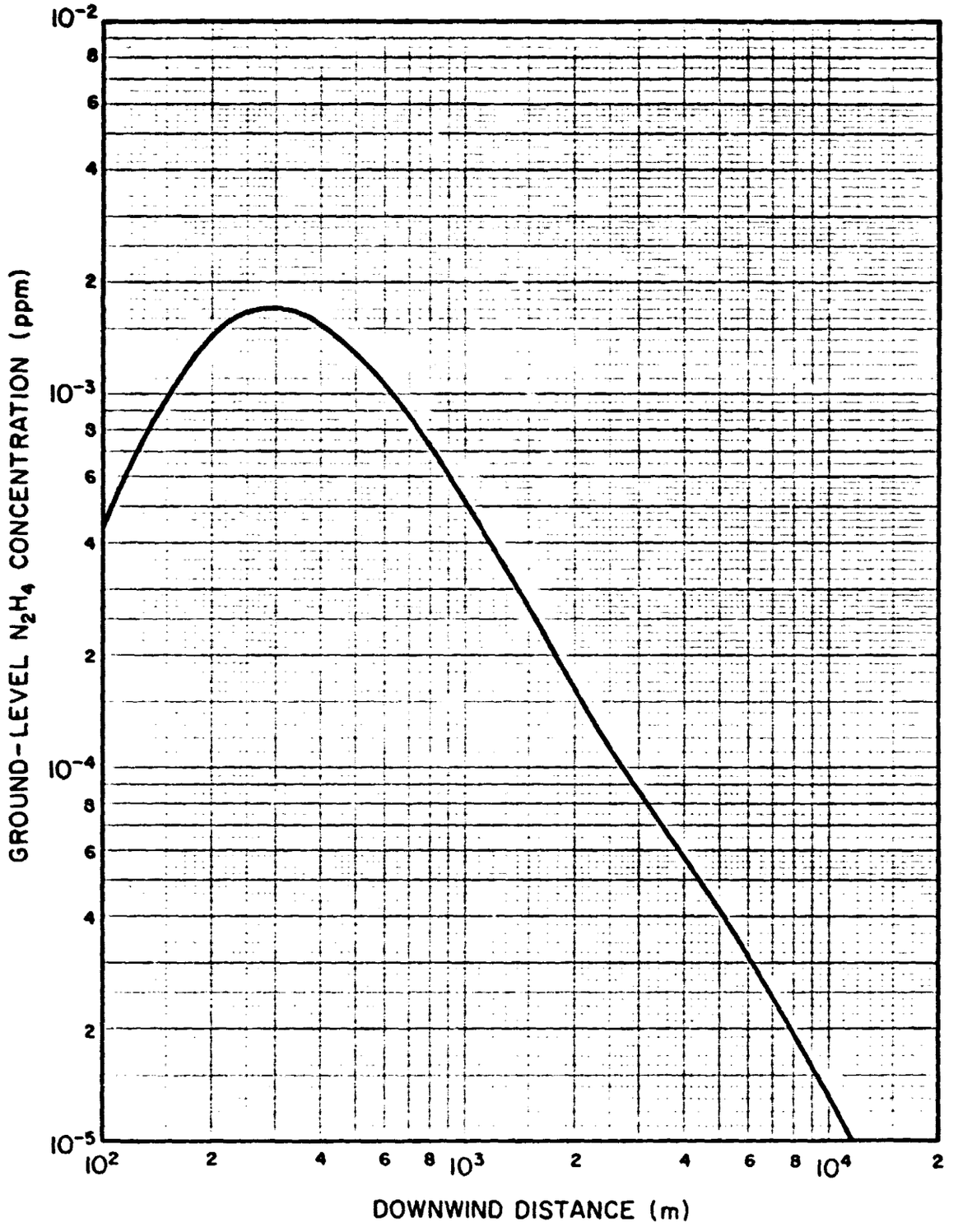

FIGURE 7-1. Preliminary estimates of N_2H_4 concentrations at ground-level downwind from the OPF Hyper Exhaust Stack.

SECTION 8

PEAK AND TIME-AVERAGE HCl CONCENTRATIONS FROM ACCIDENTAL IGNITIONS OF SRM SEGMENTS IN STORAGE AREAS

Peak and time-average HCl concentrations resulting from accidental ignitions of SRM segments stored in open areas at Kennedy Space Center (KSC) have been calculated using a quasi-continuous source model for time-average concentrations.

The calculations were performed for various source configurations specified by Dr. Koller at KSC according to the number of segments involved in the conflagration. The total solid fuel weight of the 4 segments comprising a single SRM are shown in Table 8-1. Each segment is 12 feet in diameter. In their storage configuration, the 4 segments for SRM can be stored in a line with a separation distance (center-to-center) of 34 feet. When SRM's are stored in parallel lines with a similar spacing between segments and a separation distance (center-to-center) of 31 feet between the two parallel lines. The burn configurations we have considered in the calculations are shown in Table 8-2. In addition to the SRM and 2 SRM configurations, we have considered 1 forward center SRM stored alone and another configuration in which the 2 aft segments are stored separately from the other 6 segments when 2 SRM's are stored. In the latter case, either the 2 aft segments or 6 other segments are assumed to burn separately.

Meteorological Conditions

The concentration calculations were made for very light "worst-case" wind conditions and for normal wind conditions at KSC. The meteorological conditions used in the plume-rise and concentration models described below are shown in Table 8-3. The model parameters, except for H_m, shown in the table for very light wind conditions are representative of nighttime stable conditions at KSC. The depth of the surface mixing layer H_m for these conditions is normally lower than the value of 550 meters shown in the table. However, if we had set H_m to a lower value, the buoyant plume

TABLE 8-1

SOLID FUEL WEIGHT FOR SRM SEGMENTS

Segment	Fuel Weight (lbs)
Forward	301, 125
Forward Center	273, 318
Aft Center	271, 977
Aft	261, 277

TABLE 8-2

BURN CONFIGURATIONS USED IN THE CALCULATIONS

Burn Configuration	Segments
1	Forward Center
2	Two aft segments
4 (1 SRM)	One each forward, forward center, aft center and aft segments
6	Two each forward, forward center and aft center segments
8 (2 SRM's)	Two each forward, forward center aft center and aft segments

TABLE 8-3

METEOROLOGICAL MODEL INPUT PARAMETERS

Model Parameters	Wind Conditions	
	Very Light	Moderate
$\bar{u}\{2m\}$ (m s^{-1})	1	4
p	0.25	0.15
H_m (m)	550	800
$\sigma_A\{\tau_o$=10 min$\}$ (deg)	5	8
σ_E (deg)	1.7	2.7
$\Delta\Phi/\Delta z$ (^oK m^{-1})	0.02	0.005
γ_c	0.66	0.66
T (^oK)	298.2	298.2
ρ_A (m^{-3})	1183.9	1183.9

from some of the burn configurations would have penetrated the elevated inversion at the top of the mixing layer and the plume would not have mixed to the ground. Because the objective of this study was to determine the maximum hazard distance under "worst-case" conditions, the value of H_m used in the calculations was selected to yield a maximum hazard distance. The model parameters shown in Table 8-3 for moderate wind conditions represent normal daytime conditions at KSC. Definitions of the input parameters are given in the discussions of the plume-rise and dispersion models below.

Plume-Rise Calculations

Plume rise for the quasi-continuous sources formed by the burning segments was calculated from a model developed by Briggs (1970) for continuous source emissions into a stable atmosphere. The derivation of the plume-rise model is given in Appendix A of NASA CR-129006 (Dumbauld, Bjorklund and Bowers, 1973). The height z of the cloud centroid at time t after release is given by the expression

$$\Delta h = \left[\frac{3F_c}{\bar{u}\,\gamma_c^2\, s} \left(1 - \cos\left(s^{\frac{1}{2}} t\right)\right) + \left(\frac{r_R}{\gamma_c}\right)^3 \right]^{1/3} - \frac{r_R}{\gamma_c} \qquad (8\text{-}1)$$

where

$$F_c = \frac{gQ_c}{\pi \rho_A c_p T} \qquad (8\text{-}2)$$

g = gravitational acceleration (9.8 m s^{-2})

Q_c = effective rate of heat release (cal s^{-1})

ρ_A = air density (g m^{-3})

c_p = specific heat of air at constant pressure (.24 cal g^{-1} $^oK^{-1}$)

T = air temperature (^{o}K)

s = stability parameter

$$= \frac{g}{T} \frac{\Delta\Phi}{\Delta Z} \tag{8-3}$$

$\frac{\Delta\Phi}{\Delta Z}$ = vertical gradient of ambient potential temperature

$\bar{u}$ = mean wind speed from a reference height of 2 meters to the height z

$$= \frac{\bar{u}\ \{2m\}\left(z^{1+p} - 2^{1+p}\right)}{(z-2)\ 2^{p}\ (1+p)} \tag{8-4}$$

r_R = radius of the source

γ_i = extrainment parameter (0.66)

The final plume rise from Equation (8-1) is

$$\Delta h_f = \left[\frac{6F_c}{\bar{u}\ \gamma_c^2 s} + \left(\frac{r_R}{\gamma_c}\right)^3\right]^{1/3} - \frac{r_R}{\gamma_c} \tag{8-5}$$

which occurs at the time

$$t = \pi/s^{\frac{1}{2}} \tag{8-6}$$

Inspection of Equation (8-1) and (8-4) shows that the height z is dependent on the mean wind $\bar{u}$ which is in turn dependent on z. Thus, iteration is required to determine the plume rise at any time t.

Use of the plume-rise model requires that Q_c and r_R be specified. Values of Q_c were obtained by assuming that the burning fuel releases 1100 BTU's per pound, or about 50 percent of the stoichiometric value of heat available. Also, each segment was assumed to burn at a constant rate over a period of 932 seconds. Table 8-4 shows the effective value of Q_c used in the plume-rise calculations for the various burn configurations. The values for the initial plume radious r_R shown in Table 8-4 were calculated under the assumption that the area A containing the burning segments for each configuration could, for our purposes, be represented by a circle with an equivalent area and radius r_R given by the expression

$$r_R = (A/\pi)^{1/2} \tag{8-7}$$

Finally, Table 8-4 shows the total amount of HCl released over the 932-second period which was based on the assumption that 21 percent of the fuel weight in each segments was released as gaseous HCl.

Tables 8-5 and 8-6 show the results of using the plume-rise model to calculate the centerline height of the plume and the plume radius at that height ($r_z = \gamma_r \Delta h + r_R$) at various downwind distances from the burning segment(s) for, respectively, very light and moderate wind conditions.

Quasi-Continuous Source Model for Time-Average Concentrations

The Gaussian model for calculating time-average concentrations downwind from a quasi-continuous source with a constant rate over the source emission time τ_E is given by the expression

$$\bar{\chi}(x, y, z, \tau_A) = \left[\frac{A+B}{2\tau_A}\right] \frac{Q}{2\pi \sigma_y \sigma_z \bar{u}} \left\{\exp\left[-\frac{1}{2}\left(\frac{y}{\sigma_y}\right)^2\right]\right\} \tag{8-8}$$

(Equation (8-8) continued on page 88)

TABLE 8-4

SOURCE PARAMETERS

Segment	Effective Heat Release Rate, Q_c (g cal s^{-1})	Initial Plume Radius, r_R (m)	HCl Emission Rate, Q (g s^{-1})
1	8.1288×10^7	3.7	2.7935×10^4
2	1.5541×10^8	4.9	5.3408×10^4
4 (1SRM)	3.2943×10^8	9.5	1.1321×10^5
6	5.0345×10^8	12.2	1.7302×10^5
8 (2SRM's)	6.5886×10^8	14.3	2.2643×10^5

TABLE 8-5

PLUME RISE PARAMETERS FOR VERY LIGHT WIND CONDITIONS

Downwind Distance (m)	Centerline Height (m)					Plume Radius (m)				
	Number of Segments					Number of Segments				
	1	2	4	6	8	1	2	4	6	8
100	178.2	217.7	255.3	284.3	304.3	121.2	143.7	177.9	199.9	215.2
125	199.0	242.8	286.2	319.1	341.9	135.0	160.2	198.3	222.9	239.9
160	223.1	272.1	322.6	360.3	386.4	150.9	176.6	222.4	250.1	269.4
200	244.8	298.8	356.3	398.7	428.1	165.2	197.2	244.6	275.4	296.9
250	264.0	323.5	388.1	435.5	468.4	177.9	213.5	265.6	299.7	323.4
320	277.1	342.6	415.2	468.2	505.0	186.5	226.1	283.5	321.2	347.7
338.2	277.7*	-	-	-	-	186.9	-	-	-	-
356.8	-	345.3*	-	-	-	-	227.9	-	-	-
400	-	-	422.0*	478.9*	518.7*	-	-	288.0	328.3	356.7

*Final Rise

TABLE 8-6

PLUME RISE PARAMETERS FOR MODERATE WIND CONDITIONS

Downwind Distance (m)	Centerline Height (m)					Plume Radius (m)				
	Number of Segments					Number of Segments				
	1	2	4	6	8	1	2	4	6	8
100	72.1	93.0	103.4	114.9	122.9	51.3	61.4	77.7	88.1	95.5
125	82.8	105.9	119.4	133.1	142.5	58.3	69.9	88.3	100.1	108.4
160	96.3	122.2	139.7	156.0	167.3	67.2	80.7	101.6	115.2	124.7
200	110.2	139.0	160.6	179.7	192.9	76.4	91.8	115.4	130.8	141.7
250	126.0	158.0	184.2	206.5	221.9	86.8	104.3	131.1	148.5	160.8
320	145.7	181.9	213.9	240.1	258.2	99.8	120.0	150.7	170.7	184.7
400	165.8	206.2	244.2	274.4	295.4	113.1	136.1	170.7	193.3	209.2
500	188.1	233.2	278.0	312.6	336.8	127.8	153.9	192.9	218.6	236.5
630	213.4	263.9	316.4	356.3	384.1	144.5	174.2	218.3	247.4	267.9
800	241.4	298.1	359.4	405.1	437.1	162.9	196.8	246.6	279.6	302.7
1000	268.0	331.0	401.0	452.7	488.8	180.6	218.5	274.1	311.0	336.9
1250	293.1	362.4	441.2	499.0	539.5	197.1	239.2	300.6	341.6	370.4
1600	313.3	389.1	477.1	541.4	586.4	210.5	256.8	324.4	369.5	401.4
1828.7	317.2*	-	-	-	-	213.0	-	-	-	-
1889.6	-	396.2*	-	-	-	-	261.5	-	-	-
1987.7	-	-	-	557.9*	-	-	-	-	380.5	-
2000	-	-	489.4*	-	606.2*	-	-	332.4	-	414.5

*Final Rise

(Equation (8-8) continued)

$$\frac{1}{2}\left\{\operatorname{erf}\left[\frac{x-\bar{u}(t-\tau_E)}{\sqrt{2}\,\sigma_x}\right]-\operatorname{erf}\left[\frac{x-\bar{u}t}{\sqrt{2}\,\sigma_x}\right]\right\}$$

$$\left\{\sum_{a=0}^{\infty}\left[\exp\left[-\frac{1}{2}\left(\frac{2aH_m-H+z}{\sigma_z}\right)^2\right]+\exp\left[-\frac{1}{2}\left(\frac{2aH_m+H+z}{\sigma_z}\right)^2\right]\right]\right.$$

$$\left.+\sum_{a=1}^{\infty}\left[\exp\left[-\frac{1}{2}\left(\frac{2aH_m+H-z}{\sigma_z}\right)^2\right]+\exp\left[-\frac{1}{2}\left(\frac{2aH_m-H-z}{\sigma_z}\right)^2\right]\right]\right\} \qquad (8\text{-}8)$$

where

Q = source emission rate

σ_y = standard deviation of the crosswind concentration distribution

$$= \sigma'_A\{T\}\; x_{ry}\left(\frac{x + x_y - x_{ry}\,(1-\alpha)}{x_{ry}}\right)^{\alpha} \qquad (8\text{-}9)$$

$\sigma'_A\{T\}$ = standard deviation of the wind azimuth angle in radians for the averaging time T

$$\sigma'_A\{T\} = \sigma'_A\{\tau_o\}\left(\frac{T}{\tau_o}\right)^{1/5} \qquad (8\text{-}10)$$

$$T = \begin{cases} \tau_A \;;\; 2.5 < \tau_A \leq \tau_E \\ \tau_E \;;\; \tau_A > \tau_E \end{cases} \qquad (8\text{-}11)$$

$\sigma'_A\{\tau_o\}$ = standard deviation of the wind azimuth angle in radians for the meteorological sampling time period τ_o

τ_A = concentration averaging time

x = downwind distance from the source

x_y = crosswind virtual distance

$$= \alpha x_{ry} \left(\frac{\sigma_{yR}}{\sigma'_{A\{T\}} x_{ry}} \right)^{1/\alpha} - x_R + x_{ry} (1 - \alpha) \qquad (8\text{-}12)$$

α = crosswind dispersion coefficient

x_{ry} = distance over which rectilinear crosswind cloud expansion occurs downwind from a virtual point source

σ_{yR} = standard deviation of the crosswind concentration distribution at a distance x_R from the source

σ_z = standard deviation of the vertical concentration distribution

$$= \sigma'_E (x + x_z) \qquad (8\text{-}13)$$

σ'_E = standard deviation of the wind elevation angle in radians

x_z = vertical virtual distance

$$= \frac{\sigma_{zR}}{\sigma'_E} - x_R \qquad (8\text{-}14)$$

σ_{zR} = standard deviation of the vertical concentration distribution at x_R

$\bar{u}$ = mean wind speed

$$= \left\{ \begin{array}{ll} \dfrac{\bar{u}_R \left[\left(z_2\right)^{1+p} - \left(z_1\right)^{1+p} \right]}{\left(z_2 - z_1\right) \left(z_R\right)^p \left(1+p\right)} & ; \quad \bar{u} > \bar{u}_R \\ \\ \bar{u}_R & ; \quad \bar{u} \leq \bar{u}_R \end{array} \right\} \qquad (8\text{-}15)$$

$\bar{u}_R$ = mean wind speed at the reference height z_R

p = wind profile power-law exponent

z_1 = effective lower bound of the cloud

$$= \begin{cases} H + 2.15\ \sigma_z & ;\ z_1 > 2 \\ 2 & ;\ z_1 \leq 2 \end{cases} \qquad (8\text{-}16)$$

z_2 = effective upper bound of the cloud

$$= \begin{cases} H + 2.15\ \sigma_z & ;\ z_2 < H_m \\ H_m & ;\ z_2 \geq H_m \end{cases} \qquad (8\text{-}17)$$

y = crosswind distance from the cloud centerline

H_m = depth of the surface mixing layer

H = effective height of the source above ground level

= Δh from Equation (8-1) or (8-5) (8-18)

z = height above ground level

t = time after release

σ_x = standard deviation of the alongwind concentration distribution

$$\sigma_x = \left[\left(\frac{L\{x\}}{4.3} \right)^2 + \sigma_{xo}^2 \right]^{1/2} \tag{8-19}$$

$$L\{x\} = \begin{cases} \dfrac{0.6\ \Delta\bar{u}}{\bar{u}}\ x\ ; & \Delta\bar{u} \geq 0 \\ 0 \quad ; & \bar{u} < 0 \end{cases} \tag{8-20}$$

$\Delta\bar{u}$ = vertical wind-speed shear in the layer containing the cloud

$$= \frac{\bar{u}_R}{z_R^p} \left[z_2^p - z_1^p \right] \tag{8-21}$$

σ_{xo} = standard deviation of the alongwind cloud distribution at the source

$$A = \frac{-\sqrt{2}\ \sigma_x}{\bar{u}} \left[\frac{\bar{u}\left(\tau_E - \tau_A\right)}{\sqrt{2}\ \sigma_x} \ \text{erf} \left(\frac{\bar{u}\left(\tau_E - \tau_A\right)}{2\sqrt{2}\ \sigma_x} \right) - \bar{u} \left(\frac{\tau_E + \tau_A}{\sqrt{2}\ \sigma_x} \right) \ \text{erf} \left(\frac{\bar{u}\left(\tau_E + \tau_A\right)}{2\sqrt{2}\ \sigma_x} \right) \right] \tag{8-22}$$

$$B = \frac{-2\sqrt{2}\ \sigma_x}{\sqrt{\pi}\ \bar{u}} \left[\exp\left(- \left(\frac{\bar{u}\left(\tau_E - \tau_A\right)}{2\sqrt{2}\ \sigma_x} \right)^2 \right) - \exp\left(- \left(\frac{\bar{u}\left(\tau_E + \tau_A\right)}{2\sqrt{2}\ \sigma_x} \right)^2 \right) \right] \tag{8-23}$$

Calculation Procedures

The concentrations for downwind distances between the source and the distances of maximum plume rise shown in Table 8-5 and 8-6 for the various segment configurations were calculated using Equation (8-8) at each distance x using the meteorological input parameters in Table 8-3, the source parameters in Table 8-4, and the following additional input parameters:

$$\sigma_{yR} = \sigma_{zR} = \sigma_{xo} = r_z/2.15$$

$$x_R = x$$

$$\alpha = \begin{cases} 0.9 \; ; \; \tau_A = 600\text{s and } 1800\text{s} \\ 1.0 \; ; \; \tau_A = 2.5\text{s} \end{cases} \qquad (8\text{-}24)$$

$$\beta = 1$$

$$x_{ry} = x_{rz} = 50\text{m}$$

$$z = 1.5\text{m}$$

The values of σ_{yr}, σ_{zr}, σ_{xo} and X_R at the distance of maximum plume rise were used to calculate concentrations using Equation (8-8) for all distances beyond the point of maximum cloud rise. The concentration calculations were made for nearly-instaneous peak concentrations (τ_A = 2.5s) and for 10 minute (τ_A = 600s) and 30 minute (τ_A = 1800s) averaging times.

Results of the Calculations

The results of the calculations are shown in Figures 8-1 through 8-10. Figure 8-1 shows instantaneous and 10- and 30-minute time average HCl concentrations downwind from a 1-segment burn during very light wind conditions. At distances close to the source, Figure 8-1 shows that the instantaneous and 10-minute time average concentrations are identical, a result that we expect because the segment burns for about 15.5 minutes at a constant emission rate. The 30-minute time average concentration is less because concentrations are nearly zero during part of the 30 minutes after the terminated plume has passed the receptor. At these distances close to the source, concentration decreases with increasing distance because the plume is rising faster than it is expanding and the plume begins to lose contact with the ground. As turbulence continues to cause plume expansion after maximum plume rise has been achieved, concentrations again begin to increase to a maximum value. At longer downwind distances when the terminated plume is expanding alongwind due to wind speed shear in the vertical, the 10-minute and 30-minute time averaged concentrations become more nearly identical (the plume is "long" compared to the averaging time). The remaining figures for burns of the various segment configurations show similar patterns. The highest concentrations beyond 1 kilometer from the sources occur under "worst-case" (very light wind conditions) and are greatest for the 8-segment (2SRM's) storage configuration reaching a maximum instantaneous concentration of 66 ppm HCl at 6.5 kilometers downwind from the storage area.

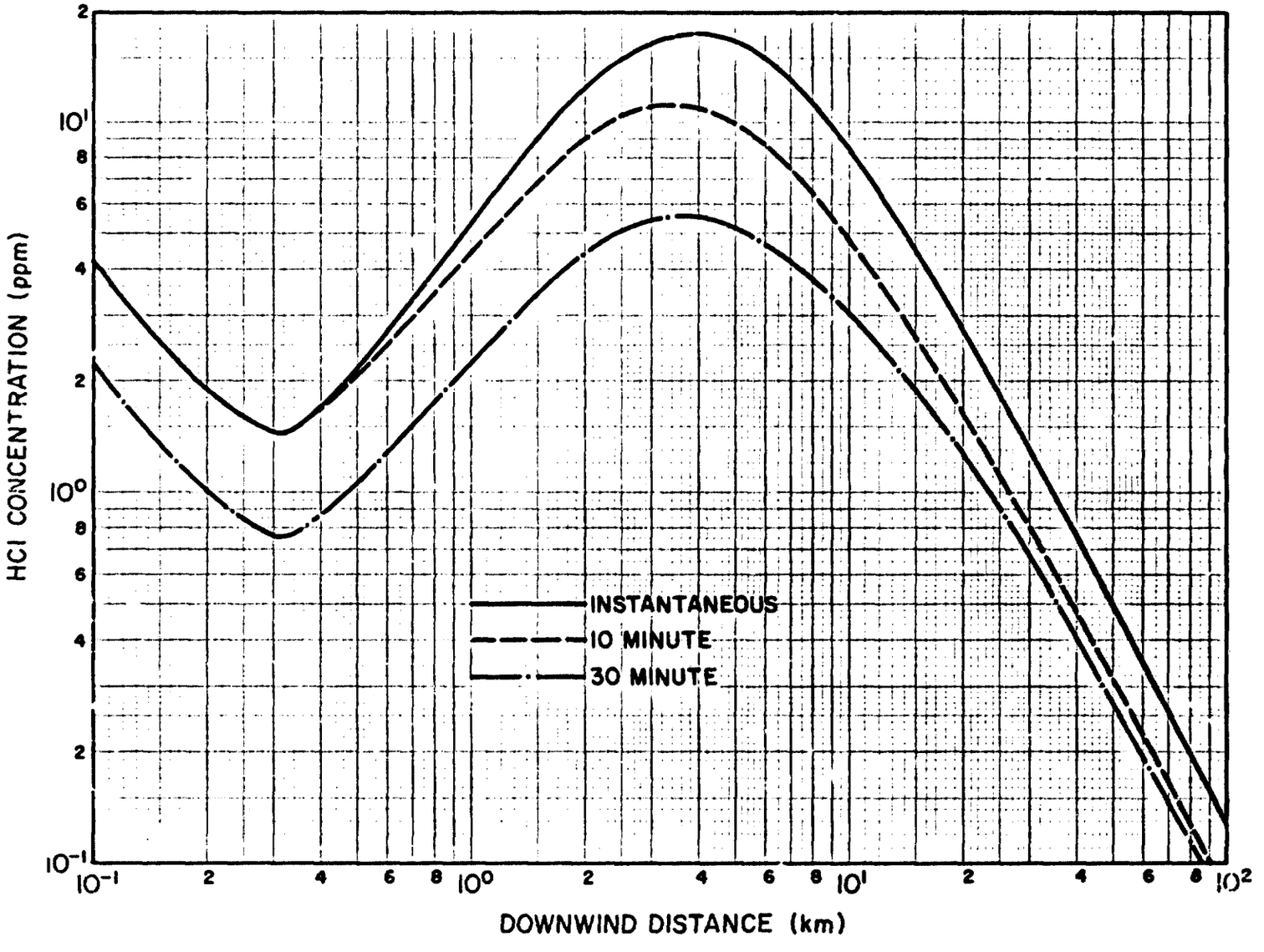

FIGURE 8-1. Instantaneous HCl concentrations and 10- and 30-minute time average HCl concentrations downwind from a 1-segment burn during very light wind conditions.

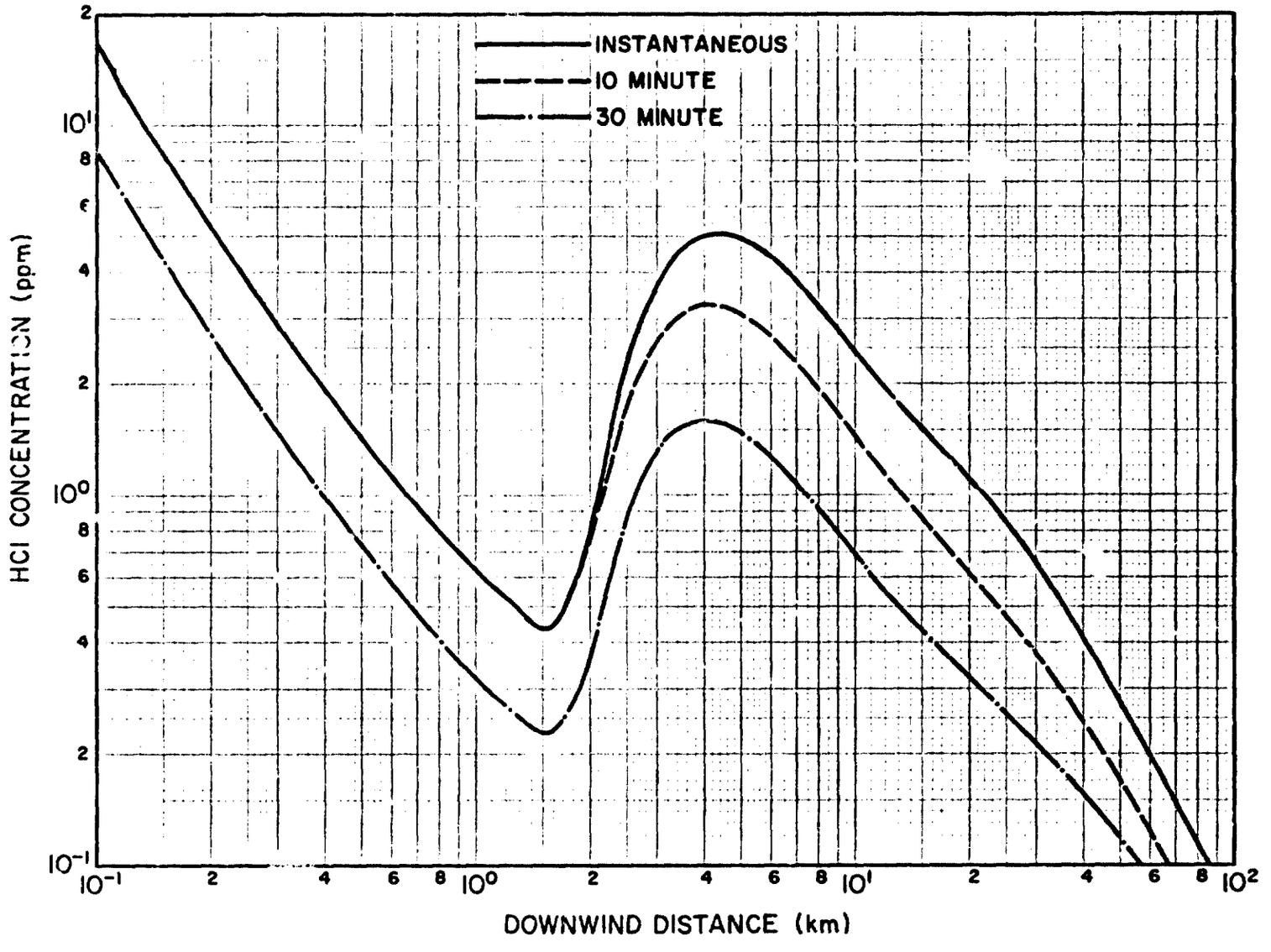

FIGURE 8-2. Instantaneous HCl concentrations and 10- and 30-minute time average HCl concentrations downwind from a 1-segment burn during moderate wind conditions.

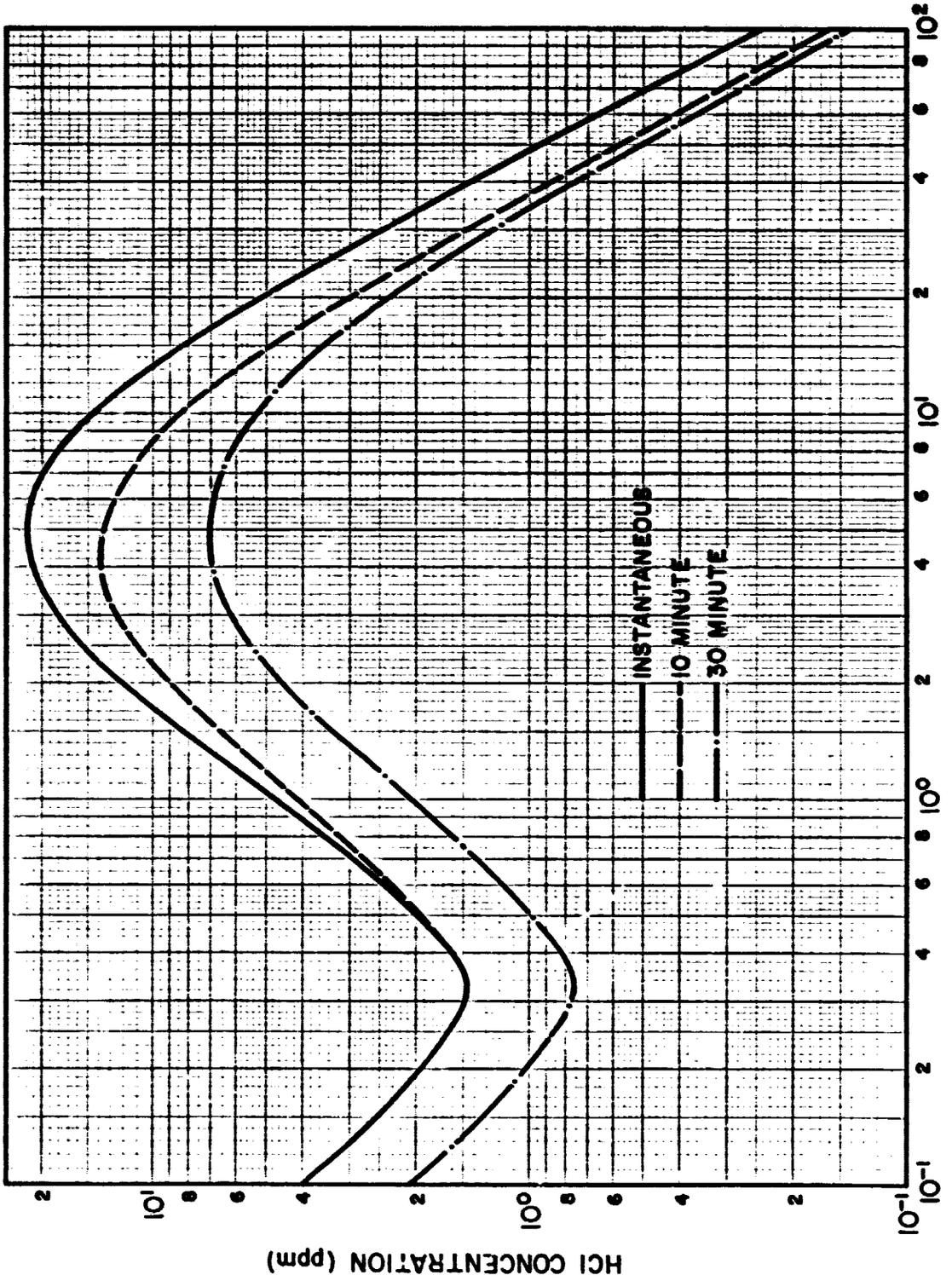

FIGURE 8-3. Instantaneous HCl concentrations and 10- and 30-minute time average HCl concentrations downwind from a 2-segment burn during very light wind conditions.

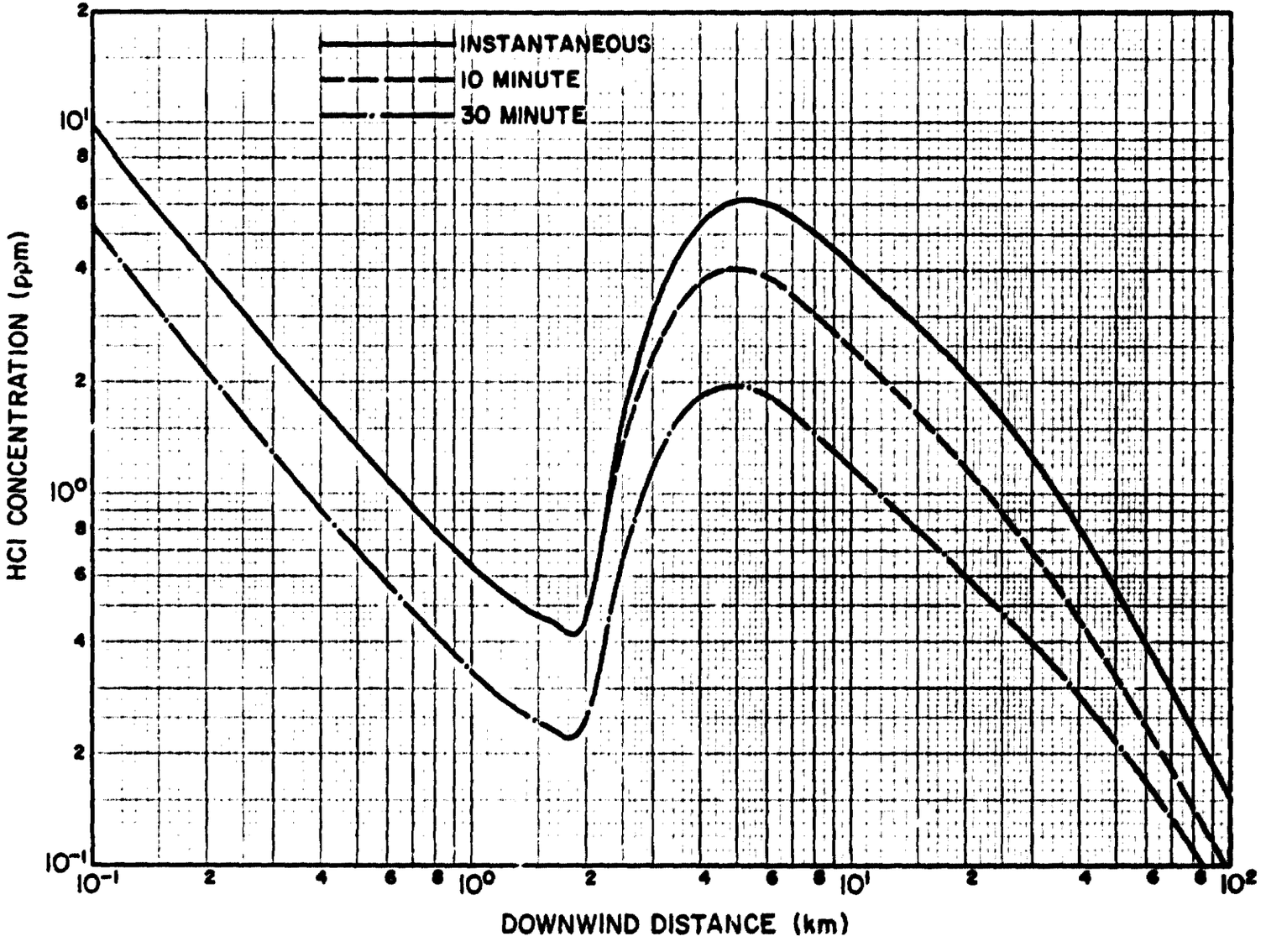

FIGURE 8-4. Instantaneous HCl concentrations and 10- and 30-minute time average HCl concentrations downwind from a 2-segment burn during moderate wind conditions.

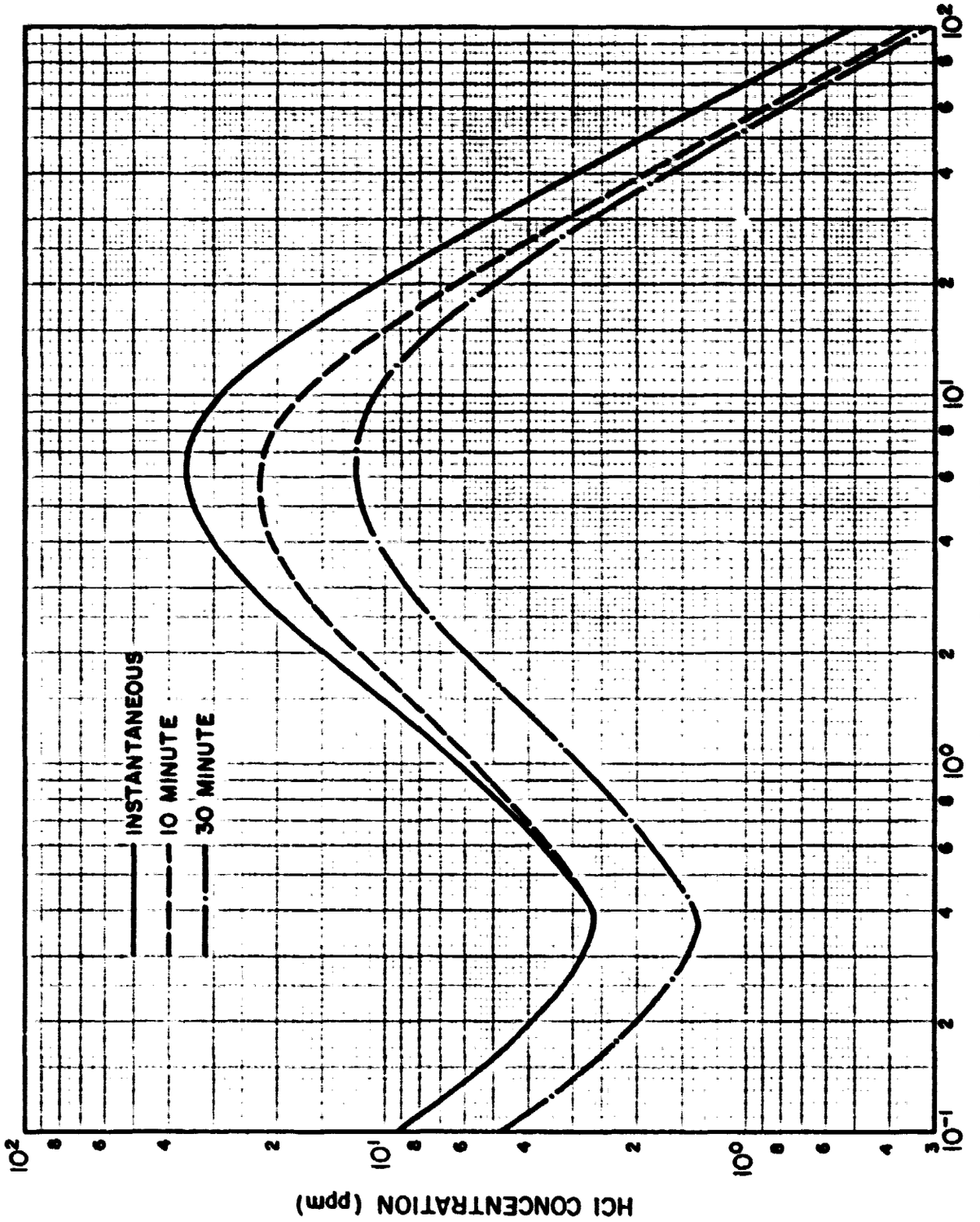

FIGURE 8-5. Instantaneous HCl concentrations and 10- and 30-minute time average HCl concentrations downwind from a 4-segment (1SRM) burn during very light wind conditions.

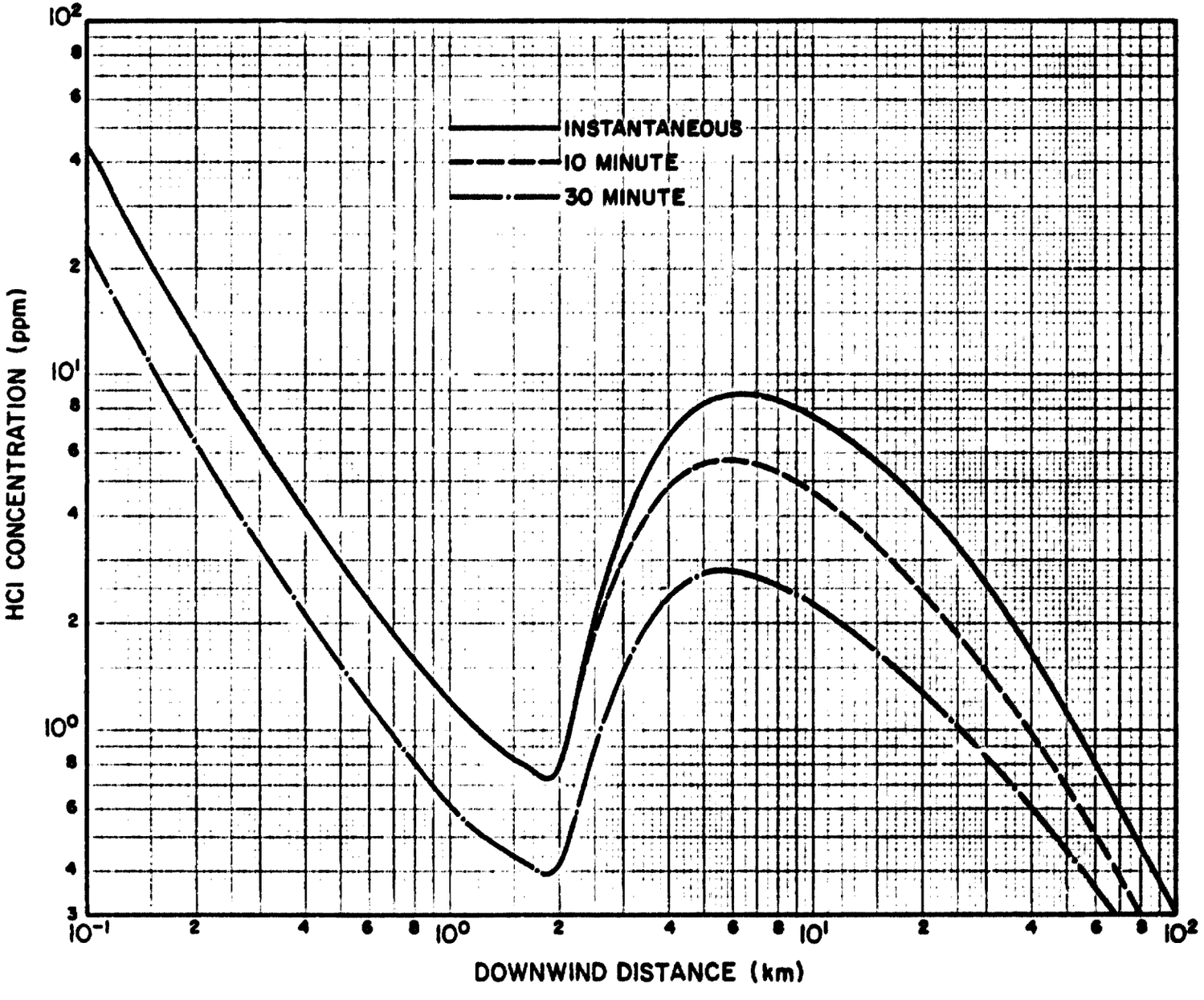

FIGURE 8-6. Instantaneous HCl concentrations and 10- and 30-minute time average HCl concentrations downwind from a 4-segment (1SRM) burn during moderate wind conditions.

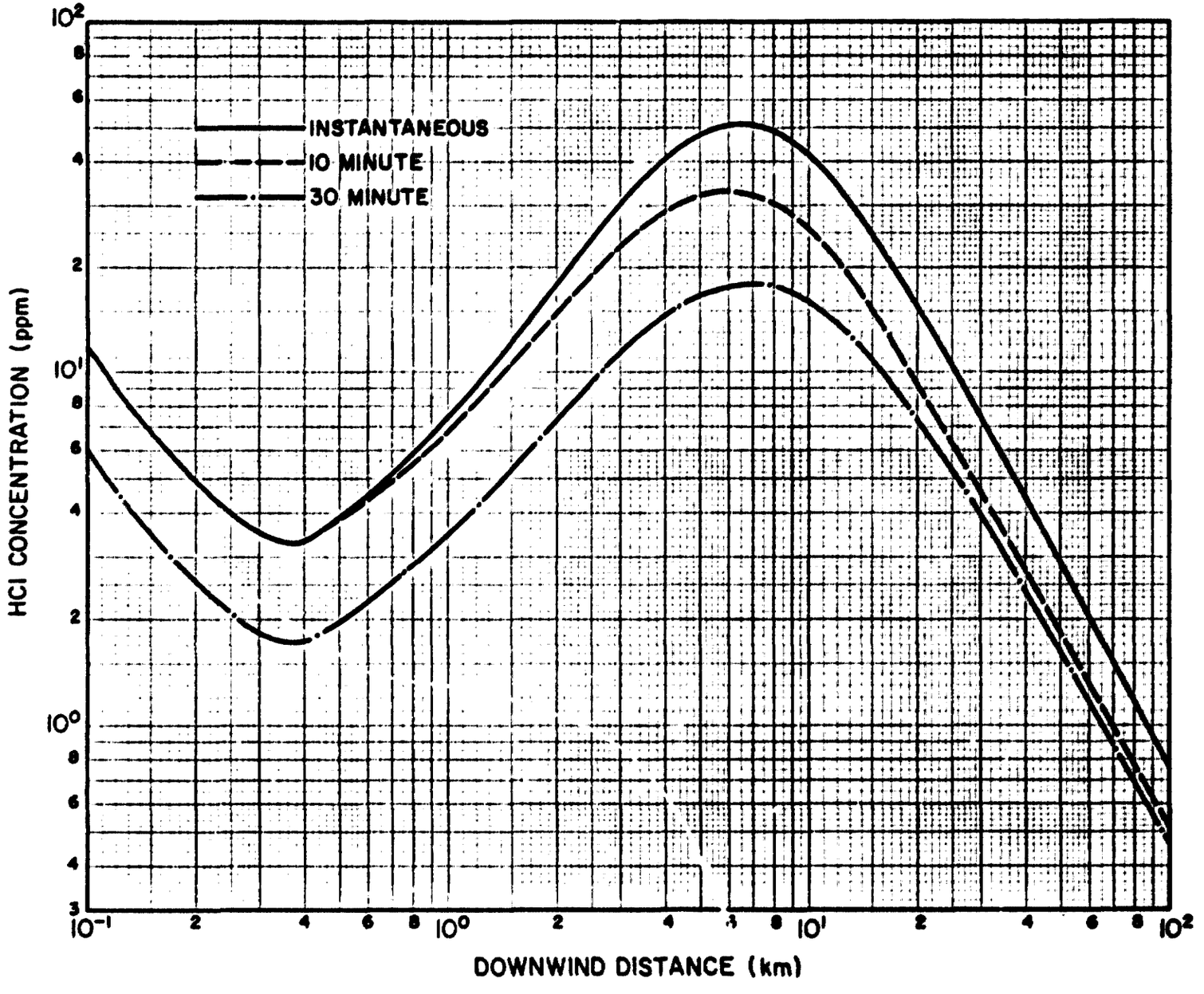

FIGURE 8-7. Instantaneous HCl concentrations and 10- and 30-minute time average HCl concentrations downwind from a 6-segment burn during very light wind conditions.

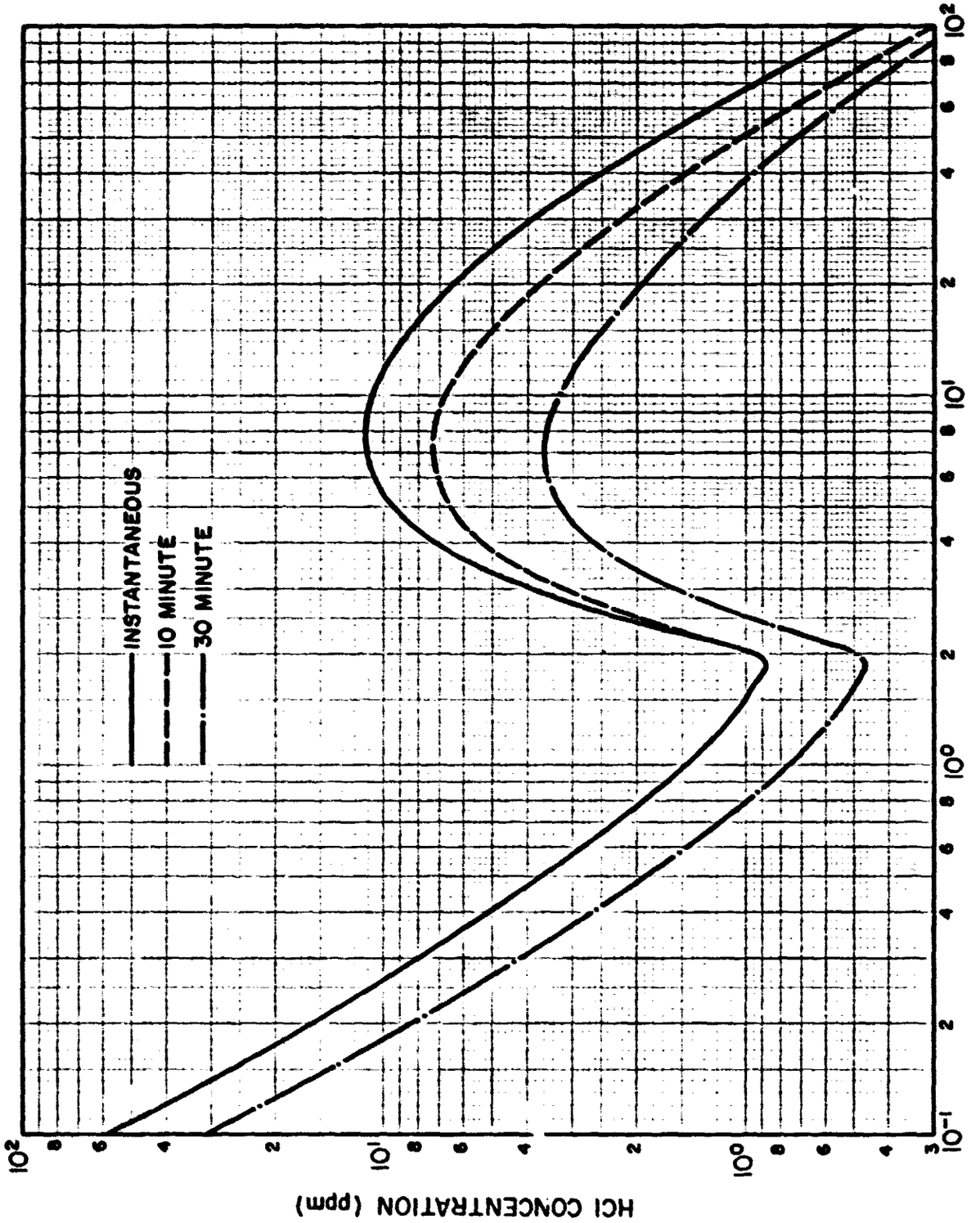

FIGURE 8-8. Instantaneous HCl concentrations and 10- and 30-minute time average concentrations downwind from a 6-segment burn during moderate wind conditions.

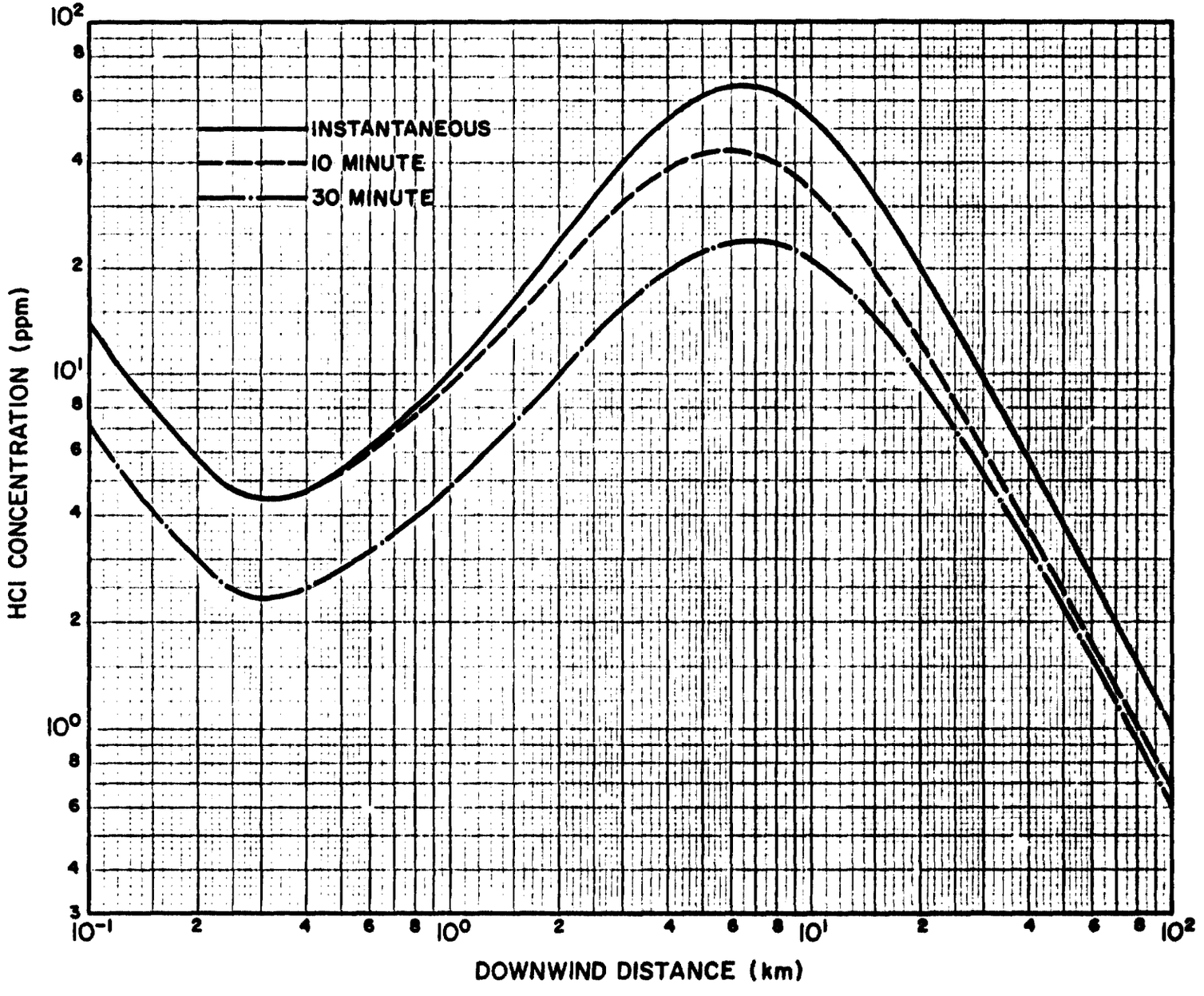

FIGURE 8-9. Instantaneous HCl concentrations and 10- and 30-minute time average HCl concentrations downwind from a 8-segment (2SRB's) burn during very light wind conditions.

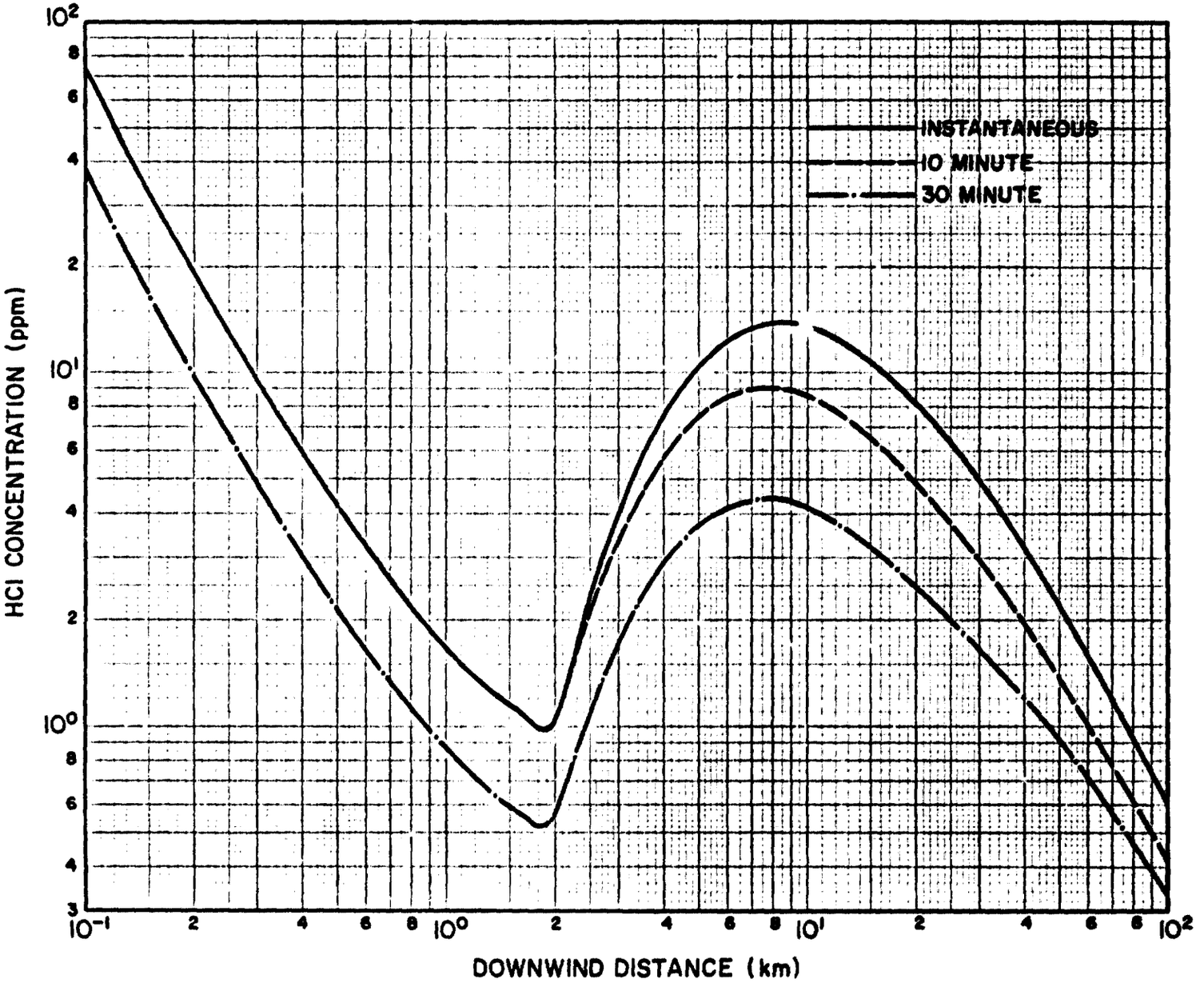

FIGURE 8-10. Instantaneous HCl concentrations and 10- and30-minute time average HCl concentrations downwind from a 8-segment (2SRM's) burn during moderate wind conditions.

SECTION 9

HAZARD CALCULATIONS FOR POSTULATED SPILLS OF MON-10 FUEL AT FUEL FARM #1, KSC

Instantaneous and time-average NO_2 concentration profiles have been calculated downwind from postulated spills of MON-10 fuel at Fuel Farm #1 at KSC. The calculations were performed for three meteorological cases specified by DF-EMS/KSC. In Case 1, the wind at a height of 2 m is assumed to be from 199° at a speed of 3 m s^{-1}. According to KSC, this wind direction takes the evaporating cloud towards the CCAFS Industrial Area at a distance of 3353 m from Fuel Farm #1. In Case 2, a wind of 4 m s^{-1} from 130° is assumed to carry the cloud towards the KSC Industrial Area located at a distance of 8534 m from Fuel Farm #1. In Case 3, a wind from 019° at a speed of 5 m s^{-1} is assumed to carry the cloud towards Cape Canaveral Harbor at a distance of 6706 meters from Fuel Farm #1.

In each case, DF-EMS/KSC suggested that we assume that the MON-10 fuel covers an area of 1600 ft^2 (148.65 m^2) within the dikes constructed at Fuel Farm #1. Recognizing that MON-10 fuel is comprised of 90% N_2O_4 and 10% NO, it was also suggested that a spill of 27,675 pounds of N_2O_4 and 3,075 pounds of NO be considered for use in the calculations. After discussion with DF-EMS/KSC, a joint decision was made to consider only the conversion of the 27,675 pounds of N_2O_4 to NO_2 gas in the calculations. Also, DF-EMS/KSC suggested an evaporation rate for MON-10 fuel of 5×10^{-3} gal min^{-1} ft^{-2}. Since MON-10 fuel has a density of 12.3 lbs gal^{-1} at 68° F, this is equivalent to an evaporation rate of 5.0045 g m^{-2} s^{-1}.

Meteorological Model Input Parameters

As noted above, the wind conditions for the calculations were specified by DF-EMS/KSC. The other meteorological input parameters we selected as being representative of meteorological conditions at KSC under

the specified wind conditions are shown in Table 9-1. The values of the wind power-law exponent p and the turbulence parameters σ_A and σ_E in Table 9-1 are conservative values based on an analysis of meteorological data from the NASA-150 meter tower at KSC (see Record, et al., 1969). That is, the use of these values in the model calculations should lead to predicted concentrations that are maximum values for the specified wind conditions. The values of the surface mixing depth H_m in Table 9-1 are considered to be average values for these wind conditions at KSC. There may be times, particularly late at night and early in the morning with winds of 3 m s^{-1} and less, when the mixing depth is lower and would act to increase concentrations at longer travel distances. The values of the dispersion coefficients α and β given in Table 9-1 are based on our experience in modeling concentrations downwind from quasi-continuous sources.

Source Model Input Parameters

The source model input parameters used in the calculations are given in Table 9-2. The values of the initial lateral (σ_{yR}) and alongwind (σ_{xo}) source dimensions were obtained by assuming the spill area of 148.65 m^2 to be circular and dividing the diameter of 13.7574 m by a factor of 4.3 to obtain the standard deviation of the concentration distribution at the source. Thus,

$$\sigma_{yR} = \sigma_{xo} = \frac{13.7574}{4.3} = 3.2 \text{ m}$$

The vertical source dimension σ_{zR} was arbitrarily set to 0.1 m. The source emission time T_E is

$$T_E = 27{,}675 \text{ lbs } N_2O_4 \times \frac{453.6 \text{g}}{1 \text{b}} \times \frac{m^2 s}{5.0045 \text{ g}} \times \frac{1}{148.65 \text{ m}^2}$$

$$= 16{,}874 \text{ s}$$

TABLE 9-1

METEOROLOGICAL MODEL INPUT PARAMETERS

Model Parameters	Case 1	Case 2	Case 3
$\bar{u}$ {2m} (m s^{-1})	3	4	5
p	0.175	0.15	0.12
H_m (m)	600	800	800
σ_A {τ_o=10 min} (deg)	8	8	8
σ_E (deg)	2.7	2.7	2.7
α	0.9	0.9	0.9
β	1.0	1.0	1.0

TABLE 9-2

SOURCE MODEL INPUT PARAMETERS

Model Parameters	Value
$\sigma_{yR} = \sigma_{xo}$ (m)	3.2
σ_{zR} (m)	0.1
X_R (m)	0
$X_{ry} = X_{rz}$ (m)	50
T_E (s)	16,874
Q (ppm m^3)	6.6708×10^9
H (m)	0

The amount of NO_2 that can be obtained from 27,675 pounds of N_2O_4 is

$$Q\ \{NO_2\} = 27{,}675\ \text{lbs}\ N_2O_4 \times \frac{22.4\ \ell}{46.01 g NO_2} \times \frac{m^3}{10^3 \ell} \times \frac{298.16^\circ K}{273.16^\circ K} \times \frac{453.6 g}{1 b}$$

$$= 6.6708 \times 10^3\ m^3$$

Since we wish the concentration to be given in parts of NO_2 per million parts of air, the above value of Q must be multiplied by 10^6, or

$$Q\ \{Q\} = 6.6708 \times 10^3 \times 10^6 = 6.6708 \times 10^9\ \text{ppm}\ m^3$$

which is the value for Q shown in Table 9-2. Finally, the source release height H is set to zero for a ground-level release. The calculations were performed for nearly-instantaneous (T_A = 2.5s), 10-minute (T_A = 600s) and 30-minute (T_A = 1800s) time-average concentrations.

Results of the Calculations

The concentration calculations were made using the quasi-continuous source model described above in Section 8. Figures 9-1 through 9-3 show calculated peak NO_2 concentrations versus downwind distance from the MON-10 fuel spill for Cases 1 through 3. In each figure, the three concentration curves represent averaging times of 2.5 seconds (instantaneous), 10- and 30-minutes. The NO_2 concentrations calculated at the distances of the CCAFS Industrial area (Case 1), KSC Industrial Area (Case 2), Cape Canaveral Harbor (Case 3) are presented in Table 9-3. The calculated 10-minute and 30-minute NO_2 concentrations at the KSC Industrial Area (Case 2) are below the lowest concentration shown in Figure 9-2.

Figure 9-4, 9-5 and 9-6 show the time profiles of instantaneous concentration for Cases 1 through 3 at the CCAFS Industrial Area, the KSC Industrial Area and Cape Canaveral Harbor. Figure 4 shows, for example,

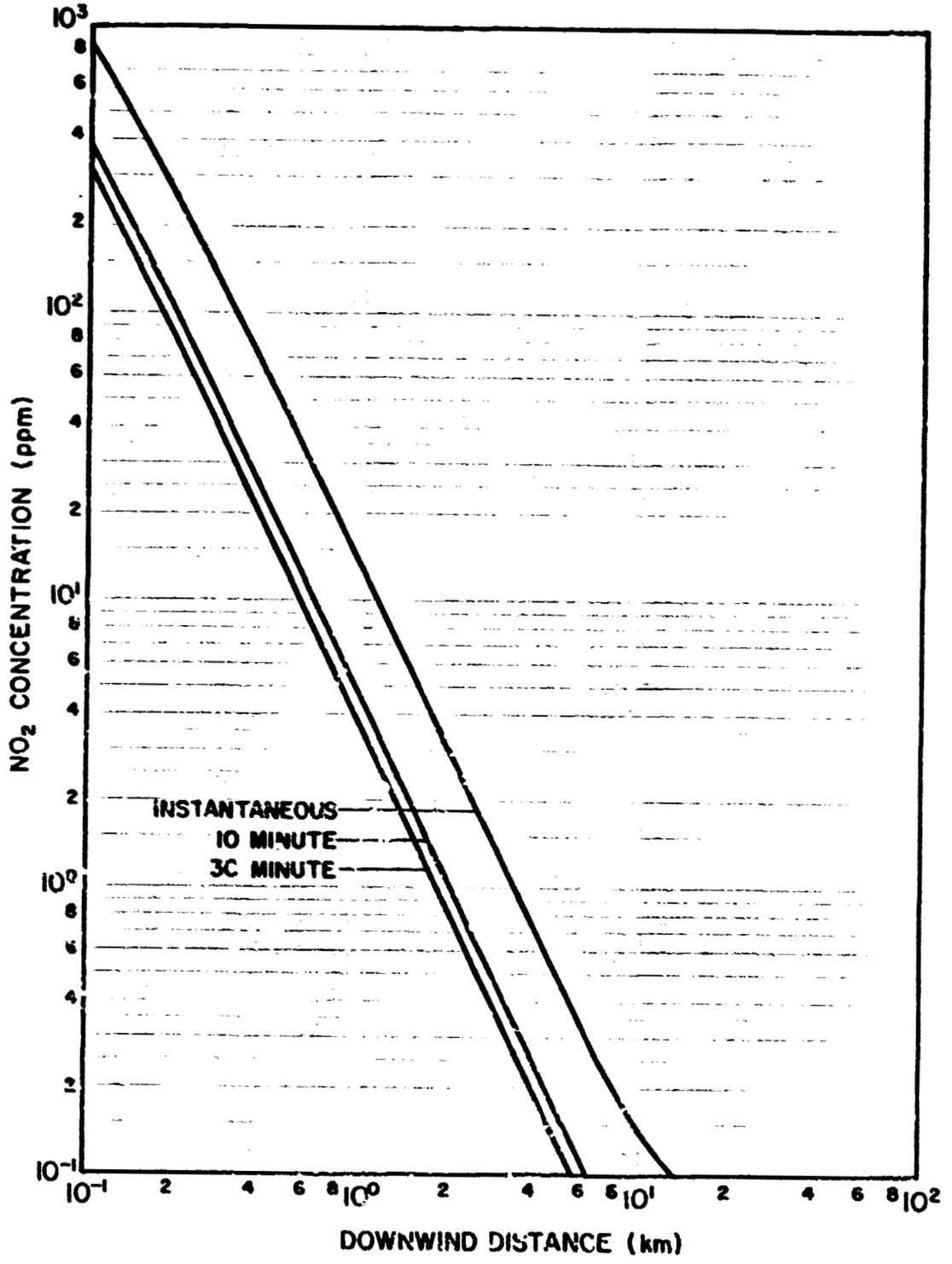

FIGURE 9-1. Instantaneous, 10- and 30-minute time average NO_2 concentrations for a 2-meter wind speed of 3 meters per second (Case 1).

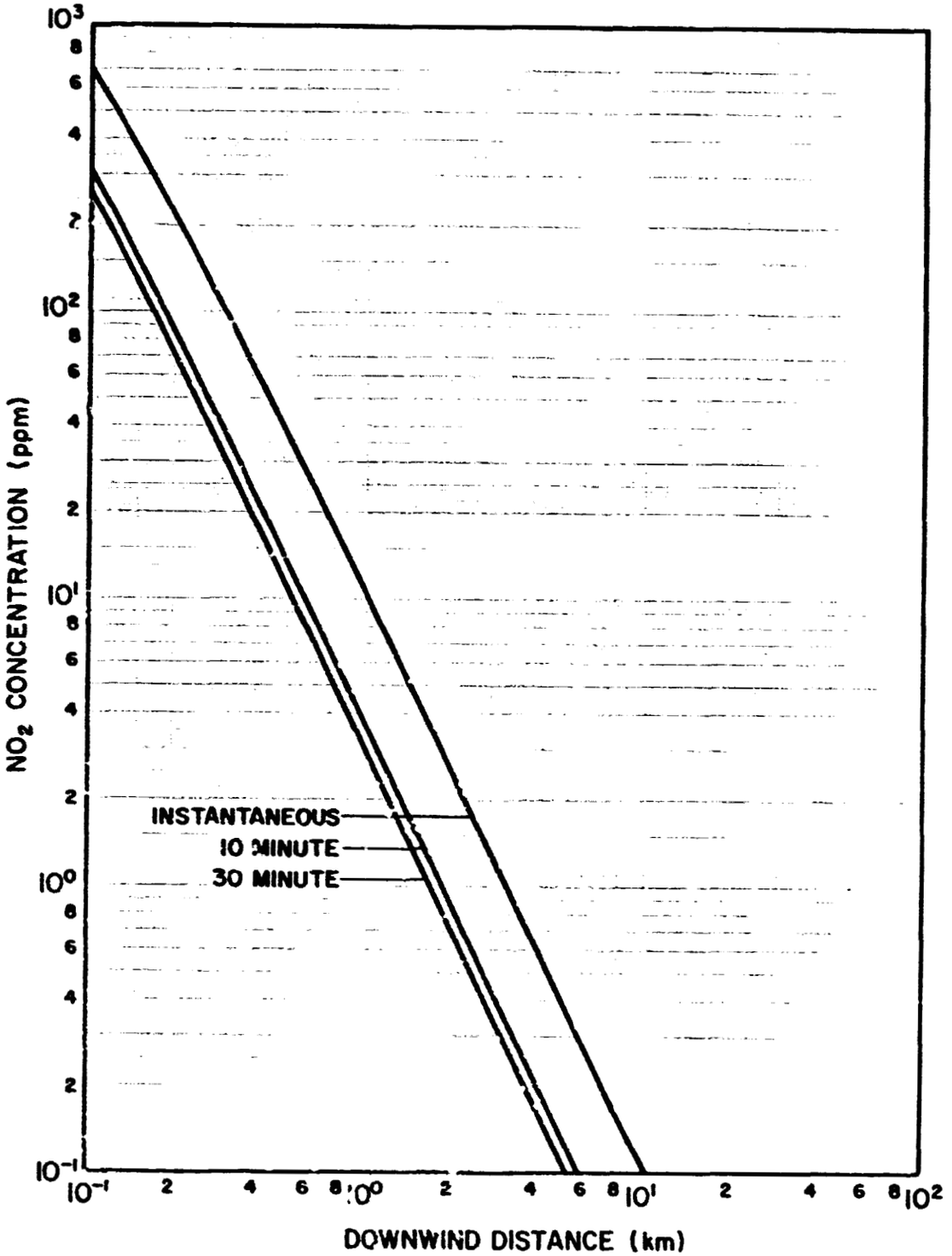

FIGURE 9-2. Instantaneous, 10- and 30-mintute time average NO_2 concentrations for a 2-meter wind speed of 4 meters per second (Case 2).

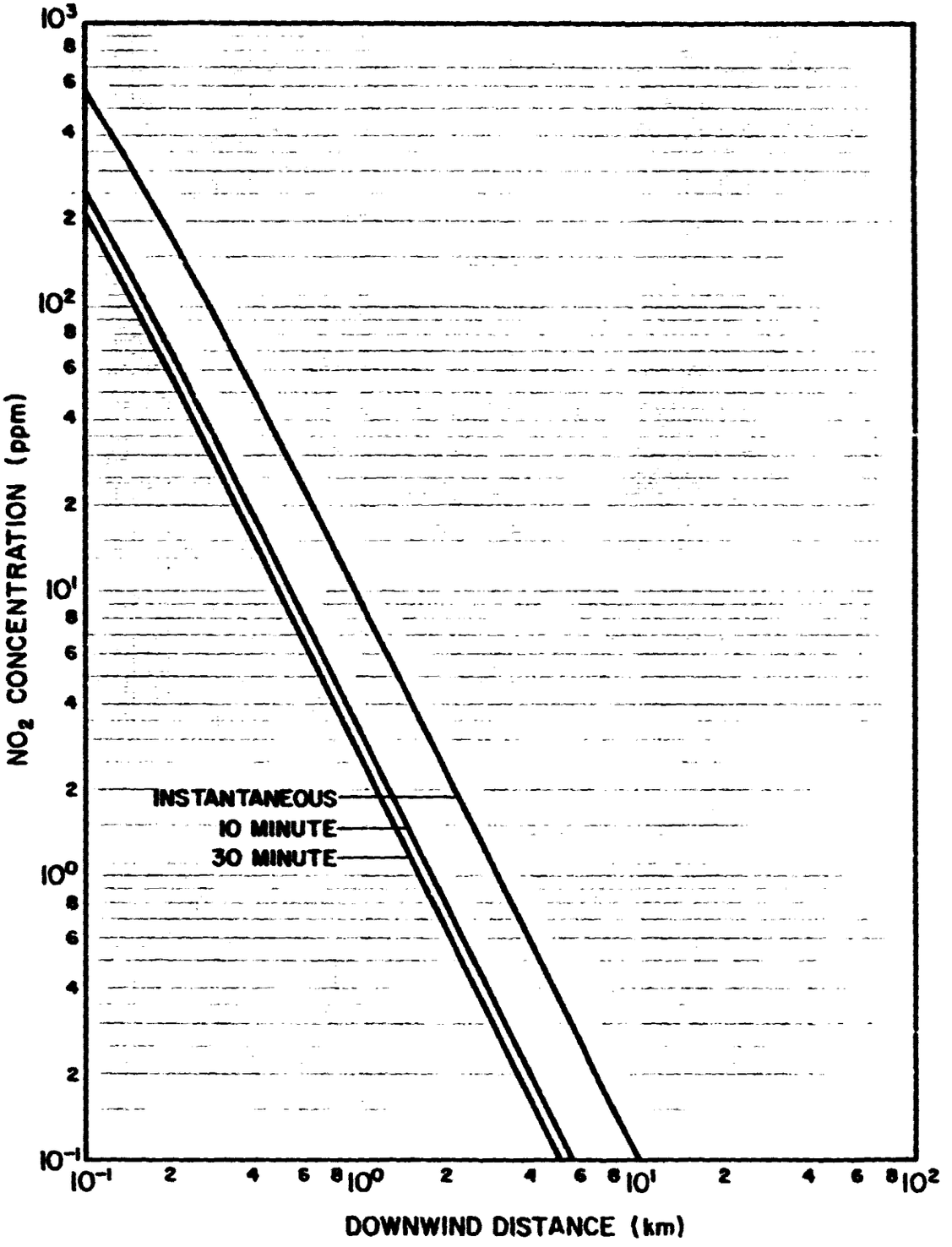

FIGURE 9-3. Instantaneous, 10- and 30-minute time average NO_2 concentrations for a 2-meter wind speed of 5 meters per second (Case 3).

TABLE 9-3

CALCULATED NO_2 CONCENTRATIONS AT THE CCAFS INDUSTRIAL AREA, KSC INDUSTRIAL AREA AND AT CAPE CANAVERAL HARBOR

	NO_2 Concentration (ppm)		
	Instantaneous	10-min	30-min
CCAFS Industrial Area (Case 1, x = 3353m)	1.1	0.37	0.30
KSC Industrial Area (Case 2, x = 8534m)	0.14	0.05	0.04
Cape Canaveral Harbor (Case 3, x = 6706 m)	0.21	0.07	0.06

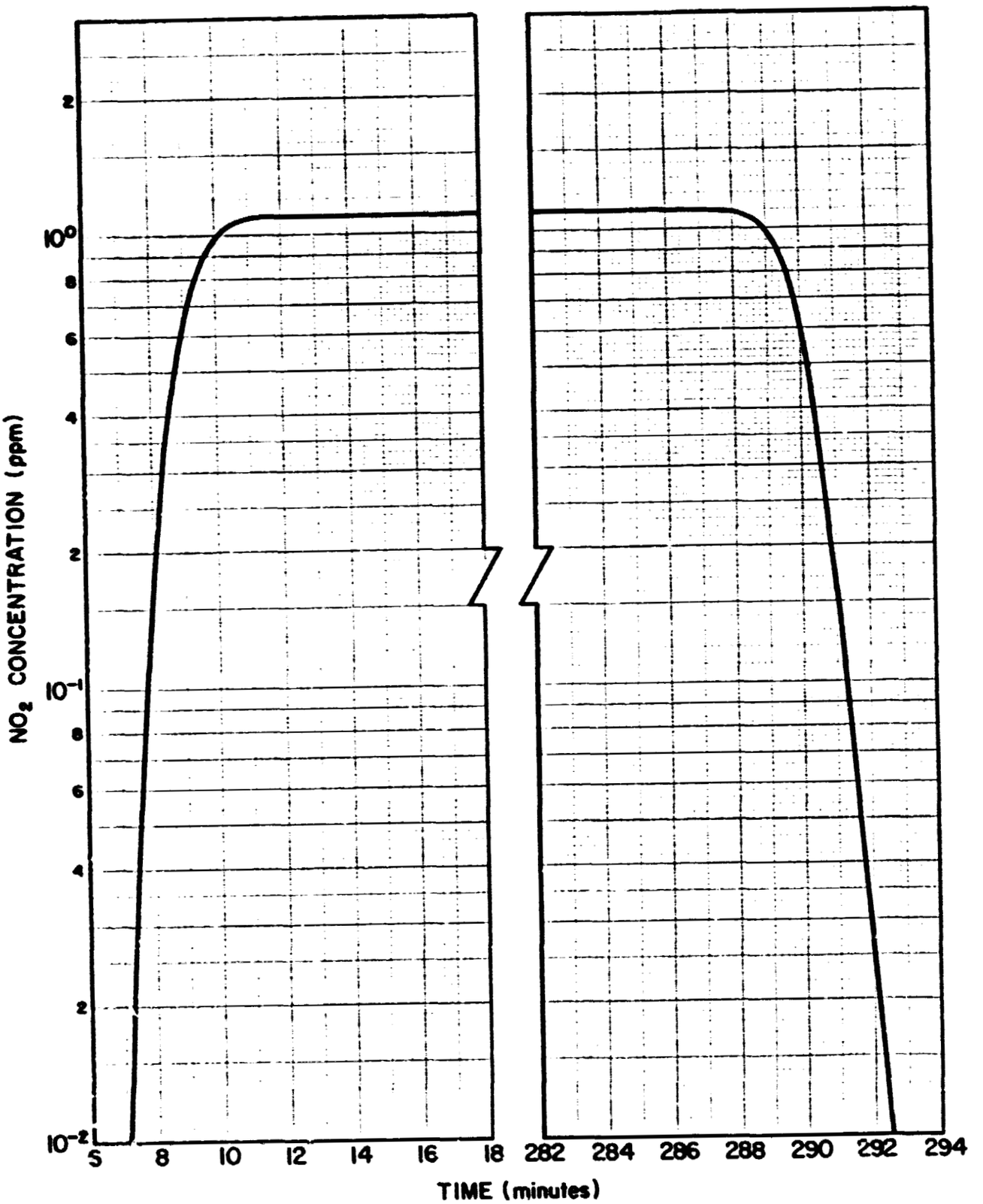

FIGURE 9-4. Time profile of instantaneous NO_2 concentrations at the CCAFS Industrial Area for a 2-meter wind speed of 3 meters per second (Case 1).

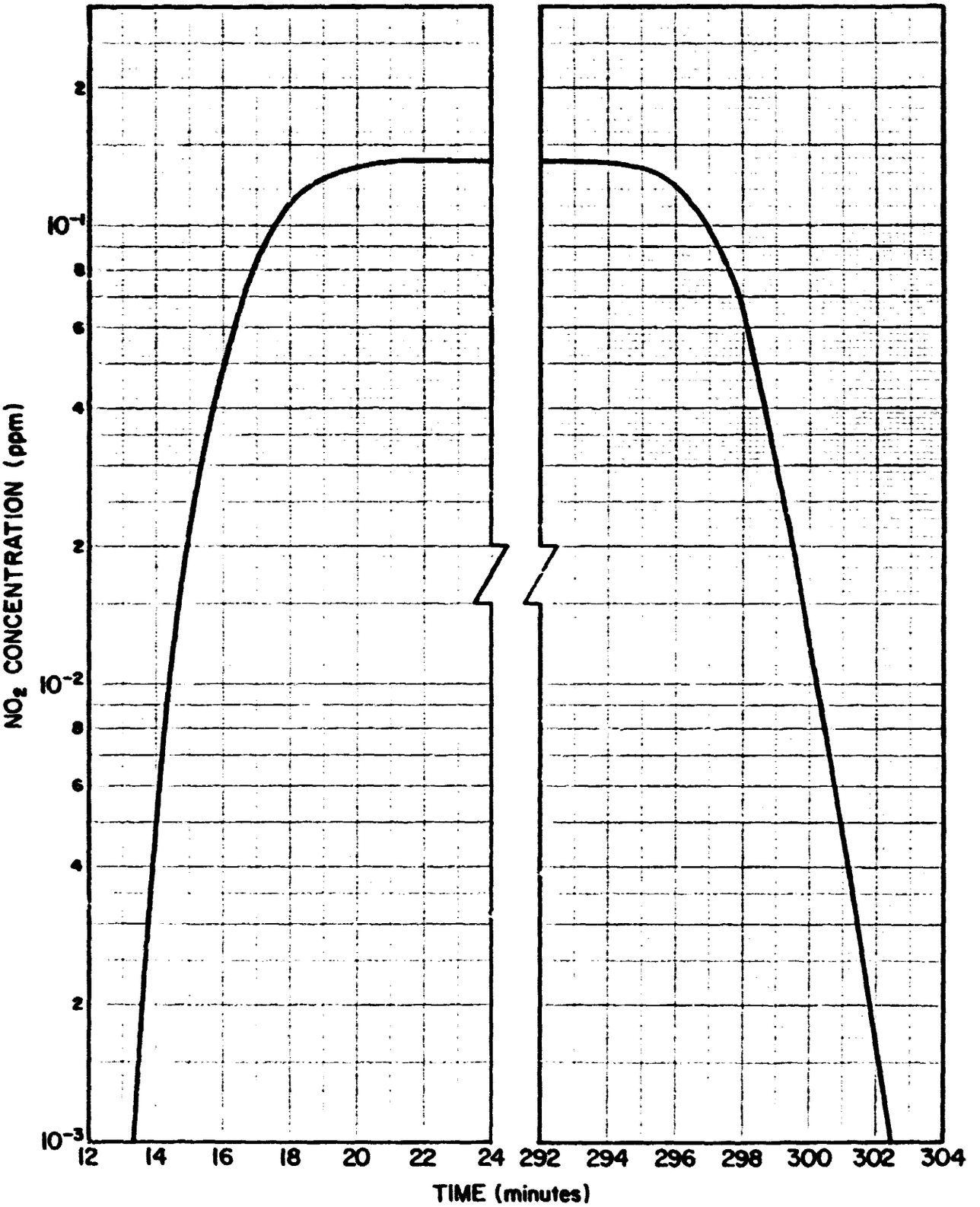

FIGURE 9-5. Time profile of instantaneous NO_2 concentrations at the KSC Industrial Area for a 2-meter wind speed of 4 meters per second (Case 2).

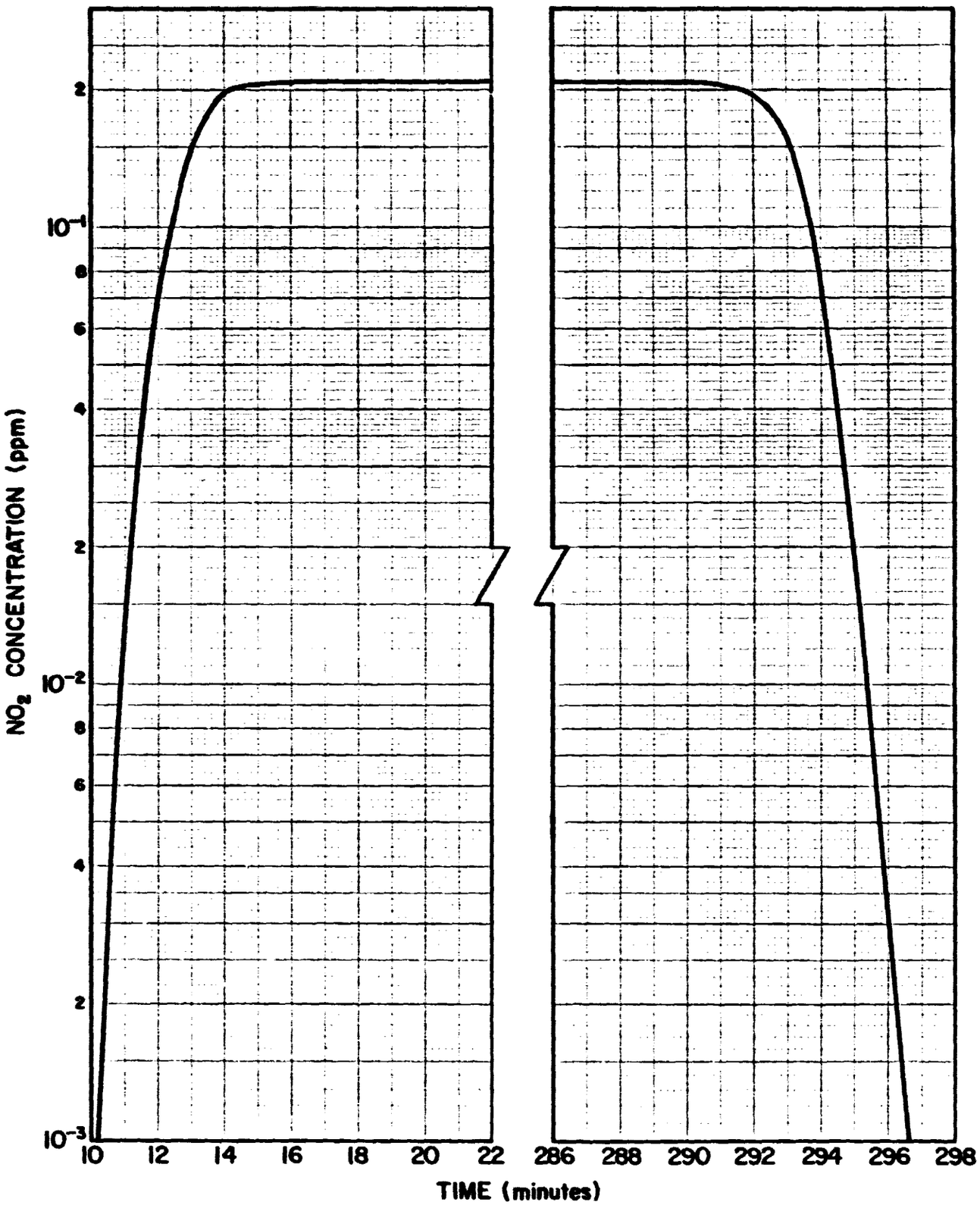

FIGURE 9-6. Time profile of instantaneous NO_2 concentrations at Cape Canaveral Harbor for a 2-meter wind speed of 5 meters per second (Case 3).

that the NO_2 concentration exceeds 1 ppm at the CCAFS Industrial Area about 10 minutes after the spill occurs and remains greater, on the average, than 1 ppm until 289 minutes after the spill occurs. The time of arrival and the passage time of various instantaneous concentration levels at the CCAFS and KSC Industrial Areas and for Cape Canaveral Harbor can be estimated from the curves in the three figures.

REFERENCES

Bjorklund, J. R. and R. K. Dumbauld, 1977: Users' instructions for the volume source diffusion models computer program and the volume/line source graphics computer program. H. E. Cramer Company, Inc. Technical Report TR-77-306-01 prepared for the U. S. Army, Dugway Proving Ground, Dugway, Utah.

Briggs, G. A., 1971: Some recent analyses of plume rise observations. In Proceedings of the Second International Clean Air Congress, Academic Press, New York.

Briggs, G. A., 1972: Chimney plumes in neutral and stable surroundings. Atm. Env., 6(7), 507-510.

Briggs, G. A., 1974: Plume rise from multiple sources. ATDL Contribution No. 91, Environmental Research Laboratories, Air Resources Atmosphric Turbulence and Diffusion Laboratory, Oak Ridge, Tennessee.

Dumbauld, R. K., J. R. Bjorklund, H. E. Cramer and F. A. Record, 1971: Handbook for estimating toxic fuel hazards. NASA CR-61326. Marshall Space Flight Center, Alabama 35812.

Dumbauld, R. K., J. R. Bjorklund and J. F. Bowers, 1973: NASA/MSFC multilayer diffusion models and computer program for operational prediction of toxic fuel hazards. NASA CR-129006, NASA - George C. Marshall Space Flight Center, Marshall Space Flight Center, Alabama 35812.

Dumbauld, R. K. and J. R. Bjorklund, 1977: Mixing-layer analysis routine and transport/diffusion application routine for EPAMS. Research and Development Tech. Rpt. ECOM-77-2. Atmospheric Sciences Laboratory, White Sands Missile Range, New Mexico 88002.

Dumbauld, R. K., J. E. Rafferty and S. F. Saterlie, 1977: Estimates of ground-level mercury concentrations from launch-pad accidents of NASA space transportation systems. H. E. Cramer Company, Inc. Technical Report TR-77-111-02. Prepared for NASA, Marshall Space Flight Center, AL 35812.

Fuchs, N. A., 1959: Evaporation and Droplet Growth in Gaseous Media. Pergammon Press, N. Y., N. Y. p. 44.

McDonald, J. E., 1960: An aid to computation of terminal fall velocities of spheres. Journ. of Meteor., 17, pp. 463-465.

Record, F. A., R. N. Swanson, H. E. Cramer and R. K. Dumbauld, 1969: Analysis of lower atmospheric data for diffusion studies. GCA Technology Division Report under Contract No. NAS8-30503, with Marshall Space Flight Center, Alabama 35812.

Robins, A. G. and I. P. Castro, 1977a: A wind tunnel investigation of plume dispersion in the vicinity of a surface mounted cube-I. The flow field. Atm. Env., 2, 291-297.

Robins, A. G. and I. P. Castro, 1977b: A wind tunnel investigation of plume dispersion in the vicinity of a surface mounted cube-II. The concentration field. Atm. Env., 2, 299-311.

Smith, M. E., 1968: Recommended guide for the prediction of the dispersion of airborne effluents. The American Society of Mechanical Engineers, New York, N. Y.

Stephens, J. B., J. S. Hickey and W. M. Greene, 1978: Space Shuttle rocket exhaust cloud rise prediction assuming January 1965 meteorological conditions. MSFC Report No. ES84-438, Marshall Space Flight Center, Alabama 35812.

Stephens, J. B. and R. K. Dumbauld, 1979: Concentration calculations for the liquid oxygen leaking from the Space Shuttle main engines during cryogenic tanking. Space Sciences Laboratory Report, Marshall Space Flight Center, AL 35812.

Thompson, R. S. and D. J. Lombardi, 1977: Dispersion of roof-top emissions from isolated buildings. EPA-600/4-77-006, Environmental Sciences Research Laboratory, U. S. Environmental Protection Agency, Research Triangle Park, North Carolina 27711.

Tyldesley, J. B. and C. E. Wallington, 1965: The effect of wind shear and vertical diffusion on horizontal dispersion. Quart. J. Roy. Met. Soc., 91, 158-174.